Homeodomain-interacting protein kinase maintains neuronal homeostasis during normal *Caenorhabditis elegans* aging and systemically regulates longevity from serotonergic and GABAergic neurons

Authors: Maria I. Lazaro-Pena[1], Adam B. Cornwell[1], Carlos A. Diaz-Balzac[2], Ritika Das[1,3,4], Nicholas Macoretta[3], Juilee Thakar[1,5,6], Andrew V. Samuelson[1*]

Affiliations:
[1] Department of Biomedical Genetics, University of Rochester Medical Center, Rochester, New York, USA
[2] Division of Endocrinology, Diabetes and Metabolism, Department of Medicine, University of Rochester Medical Center, Rochester, New York, USA
[3] Department of Biology, University of Rochester, Rochester, New York, USA
[4] Department of Cell Biology, Skirball Institute of Biomolecular Medicine, NYU School of Medicine, New York, New York, USA.
[5] Department of Biostatistics and Computational Biology, University of Rochester Medical Center, 601 Elmwood Avenue, Rochester, NY 14642, USA
[6] Department of Microbiology and Immunology, University of Rochester Medical Center, 601 Elmwood Avenue, Rochester, NY 14642, USA

* Corresponding author. Andrew_Samuelson@URMC.Rochester.edu

Author Contributions: M.I.L.P. designed, conducted, and analyzed the majority of experiments. A.B.C. designed and conducted the genomic analyses in Fig. 2 & 4 and associated supplements, and analyzed data for figure supplements 3 and 9. C.A.D.B. assisted in the completion of multiple experiments. R.D. designed and conducted the experiments in Fig 1A, F and Fig. 4. N.M. designed and conducted the experiments in Fig Sup 9. A.V.S. oversaw the project from concept to completion, contributing primarily to experimental design and the analysis and interpretation of results. J.T. contributed to the genomic analyses. M.I.L.P., A.B.C. and A.V.S. wrote the manuscript.

Competing Interest Statement: The authors have no competing interests.

Abstract

Aging and the age-associated decline of the proteome is determined in part through neuronal control of evolutionarily conserved transcriptional effectors, which safeguard homeostasis under fluctuating metabolic and stress conditions by regulating an expansive proteostatic network. We have discovered the *Caenorhabditis elegans* homeodomain-interacting protein kinase (HPK-1) acts as a key transcriptional effector to preserve neuronal integrity, function, and proteostasis during aging. Loss of *hpk-1* results in drastic dysregulation in expression of neuronal genes, including genes associated with neuronal aging. During normal aging *hpk-1* expression increases throughout the nervous system more broadly than any other kinase. Within the aging nervous system, *hpk-1* is co-expressed with key longevity transcription factors, including *daf-16* (FOXO), *hlh-30* (TFEB), *skn-1* (Nrf2), and *hif-1,* which suggests *hpk-1* expression mitigates natural age-associated physiological decline. Consistently, pan-neuronal overexpression of *hpk-1* extends longevity, preserves proteostasis both within and outside of the nervous system, and improves stress resistance. Neuronal HPK-1 improves proteostasis through kinase activity. HPK-1 functions cell non-autonomously within serotonergic and GABAergic neurons to improve proteostasis in distal tissues by specifically regulating distinct components of the proteostatic network. Increased serotonergic HPK-1 enhances the heat shock response and survival to acute stress. In contrast, GABAergic HPK-1 induces basal autophagy and extends longevity. Our work establishes *hpk-1* as a key neuronal transcriptional regulator critical for preservation of neuronal function during aging. Further, these data provide novel insight as to how the nervous system partitions acute and chronic adaptive response pathways to delay aging by maintaining organismal homeostasis.

Keywords: Neuronal cell-nonautonomous control, gene expression, proteostasis, longevity, aging, stress response, autophagy, homeodomain interacting protein kinase

Introduction

The gradual decline of function within the proteome (proteostasis) is a characteristic of aging, which precipitates the onset and progression of a growing number of age-associated diseases (Balch et al., 2008; Gidalevitz et al., 2006; Gidalevitz et al., 2010; Kikis et al., 2010; Morimoto, 2011, 2019; Sala et al., 2017; Taylor and Dillin, 2011): Alzheimer's disease (AD), Parkinson's disease (PD), Huntington's disease, and Amyotrophic Lateral Sclerosis (ALS) are neurodegenerative diseases driven by genetic alterations that typically predispose a mutant protein isoform to aggregate and have toxic gain of function properties on the neuronal proteome. Outside of the nervous system age-associated proteostatic decline also leads to disease, for example: the onset of diabetes mellitus (Jaisson and Gillery, 2014); thus the decline in proteostasis during normal aging is not limited to the nervous system. A growing number of studies suggest that aging is not simply the result of the stochastic accumulation of damage, but is determined through genetics and coordinated mechanisms across tissues and cell types (Labbadia and Morimoto, 2015; Lazaro-Pena et al., 2022; Lopez-Otin et al., 2013). Proteostatic decline corresponds with the age-associated breakdown of a large proteostasis network (PN), which integrates stress-responsive control of protein folding, degradation, and translation in response to myriad cell intrinsic and non-autonomous signals. And yet, while major components of the proteostatic network have been identified, it is still poorly understood how multi-cellular organisms maintain systemic proteostasis within and across tissues to delay aging.

The relatively simple metazoan animal *Caenorhabditis elegans* (*C. elegans*) is a premier model system to learn how proteostasis is coordinated across cell- and tissue-

82 types in response to myriad signals. Discoveries of cell non-autonomous signaling first
83 made in *C. elegans* have evolutionarily conserved components, and revealed that the
84 nervous system acts as a key cell non-autonomous regulator of organismal proteostasis
85 and longevity (reviewed in (Miller et al., 2020)). For example, a pair of thermosensory
86 neurons systemically regulate the heat shock response (HSR) in a serotonin-dependent
87 manner (Prahlad et al., 2008; Tatum et al., 2015). In contrast, a second regulatory
88 component from the GABAergic and cholinergic systems normally limits muscle cell
89 proteostasis (Garcia et al., 2007; Silva et al., 2013).

90 In *C. elegans,* the transcriptional co-factor homeodomain-interacting protein
91 kinase (HPK-1), preserves proteostasis and organismal longevity (Berber et al., 2016;
92 Das et al., 2017; Samuelson et al., 2007). We first identified *hpk-1* in a genome-wide RNAi
93 for genes that are essential for decreased insulin-like signaling (ILS) to extend longevity
94 (Samuelson et al., 2007). Additionally, we have previously shown that HPK-1 extends
95 longevity through distinct genetic pathways defined by HSF-1, and the target of rapamycin
96 complex 1 (TORC1) (Das et al., 2017). Activation by either metabolic or genotoxic
97 stressors has been observed from yeast to mammals, suggesting that this family of
98 transcriptional cofactors arose early in evolution to couple metabolic and stress signaling
99 (Hofmann et al., 2003; Kim et al., 2006; Lee et al., 2008; Shojima et al., 2012).

100 In general, mammalian HIPK family members regulate the activity of transcription
101 factors (TFs), chromatin modifiers, signaling molecules and scaffolding proteins in
102 response to cellular stress (Calzado et al., 2007; de la Vega et al., 2012; Song and Lee,
103 2003a, b). For example, nutrient stress, such as glucose deprivation can activate Hipk1

104 and Hipk2 (Ecsedy et al., 2003; Garufi et al., 2013; Song and Lee, 2003b). Conversely,
105 hyperglycemia triggers HIPK2 degradation via the proteasome (Baldari et al., 2017).

106 We sought to identify the tissue- and cell-types in which the HPK-1 transcriptional
107 circuits acts to extend longevity, increase resistance to acute proteotoxic stress, and
108 which PN components are regulated across tissues. We have discovered that HPK-1
109 functions as a key regulator of the proteostatic response, originating in the nervous
110 system of *C. elegans*. We find that *hpk-1* is the most broadly upregulated kinase during
111 normal *C. elegans* aging, predominantly within the nervous system, and acts to preserves
112 neuronal function and proteostasis within the nervous system. Further, HPK-1 kinase
113 activity within the nervous system initiates cell non-autonomous signals that trigger
114 protective peripheral responses to maintain organismal homeostasis. Responses can
115 qualitatively differ depending on the neuronal type from which they arise: serotonergic
116 HPK-1 activity increases thermotolerance and protects the proteome from acute stress
117 by enhancing the HSR, without increasing lifespan or altering basal autophagy. In
118 contrast, GABAergic HPK-1 activity induces autophagy to extend longevity, without
119 altering thermotolerance. We posit that serotonergic HPK-1 signaling responds to acute
120 proteotoxic stress, whereas GABAergic HPK-1 responds to chronic metabolic changes
121 mediated through target of rapamycin complex 1 (TORC1) (Das et al., 2017). Yet, each
122 of these distinct adaptive responses is sufficient to activate the PN and improve
123 proteostasis outside of the nervous system. Our findings reveal HPK-1 as a key neuronal
124 regulator in coordinating adaptive metabolic and stress response pathways across
125 tissues to delay aging throughout the animal.

126 **Results**

127 **HPK-1 acts from neuronal tissue to promote longevity and health span.**

128 To precisely determine where HPK-1 functions in the regulation of longevity, we
129 overexpressed *hpk-1* within neuronal (*rab-3p*), muscle (*myo-3p*), intestine (*ges-1p*) or
130 hypodermal (*dpy-7p*) tissues to identify where activity was sufficient to increase lifespan.
131 Increased neuronal expression of *hpk-1* was sufficient to increase lifespan by 17%, which
132 is comparable to constitutive overexpression of *hpk-1* throughout the soma (*Figure 1A*)
133 (Das et al., 2017). In contrast, transgenic animals overexpressing *hpk-1* in either
134 muscular, intestinal, or hypodermal cells had no significant change in lifespan (*Figure 1B-*
135 *D*). These results were somewhat unexpected, as we previously found that loss of *hpk-1*

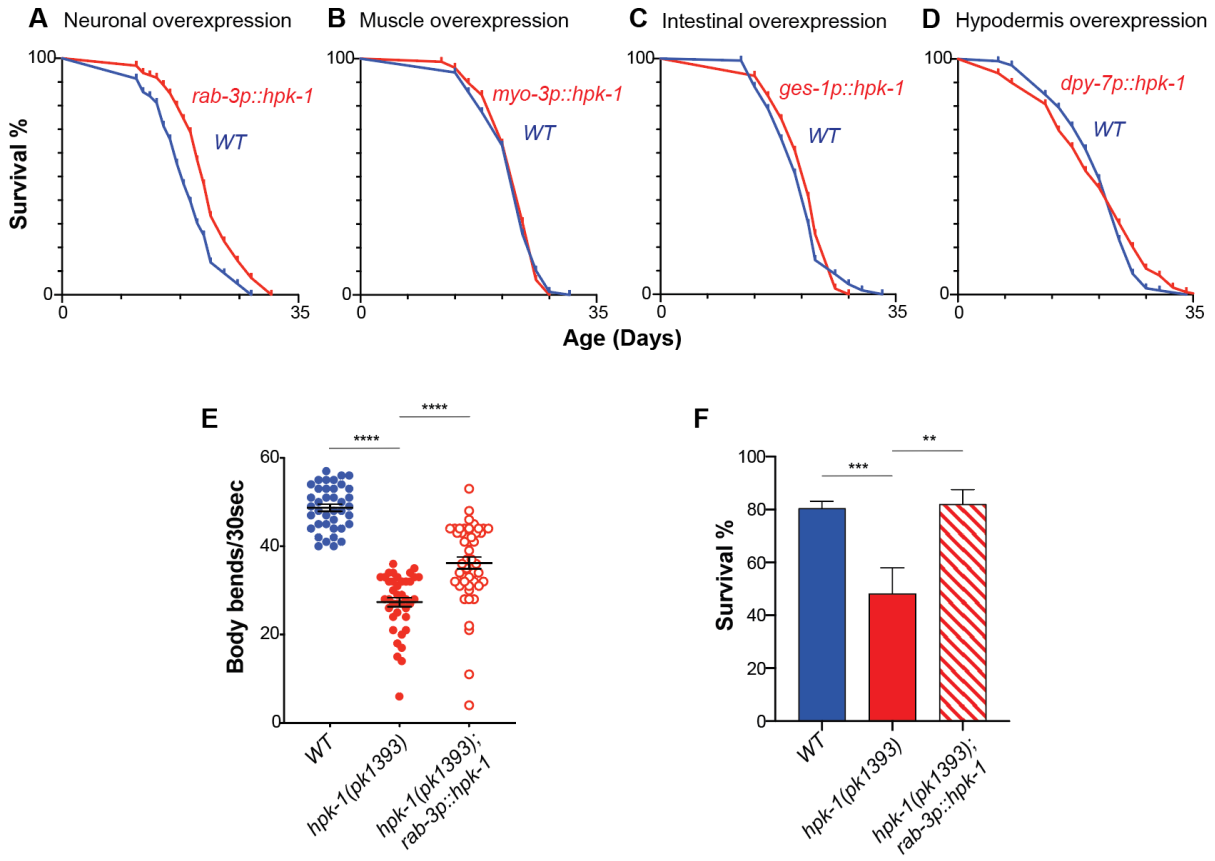

Figure 1. Neuronal HPK-1 extends longevity and promotes health span.
Lifespan curves of animals overexpressing *hpk-1* (red line) in the nervous system **(A)**, muscle **(B)**, intestine **(C)** and hypodermis **(D)** compared with control non-transgenic siblings (blue line). ($n \geq 175$, log-rank test, $P < 0.0001$ for A, $n \geq 78$ for B, $n \geq 82$ for C and $n \geq 105$ for D). Lifespan graphs are representative of two biological replicates. **(E)** Frequency of body bends of *wild type*, *rab-3p::hpk-1* and *hpk-1(pk1393); rab-3p::hpk-1* day 2 adult animals ($n \geq 48$). **(F)** Survival of day 1 adult animals subjected to heat shock treatment. Graph represents one of the two individual trials ($n \geq 66$). See *Supplementary Files 1, 2 and 3* for details and additional trials.

136 solely within either neuronal, intestinal, or hypodermal cells is sufficient to shorten lifespan
137 (Das et al., 2017). *hpk-1* is broadly expressed during embryogenesis and larval
138 development, but is only expressed within the nervous system in adult animals (Berber
139 et al., 2013; Berber et al., 2016; Das et al., 2017; Raich et al., 2003). Furthermore, *hpk-1*
140 and orthologs are known to have roles in development, differentiation and cell fate-
141 specification (Berber et al., 2013; Blaquiere and Verheyen, 2017; Calzado et al., 2007;
142 Hattangadi et al., 2010; Rinaldo et al., 2007; Rinaldo et al., 2008; Steinmetz et al., 2018).
143 Therefore, we conclude that HPK-1 functions primarily within the nervous system to
144 regulate aging.

145 We performed a locomotion assay to test whether neuronal *hpk-1* could rescue an
146 age-associated decline in movement, a readout of *C. elegans* healthspan (Berber et al.,
147 2016; Das et al., 2017; Herndon et al., 2002; Huang et al., 2004; Samuelson et al., 2007).
148 As expected, *hpk-1(pk1393)* null mutants displayed a reduced frequency of body bends
149 at day 2 of adulthood (*Figure 1E*). Increased expression of *hpk-1* in neurons was sufficient
150 to partially mitigate the locomotion defect of *hpk-1* null mutants. Thus, HPK-1 activity
151 within the nervous system is sufficient to improve healthspan. Further, HPK-1 also retains
152 essential functions for adult healthspan outside of the nervous system; as *hpk-1* is no
153 longer expressed with translational reporters outside of the nervous system in adult
154 animals (Das et al., 2017).

155 We next asked whether neuronal *hpk-1* expression would be sufficient to rescue
156 the ability of animals to survive acute stress. We and others previously found that in the
157 absence of *hpk-1*, animals are vulnerable to thermal stress (Berber et al., 2016; Das et
158 al., 2017). Restoring *hpk-1* expression solely within the nervous system was sufficient to

159 fully rescue the reduced thermotolerance of *hpk-1* null mutant animals (Fig. 1F).
160 Collectively, these findings are consistent with the notion that *hpk-1* primarily acts within
161 the nervous system to regulate aging and stress resistance.

162 ***hpk-1* expression increases broadly during normal aging.**

163 We sought to determine whether *hpk-1* mRNA expression changes during normal
164 aging. Adult *C. elegans* are composed of 959 somatic cells, of which 302 are neuronal;
165 all somatic cells are all post-mitotic and arise from an invariant lineage. A recent
166 comprehensive single-cell analysis of age-associated changes in gene expression
167 throughout the *C. elegans* identified 211 unique "cell-clusters" within the aging soma:
168 groups of cells within a lineage or tissue defined by gene expression profiles (Roux et al.,
169 2022). The "*C. elegans* Aging Atlas" analysis identified 124 neuronal cell clusters and
170 obtained age-associated changes in gene expression for 122, with high concordance of
171 overall gene expression between neuron clusters to a previous project, which mapped
172 the complete gene expression profiles of the *C. elegans* nervous system in late larval
173 animals (The CeNGEN project (Taylor et al., 2021)). The *C. elegans* Aging Atlas provides
174 the means to investigate age-associated changes in gene expression at an
175 unprecedented level of resolution.

176 Using the *C. elegans* Aging Atlas dataset, in which differentially expressed genes
177 were identified within each cell cluster in old versus young animals, we find that *hpk-1*
178 expression increases during aging within 48 cell clusters: broadly within the nervous
179 system and in eleven non-neuronal cell clusters (*Figure 2-figure supplement 1*, see
180 Materials and methods). With aging, neuronal expression of *hpk-1* increased within
181 interneurons, motor neurons, sensory neurons, and all neuronal sub-types (cholinergic,

182 dopaminergic, GABAergic, serotonergic, and glutamatergic). We found no cell-clusters in
183 which *hpk-1* is downregulated during normal aging. It is well known that many longevity-
184 associated TFs increase lifespan when overexpressed and shorten lifespan when lost
185 (reviewed in (Denzel et al., 2019)), which infers these TFs might be upregulated, or
186 become chronically activated, during normal aging. A major finding of the *C. elegans*
187 Aging Atlas study was that many longevity-associated TFs are upregulated during normal
188 aging in more than 200 cell-type clusters (Roux et al., 2022). Increased expression of
189 longevity-associated TFs is thought to reflect an age-associated adaptive response to
190 dysregulation of homeostatic mechanisms and accumulating damage (Roux et al., 2022).
191 We posit *hpk-1* neuronal expression increases during normal aging in wild-type animals
192 to mitigate accumulating damage and cellular dysfunction.

193 **During normal aging, *hpk-1* is neuronally co-expressed with longevity-associated**
194 **TFs*.***

195 We next assessed whether the age-associated increase in expression of *hpk-1*
196 spatially correlated with expression of *any* TFs, and then segregated co-expression into
197 neuronal and non-neuronal subgroups. Seventy-one TFs were differentially co-expressed
198 with *hpk-1* during aging within three or more neuron clusters, thirty within non-neuronal
199 clusters, with an overlap of twenty-one TFs between neurons and non-neurons (*Figure*
200 *2A-figure supplement 2* and *Supplementary File 4*). Overall, twenty-six of these TFs have
201 previously been implicated in longevity. There are ten TFs upregulated with aging that
202 are broadly co-expressed with *hpk-1* in the nervous system (in 9 or more neuronal
203 clusters), six of which have previously been linked to longevity: *daf-16* (FOXO, overlaps
204 in 19/37 neuronal clusters)*, hlh-30* (TFEB, 18/37)*, dpy-22* (mediator complex subunit 12L,

15/37), *gei-3* (10/37), *skn-1* (NRF2, 10/37), and *hif-1* (hypoxia inducible factor 1, 10/37) (*Figure 2B*) (An and Blackwell, 2003; Chen et al., 2009; Fawcett et al., 2015; Kenyon et

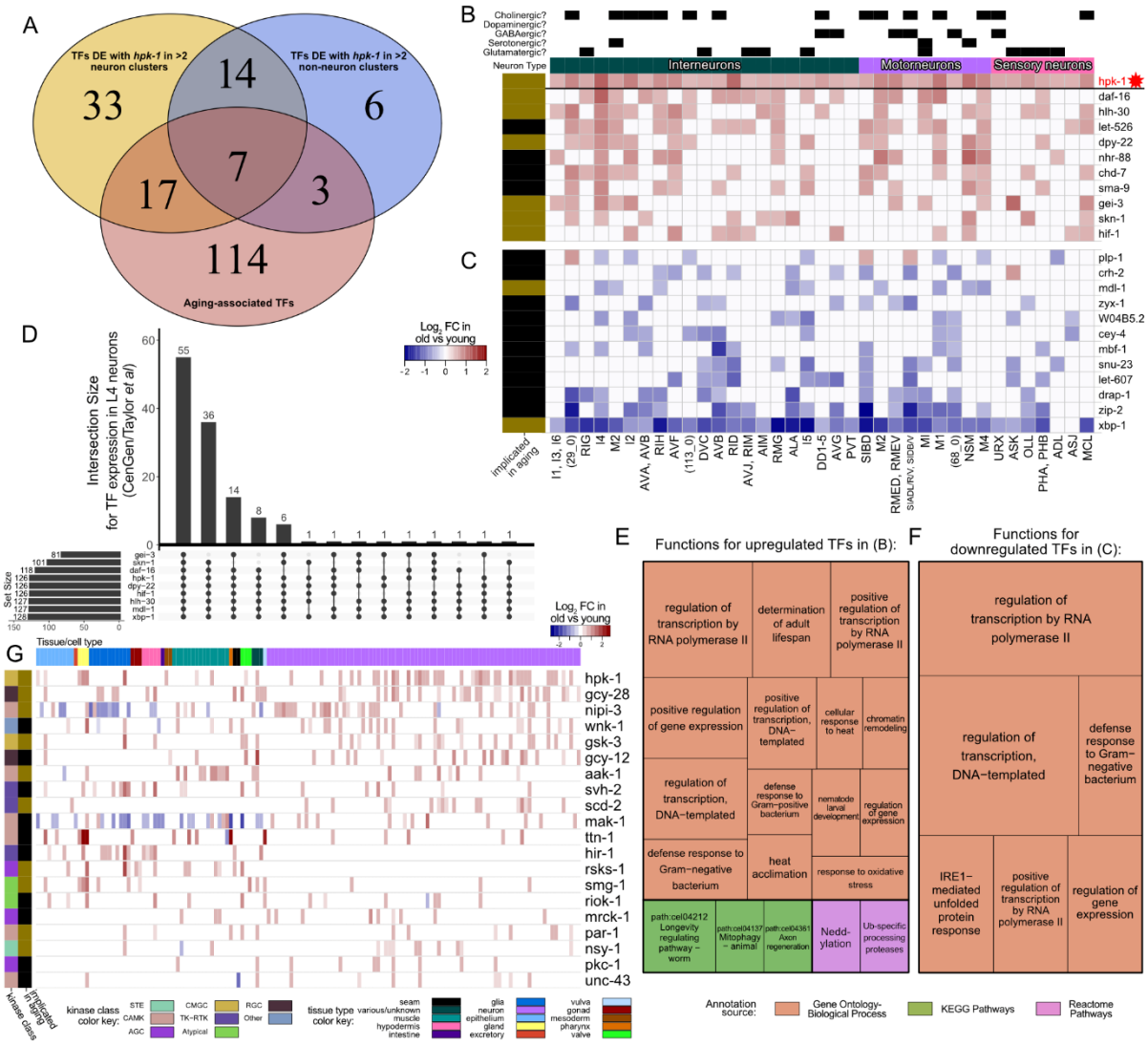

Figure 2. During normal aging *hpk-1* is the most broadly upregulated kinase and is co-expressed with key longevity-associated transcription factors within the nervous system.
(A) Venn diagram depicting transcription factors (TFs) with significant age-associated differential expression with *hpk-1* within three or more of the 36 neuronal and/or 11 non-neuronal cell clusters (yellow and blue, respectively), along with TFs that have previously been implicated in *C. elegans* longevity (red). **(B, C)** Heat map of neuronal cell clusters in which *hpk-1* expression increases during normal aging along with most broadly co-expressed TFs (≥ 9 cell-clusters). Positive (red) and negative (blue) fold change with aging of a given TF are shown in (**B**) and (**C**), respectively, grouped by average across the indicated clusters. Neuronal types, subtypes, cell-cluster or individual neuronal pair, as well as whether a TF has previously been implicated in aging is indicated. Primary data for this analysis was generated in the *C. elegans* Aging Atlas (Roux et al., 2022) and significant differences in expression with aging were determined by filtering differential expression results from a comparison of old vs young animals, based on adjusted p-values <0.05 and a $\log_2$ foldchange magnitude of at least 0.5 (between days 8,11,15 and days 1,3,5). **(D)** *hpk-1* is broadly co-expressed with the aging-implicated TFs **(B, C)** in late larval stage animals. Vertical bars show the number of neurons expressing TFs or *hpk-1* in the intersection indicated by the filled dots. The number of neurons each individual gene is found expressed is given by the horizontal bars, "set size". Primary data for this analysis was generated in the CenGEN project, expression was determined based on their "medium" stringency threshold of average TPM per neuron type ≥ 0.1 (Taylor et al., 2021). **(E, F)** Functions and pathways associated with two or more of the TFs listed in **(B)** and **(C)**, respectively. **(G)** *hpk-1* is differentially expressed with age in more cell clusters than any other kinase, and mostly in neurons. Heatmap shows $\log_2$ foldchange in old vs young animals for kinases with differential expression in ≥10 cell clusters. Primary data for this analysis was generated in the *C. elegans* Aging Atlas (Roux et al., 2022) and filtered for significant age-associated expression changes as described in **(B, C)**. See *Supplementary Files 4 and 5* for dataset.

207 al., 1993; Lapierre et al., 2013; Lin et al., 1997; Ogg et al., 1997; Roux et al., 2022;
208 Suriyalaksh et al., 2022; Tacutu et al., 2012; Zhang et al., 2009). Conversely, there was
209 an inverse correlation with 14 TFs (9 or more clusters, (*Figure 2C*); only two of which have
210 previously been implicated in longevity, *xbp-1* (X-box binding protein 1) a key regulator of
211 the endoplasmic reticulum unfolded protein response (ER-UPR), and *mdl-1* (MAX
212 dimerization protein) (Johnson et al., 2014; Nakamura et al., 2016; Riesen et al., 2014).
213 Of note, *mdl-1* is a Myc-family member with opposing roles in longevity from *mxl-2* (Mlx)
214 (Johnson et al., 2014), and *mxl-2* is required for *hpk-1* to extend longevity. (Das et al.,
215 2017).

216 In non-neuronal clusters we found a much smaller subset of TFs with
217 corresponding positive age-associated fold-changes (see Appendix 1). Similar to *hpk-1,*
218 all of the aforementioned longevity-associated TFs are broadly expressed throughout the
219 nervous system by late larval development, with the exception of the nematode specific
220 gene *gei-3*, for which overlap is restricted to a subset of neurons (*Figure 2D*). TFs with
221 age-associated increases in co-expression with *hpk-1* are associated with positive
222 regulation of adult lifespan, heat and oxidative stress response, bacterial innate immunity,
223 chromatin remodeling, development, mitophagy, axon regeneration, neddylation, and
224 ubiquitination (*Figure 2E*). TFs inversely correlated with *hpk-1* broadly across neuronal
225 cell-clusters have been implicated in the ER unfolded protein response and the innate
226 immune response (*Figure 2F*). These findings suggest that during normal aging, *hpk-1* is
227 induced within the nervous system in tandem with key longevity transcription factors to
228 mitigate the physiological effects of aging.

229 The first discovery of a putative link between *hpk-1* and longevity was from our
230 genome-wide RNAi screen that identified 103 genes that were essential for decreased
231 insulin-like signaling (ILS) to extend longevity (Samuelson et al., 2007): at 25°C loss of
232 *hpk-1* reduced *daf-2(e1370)* (insulin/IGF1 receptor) and wild-type lifespans to a similar
233 extent, but did not substantially further reduce *daf-2(e1370);daf-16(mfDf47)* lifespan
234 (reported in Sup Table S2 of (Samuelson et al., 2007) and this study (*Figure Supplement*
235 *3A-C*)). However, animals maintained at 25°C experience chronic, mild heat stress (Das
236 et al., 2017), which complicates genetic analysis of lifespan as animals lacking either *daf-*
237 *16* or *hpk-1* also have impaired survival to thermal stress. To more rigorously decipher
238 the genetic interactions between *hpk-1, daf-16* and reduced ILS we repeated these RNAi
239 experiments under basal temperatures (20°C). We found *hpk-1(RNAi)* had only a mild
240 detrimental effect on *daf-2(e1370)* lifespan; in wild-type and *daf-2(e1370);daf-*
241 *16(mgDf47)* similar results were found between 20 and 25°C (*Figure Supplement 3D-F*,
242 and *Supplementary File 1*), which suggests HPK-1 and DAF-16 have overlapping
243 longevity functions, and decreased ILS extends longevity independently from HPK-1
244 functions outside of the nervous system.

245 Based on the extensive neuronal overlap in co-expression between *daf-16* and
246 *hpk-1*, and previous findings suggesting ILS functions within the nervous system to
247 regulate longevity (Apfeld and Kenyon, 1998; Wolkow et al., 2000), we revisited whether
248 *hpk-1* and ILS genetically intersect. The nervous system of *C. elegans* is largely refractory
249 to RNAi, as these cells do not express *sid-1*, which is necessary for dsRNA transport in
250 neurons (Kamath et al., 2003; Timmons et al., 2001; Winston et al., 2002). Enhanced
251 neuronal RNAi is obtained by ectopic neuronal expression of *sid-1* (Calixto et al., 2010),

252 which we next explored in greater detail. We assessed lifespan in transgenic animals
253 overexpressing *hpk-1* in a neuronal enhanced RNAi background (i.e., *unc-119p::sid-*
254 *1::YFP; eri-1(mg366)*; *hpk-1(oe)*) and (*Supplementary File 1*). The combination of
255 inactivating *daf-2* within the nervous system and overexpression of *hpk-1* failed to further
256 increase lifespan (p-value = 0.2, *Figure Supplement 3G*). Collectively, these results
257 suggest neuronal HPK-1 share overlapping mechanisms of longevity control with
258 decreased ILS and activated DAF-16 to extend longevity.

259 ***hpk-1* is the most broadly upregulated kinase during normal aging**

260 We were surprised to find that *hpk-1* mRNA expression increased during aging, as
261 kinase regulation at the level of gene expression seemed atypical. Therefore, using the
262 *C. elegans* Aging Atlas dataset we assessed whether any of the 438 *C. elegans* kinases
263 (Zaru et al., 2017) are differentially expressed during aging: 115 kinases are upregulated
264 and conversely 120 are downregulated in at least one cell cluster, while 254 kinases do
265 not change expression (*Figure supplement 4, Supplementary File 5*). *hpk-1* is upregulated
266 in more cell-clusters than any other kinase, while *hpk-1* is upregulated in 48, the next
267 most broadly upregulated kinase is *gcy-28* (38 cell-clusters), which encodes the ortholog
268 of natriuretic peptide receptor 1 and is involved in chemotaxis, olfactory behavior, and
269 sensory perception (Li and van der Kooy, 2018; Shinkai et al., 2011; Tsunozaki et al.,
270 2008). During normal aging, only 14 kinases are downregulated in 10 or more cell-
271 clusters (see Appendix 2). Only 20 kinases are upregulated in ten or more cell-clusters
272 (*Figure 2G-figure supplement 4*). In addition to *hpk-1* and *gcy-28*, five other kinases that
273 have previously been linked to longevity are also broadly upregulated during normal
274 aging: *nipi-3* (a Tribbles pseudokinase that positively regulates SKN-1 (Wu et al., 2021),

275 *aak-1* (AMP-activated kinase catalytic subunit alpha-2) (Lee et al., 2009), *scd-2* (ALK
276 receptor tyrosine kinase) (Shen et al., 2007), *rsks-1* (ribosomal protein S6 kinase)
277 (Hansen et al., 2007; Pan et al., 2007), and *smg-1* (SMG1 nonsense mediated mRNA
278 decay associated PI3K related kinase) (Masse et al., 2008). We previously demonstrated
279 that HPK-1 is an essential component of TORC1-mediated longevity and autophagy (Das
280 et al., 2017). Interestingly we find that only two of 11 TOR-associated genes: *rsks-1* and
281 *aak-1,* are upregulated during aging in three or more cell-clusters (Blackwell et al., 2019;
282 Hindupur et al., 2015; Pan et al., 2007). We find *rsks-1* is exclusively upregulated outside
283 of the nervous system and has poor overlap with *hpk-1* (2/13). *aak-1* is primarily but not
284 exclusively upregulated outside of the nervous system during aging, with some overlap
285 with *hpk-1*. In future studies it will be interesting to dissect whether HPK-1 intersects with
286 these components of TORC1 signaling within and/or outside of the nervous system.

287 **HPK-1 preserves integrity of the *C. elegans* nervous system.**

288 Based on the neuronal HPK-1 capacity to promote longevity, we sought to
289 determine whether HPK-1 preserves the anatomy and physiology of the nervous system
290 during aging. To assess age-associated changes in neuroanatomy of ventral and dorsal
291 cord motor neurons (VD and DD), we used the *unc-25p::GFP* cell-specific reporter (*Figure*
292 *3A*) (Cinar et al., 2005; Kraemer et al., 2003). Aged populations of *hpk-1* mutant animals
293 displayed more than a 3-fold difference in VD axonal breaks and more than a 2-fold
294 difference in DD axonal breaks compared to wild type animals (*Figure 3A-B, D*). These
295 age-associated breaks could be rescued by neuronal expression of *hpk-1* (*Figure 3C*).
296 Importantly, young wild-type and *hpk-1* mutant animals did not show neuronal breaks

297 (*Figure 3B*). Thus, loss of *hpk-1* does not disrupt axon formation during development,
298 rather HPK-1 preserves axonal integrity in aging motor neurons.

299 In *C.*
300 *elegans,* locomotion is
301 controlled by
302 acetylcholine-releasing
303 excitatory motor neurons
304 and GABA (γ-
305 aminobutyric acid)-
306 releasing-inhibitory
307 motor neurons
308 (Jorgensen and Nonet,
309 1995; Richmond and
310 Jorgensen, 1999). Thus,
311 locomotion is a useful
312 readout to assess
313 neurotransmission. To
314 examine the role of *hpk-*
315 *1* in synaptic
316 transmission, we
317 performed a paralysis
318 assay after
319 acetylcholinesterase

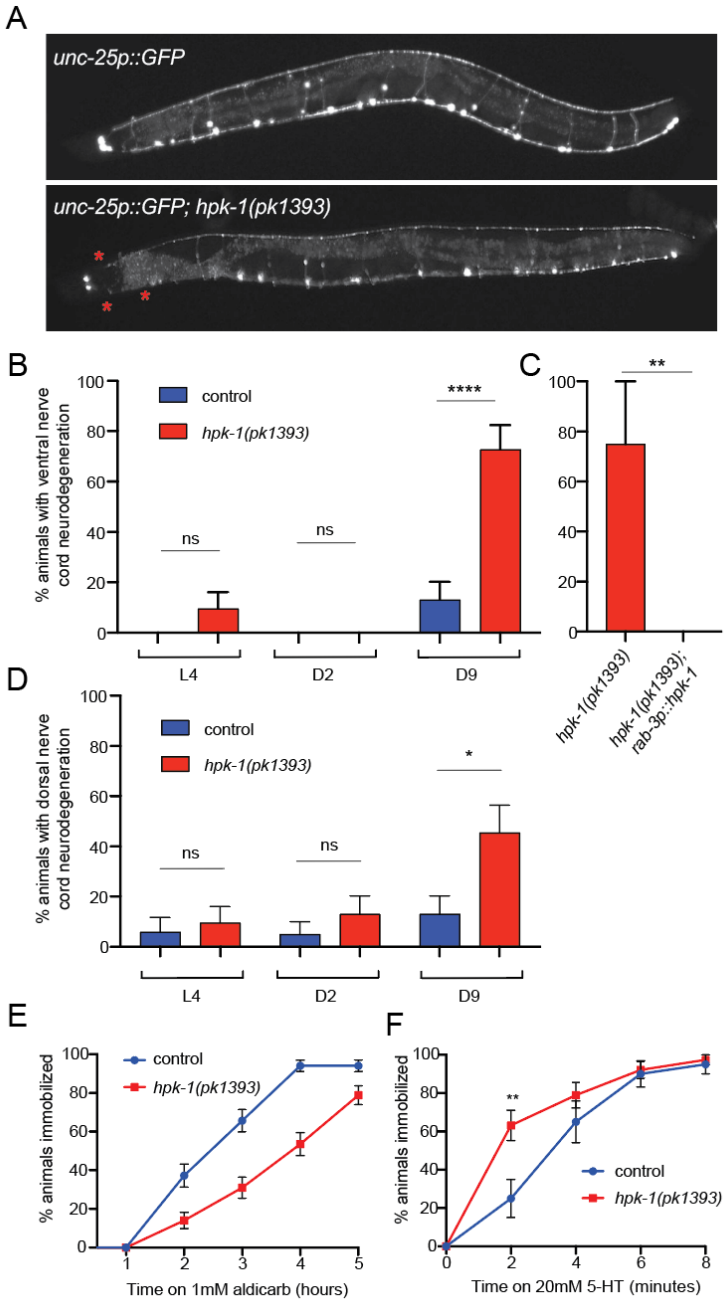

Figure 3. Neuronal HPK-1 maintains neuronal integrity during aging.
(A) Fluorescent micrographs of control and *hpk-1(pk1393)* 9 day old animals expressing GFP in GABAergic DD and VD motor neurons. Asterisks (*) indicate axonal breaks in the motor neurons. **(B)** Percentage of wild type and *hpk-1* mutant animals with neurodegeneration in VD motor neurons (n≥23). **(C)** Percentage of *hpk-1* rescue animals with neurodegeneration in VD motor neurons (n≥10). **(D)** Percentage of wild type and *hpk-1* mutant animals with neurodegeneration in DD motor neurons (n≥20). Percentage of immobilized animals after exposure to aldicarb (n≥67) **(D)** and to 20mM 5-HT (n≥38) **(E)**. *T* test analysis with $^{**}P < 0.01$ and $^{***}P < 0.001$. See *Supplementary Files 6, 7 and 8* for details and additional trials.

320 inhibition with aldicarb, where mutations that impair cholinergic signaling cause a
321 reduction in rate of paralysis (Mahoney et al., 2006; Oh and Kim, 2017). Therefore,
322 mutants with lower synaptic transmission undergo reduced paralysis (i.e., animals are
323 resistant), while mutants with higher synaptic transmission exhibit greater sensitivity.
324 Interestingly, *hpk-1* mutants showed increased aldicarb resistance by L4/YA (*Figure 3E*),
325 suggesting that loss of *hpk-1* reduces cholinergic synaptic transmission and that HPK-1
326 normally preserves neuronal function.

327 *C. elegans* serotonin (5-HT) signaling in conjunction with dopamine (DA)
328 modulates locomotion; animals treated with exogenous 5-HT exhibit paralysis over time.
329 In a paralysis assay with exogenous 5-HT, we observed that late L4/YA *hpk-1* mutant
330 animals paralyzed sooner: at 2 minutes of 5-HT treatment, 63% of mutants were
331 immobilized compared to 25% of wild type animals immobilized (*Figure 3F*). Based on
332 the aforementioned findings, we conclude that HPK-1 prevents an age-associated decline
333 in axonal and synaptic integrity.

334 **Loss of *hpk-1* results in neuronal dysregulation of neuronal gene expression**

335 We sought to gain deeper insight into how loss of *hpk-1* negatively impacted the
336 *C. elegans* nervous system. To identify early transcriptional dysregulation events that
337 occur due to the absence of *hpk-1*, we conducted bulk RNA-sequencing of day 2 adult
338 wild-type and *hpk-1(pk1393)* null mutant animals, an age at which axonal breaks have
339 yet to occur (*Figure 3B, D*), but after neuronal function has begun to decline (*Figure 3E,*
340 *F*). Differential expression analysis identified 2201 total genes with significant expression
341 changes with loss of *hpk-1*, 1853 upregulated and 348 downregulated (adjusted p-value
342 < 0.05 and $\log_2$ foldchange magnitude ≥ 1) (*Figure 4A* and *Supplementary File 9*).

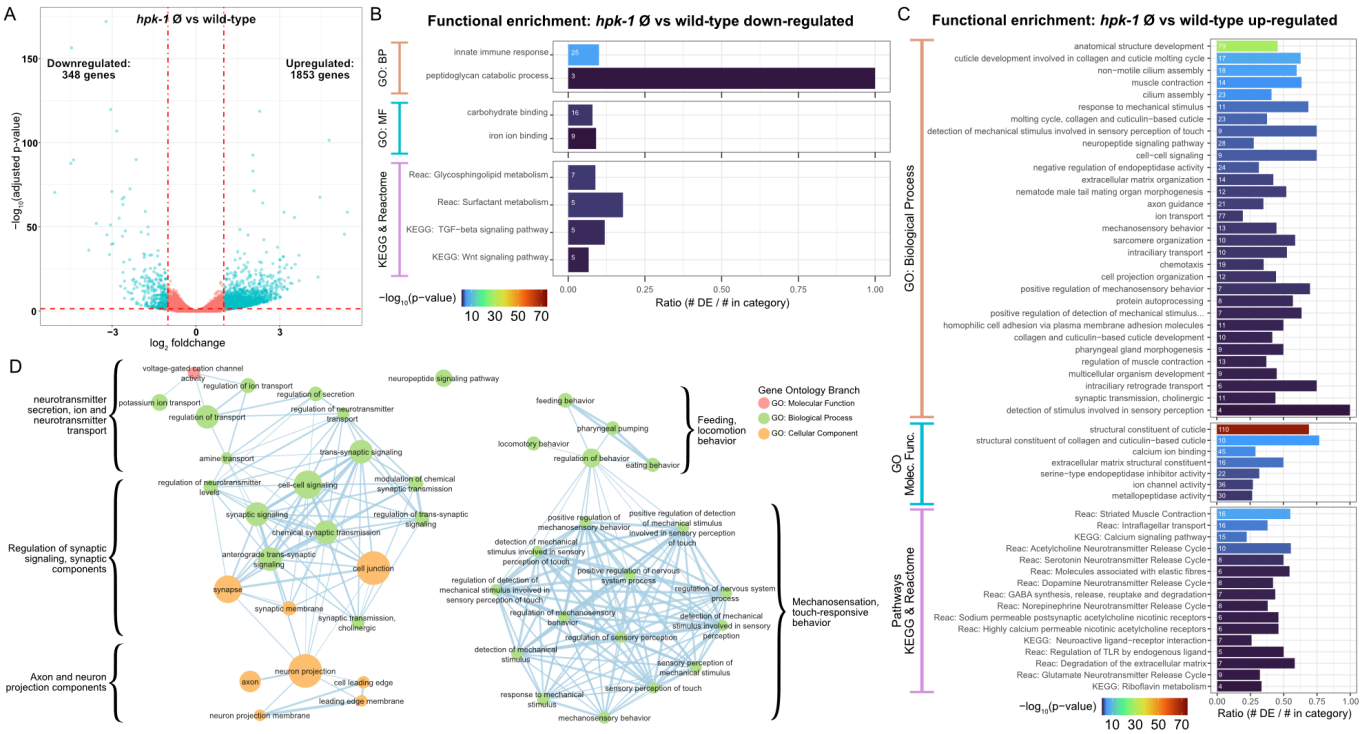

Figure 4. Loss of *hpk-1* results in broad dysregulation of neuronal gene expression.
(A) Differential expression analysis for RNA-Seq of day 2 adult *hpk-1* null mutant animals (n=3) compared to N2 wild-type animals (n=3) identified 2,201 genes with significantly altered expression with loss of *hpk-1* (adjusted p-value < 0.05 and $|\log_2$ foldchange$| \geq 1$), 84% of which were upregulated in the mutants. The volcano plot illustrates the criteria applied for selecting genes with significant and substantial expression changes, shown as blue dots: vertical dashed lines are the foldchange threshold and the horizontal dashed line is the p-value threshold. **(B, C)** Enrichment for functions and pathways associated with the 348 downregulated genes **(B)** or the 1853 upregulated genes **(C)** in *hpk-1* animals yields innate immune response as the most significantly over-represented term for downregulated genes, but reveals a large number of significant associations to pathways and processed for the upregulated genes- many of which are associated with neurons and neuronal signaling. Each bar represents a functional term or pathway from the Gene Ontology (GO), KEGG, or Reactome databases, as indicated. Bar colors show the $-\log_{10}$ transformed enrichment p-value. The number in each bar is the size of the overlap between the set of differentially expressed genes and the genes in the term or pathway. The x-axis indicates the fraction of the total genes in the term or pathway that were differentially expressed. All results shown have significant enrichment after adjustment for multiple testing. **(D)** Functional enrichment for 283 genes upregulated with *hpk-1* loss that are specific to, or enriched in, *C. elegans* neurons shows broad dysregulation of functions associated with neurons including neurotransmitter transport and release, cell-cell junctions, axons, neuropeptides, and sensory processes, among others. 880 genes uniquely expressed or significantly enriched in neurons were derived from bulk tissue-specific RNA-Seq profiling results in (Kaletsky et al., 2018) and 32% of these are significantly upregulated in *hpk-1* null animals. See *Supplementary Files 9 and 10* for dataset and additional analysis.

Functional enrichment with over-representation analysis was performed for the up- and down-regulated genes separately (GOSeq, adjusted p-value < 0.01). Among down-regulated genes, we find 25 genes implicated in the innate immune response, as well as TGF-beta and WNT signaling (five ubiquitin ligase complex component genes), glycosphingolipid metabolism, and surfactant metabolism. (*Figure 4B*). By contrast, more than 50 GO terms and pathways were enriched for the upregulated genes. The most significantly enriched single term reveals a substantial number of cuticle and collagen

350 associated genes as dysregulated (*Figure 4C*). Upregulation of some collagens and
351 ECM-remodeling processes have been associated with longevity in *C. elegans* (Ewald et
352 al., 2015; Rahimi et al., 2022). Alternatively, aberrant upregulation could lead to stiffening
353 of the cuticle, a hallmark of aged *C. elegans* and some progeric mutants (Ewald et al.,
354 2015; Rahimi et al., 2022).

355 A striking number of other functions significantly enriched in the *hpk-1* upregulated
356 genes from across GO, KEGG, and Reactome are related to neuronal function and
357 signaling, including: neuropeptide and neurotransmitter pathways, mechanosensation,
358 chemotaxis, and axon guidance, among others (*Figure 4C*). To explore further, we looked
359 at the *hpk-1* null upregulated genes in the context of a curated compendium of genes with
360 functions that are important for the nervous system (Hobert, 2013), as well as genes
361 identified as uniquely expressed in neurons or significantly enriched in neurons from
362 tissue-specific bulk RNA-Seq (Kaletsky et al., 2018).

363 Among 1496 genes known, or expected through homology, to function in the
364 nervous system, 264 are upregulated with loss of *hpk-1*, representing a much larger
365 overlap than expected by chance (hypergeometric test p-value < 0.0001) (*Supplementary*
366 *File 10*). Genes with higher fold-change of expression in *hpk-1* mutants were associated
367 with ciliated sensory neurons (motor proteins, sensory cilia transport), calcium binding,
368 and neuropeptides. We find that 55 of these neuron-associated genes are normally
369 upregulated with age in wild-type animals in at least one cell cluster in the *C. elegans*
370 Aging Atlas, 87 are downregulated with age, with the remaining having mixed or no
371 significant age-associated changes. This suggests that while loss of *hpk-1* results in

372 expression of some genes associated with aging, the bulk of differentially expressed
373 genes at day 2 of adulthood are consistent with dysregulation of neuronal gene
374 expression. Refined genetic perturbation within the nervous system coupled with single
375 cell RNA-sequencing over time would be required to fully reveal the impact of HPK-1
376 function on age-associated changes in gene expression.

377 We next investigated how many of these genes are predominantly- or exclusively-
378 expressed in neurons, based on a set of 880 neuron-enriched and neuron-specific genes
379 (Kaletsky et al., 2018). We found that 15% of all *hpk-1* upregulated genes are enriched
380 or specific to neurons in wild-type animals (283 genes, hypergeometric test p-value <
381 0.0001) whereas only five *hpk-1* down-regulated genes normally exhibit such neuron-
382 restricted expression. To determine what functions are over-represented among the
383 upregulated neuronally expressed genes, we ran Gene Ontology enrichment analysis.
384 Representing these results as a network, and clustering terms which have overlapping
385 gene associations, we identified some major themes: neurotransmitter and ion transport,
386 synaptic components and signaling, axon and neuron projection components, feeding
387 and locomotion behavior, mechanosensation and touch-responsive behavior are all
388 upregulated in the absence of *hpk-1* (*Figure 4D*). Among all genes upregulated in the
389 *hpk-1* null mutants, the largest group correspond to genes related to neuropeptide
390 encoding, processing and receptors. Neuropeptides are short sequences of amino acids
391 important for neuromodulation of animal behavior, broadly expressed in sensory, motor
392 and interneurons. Of the 120 neuropeptide-encoding genes in the *C. elegans* genome,
393 40 (33%) are upregulated in the *hpk-1* null mutants. Nine of these are insulin-related (*ins*),
394 which suggest increased *hpk-1* expression during normal aging or *hpk-1* overexpression

395 may positively affect longevity through decreased *ins* neuropeptide expression. We
396 surmise that many of the neuronal genes that are induced in the absence of *hpk-1* might
397 be compensatory responses to maintain neuronal function. We describe the major types
398 of neuronal processes with increased expression in *hpk-1* null mutant animals in greater
399 detail in Appendix 3, and assess whether loss of *hpk-1* disrupts proteostasis within the
400 nervous system in the next section.

401 **Neuronal HPK-1 regulates proteostasis cell intrinsically and cell non-**
402 **autonomously via neurotransmission.**

403 We hypothesized that HPK-1 maintains neuronal function by fortifying the neural
404 proteome. We measured polyglutamine toxic aggregate formation in neuronal cells (*rgef-*
405 *1p::Q40::YFP*) of animals overexpressing *hpk-1* pan-neuronally (*rab-3p*). These animals
406 showed decreased number of fluorescent foci within the nerve ring (*Figure 5Ai - iii, B*). To
407 assess whether this was associated with improved neuronal function, we assessed
408 alterations in locomotion capacity (body bends) after placement in liquid. Increased
409 neuronal expression of *hpk-1* significantly increased the average number of body bends
410 (17.7 ± 1 vs 12.5 ± 1.2 bends/30sec), suggesting that neuronal expression of *hpk-1*
411 improves proteostasis in the nervous system and mitigates locomotion defects associated
412 with the decline in proteostasis (*Figure 5C*).

413 We next tested whether HPK-1 was necessary to preserve proteostasis within
414 neurons. We crossed the *rgef-1::Q40::YFP* reporter with neuronal enhanced RNAi
415 background (*sid-1(pk3321);unc-119p::sid-1*) and assessed whether neuronal inactivation
416 of *hpk-1* hastened age-associated proteostatic decline. Animals with neuronal *hpk-1*
417 inactivation had a significant increase in foci number within neurons and a decreased

418 number of body bends in liquid (19.7 ± 0.8 vs 25.5 ± 1.1 bends/30sec) (*Figure 5Aiv, D,*
419 *E*). Thus, HPK-1 functions cell intrinsically to maintain neuronal proteostasis.

420 We next assessed whether neuronal HPK-1 activates a cell non-autonomous
421 signal to regulate proteostasis in distal tissues. We used a proteostasis reporter
422 expressed exclusively in muscle tissue (*unc-54p::Q35::YFP*); animals display an age-
423 associated accumulation of fluorescent foci, which are proteotoxic aggregates, and
424 become paralyzed as muscle proteome function collapses (Lazaro-Pena et al., 2021;
425 Morley et al., 2002). Animals with increased neuronal *hpk-1* expression had significantly
426 decreased fluorescent foci in muscle tissue (*Figure 5Fi-ii*). For instance, at day 3 of
427 adulthood, animals overexpressing neuronal HPK-1 had an average of 21 ± 0.9 polyQ
428 aggregates, while control animals had an average of 26 ± 1.1 polyQ aggregates (*Figure*
429 *5G*). In *C. elegans*, the age-related progressive proteotoxic stress of muscle polyQ
430 expression is pathological and results in paralysis. Of note, increased *hpk-1* expression
431 in neurons was sufficient to reduce paralysis; at day 13 of adulthood only 61% ± 0.10 of
432 neuronal *hpk-1* overexpressing animals were paralyzed compared to 81% ± 0.08 of
433 paralyzed control animals (*Figure 5H*). Thus, increased neuronal HPK-1 activity is
434 sufficient to improve proteostasis cell non-autonomously.

435 We confirmed that the kinase activity is essential for HPK-1 to improve
436 proteostasis. We find the kinase domain of HPK-1 is highly conserved from yeast to
437 mammals, both at the amino acid level and predicted tertiary structure, based on multiple
438 sequence alignments, AlphaFold structure prediction, and visualization with PyMol
439 (*Figure supplement 5*) (DeLano, 2002; Jumper et al., 2021; Varadi et al., 2022). We
440 mutated two highly conserved residues within the kinase domain, K176A and D272N,

441 which are known to be essential for the kinase activity of HPK-1 orthologs (He et al.,

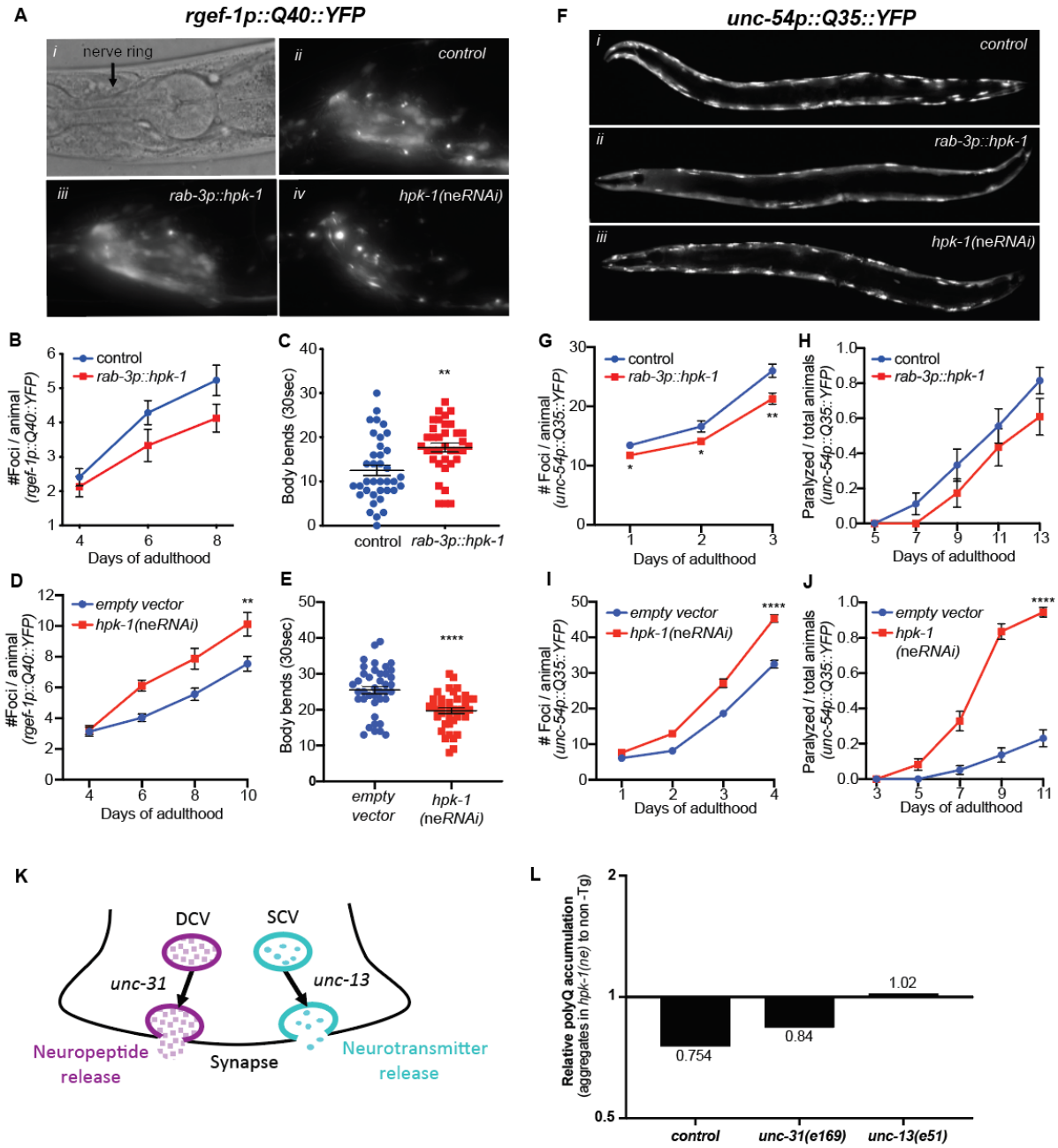

Figure 5. Neuronal HPK-1 prevents the decline in proteostasis through neurotransmitter release.
(A) Nomarski (*i*) and fluorescent (*ii-iv*) micrographs of animals expressing polyglutamine fluorescent reporter within the nervous system. (**B** and **C**) Quantification of foci in the nerve ring (B) and body bend frequency (C) (n≥21 for B and n≥36 for C). (**D** and **E**) Quantification of foci in the nerve ring (D) and frequency of body bends (E) in neuronal enhanced RNAi animals (n≥19 for D and n≥39 for E). **(F)** Fluorescent micrographs of animals expressing the polyglutamine fluorescent reporter in muscle. (**G** and **H**) Quantification of foci in muscle (G) and paralysis rate (H). Graphs are representative of 5 individual transgenic lines (n≥18 for G and n≥23 for H). (**I** and **J**) Quantification of foci in muscle (I) and paralysis rate (J) in neuronal enhanced RNAi animals (n≥22 for I and n≥73 for J). **(K)** Neuropeptides and neurotransmitters are essential for neuronal signaling; vesicle release depends on *unc-31* and *unc-13*, respectively. (**L**) Quantification of relative *polyQ* fluorescent foci in muscle cells after *rab-3p::hpk-1* overexpression in control, *unc-31(e169)* and *unc-13(e51)* animals; see *figure supplement 6* for absolute values. *T* test analysis with $^{**}P < 0.01$ and $^{***}P < 0.001$. See *Supplementary Files 11, 2, and 12* for details and additional trials.

442 2010), and tested whether these kinase-dead mutant versions could improve proteostasis
443 when neuronally overexpressed. In contrast to wild-type HPK-1 (*Figure 5G, H*), neither
444 mutant had any effect on either polyglutamine foci accumulation (*Figure supplement 5C,*
445 *D*) or paralysis (*Figure supplement 5E, F*) in muscle cells (*unc-54p::Q35::YFP*); thus,
446 increased *hpk-1* expression improves proteostasis through kinase activity.

447 We tested whether neuronal HPK-1 is required for maintaining proteostasis in
448 distal muscle cells. Neuronal inactivation of *hpk-1* (*sid-1(pk3321); unc-119p::sid-1; unc-*
449 *54p::Q35::YFP; hpk-1(RNAi)*) was sufficient to hasten the collapse of proteostasis,
450 significantly increasing the number of polyQ aggregates (45 $\pm$ 1 vs 32 $\pm$ 1.1 at day 4) and
451 paralysis rate (84% $\pm$ 0.04 vs 14% $\pm$ 0.04 at day 9) (*Figure 5Fiii, I, J*). Thus, HPK-1 function
452 within the nervous system impacts proteostasis in distal muscle tissue, which implies that
453 HPK-1 coordinates organismal health through cell non-autonomous mechanisms.

454 To identify the signaling mechanism through which HPK-1 regulates distal
455 proteostasis, we tested whether either neuropeptide or neurotransmitter transmission are
456 essential for cell non-autonomous regulation of proteostasis (using *unc-31* and *unc-13*
457 mutant animals, respectively *Figure 5K*). Neuronal expression of *hpk-1* in *unc-31* mutants
458 improved proteostasis in the absence of neuropeptide transmission and dense core
459 vesicles, as increased neuronal *hpk-1* expression still delayed the age-associated
460 accumulation of aggregates within muscle cells. In contrast, in the absence of
461 neurotransmitter function, neuronal expression of *hpk-1* in *unc-13* mutants failed to
462 improve proteostasis in muscle tissue (*Figure 5L- see figure supplement 6*). We conclude
463 that HPK-1 mediated longevity-promoting cell non-autonomous signaling occurs through
464 neurotransmission.

465 **Neuronal HPK-1 induces molecular chaperones and autophagy in distal tissues.**

466 We sought to identify the components of the PN that are cell non-autonomously
467 regulated via HPK-1 activity in the nervous system. We tested whether increasing levels
468 of neuronal *hpk-1* alters the expression of molecular chaperones (*hsp-16.2p::GFP*).
469 Increased neuronal expression of *hpk-1* in wild type animals did not alter the basal
470 expression of molecular chaperones (*Figure 6A*). In contrast, after heat shock, increased
471 neuronal *hpk-1* expression resulted in hyper-induction of *hsp-16.2p::GFP* expression,
472 particularly in the pharynx and head muscles, but surprisingly not within intestinal cells
473 (*Figure 6B-E*). We conclude that while *hpk-1* is required for the broad induction of

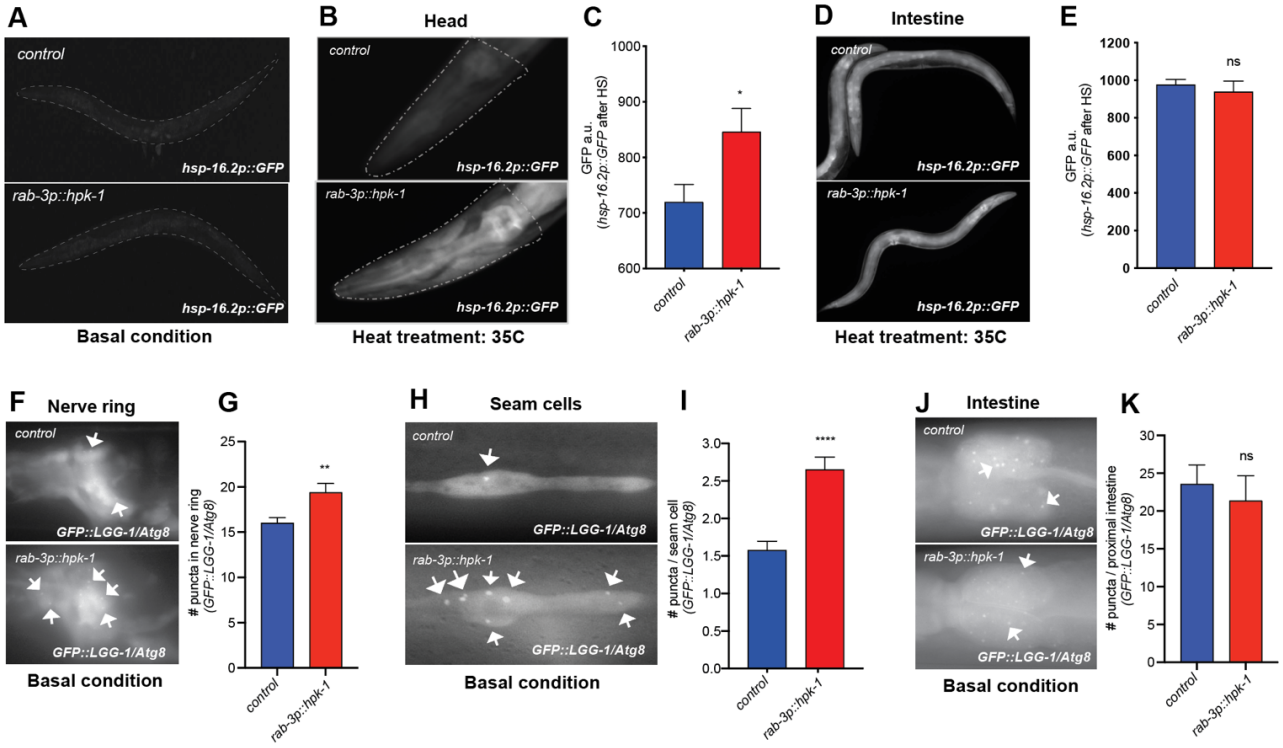

Figure 6. Neuronal HPK-1 induces the proteostatic network in distal tissues.
(**A**) Fluorescent micrographs of animals expressing *hsp-16.2p::GFP* in basal conditions. (**B** and **C**) Fluorescent micrographs (B) and fluorescent density quantification (C) of control and *rab-3p::hpk-1* day 1 adult animals expressing *hsp-16.2p::GFP* after heat shock (35°C) for 1 hour at (n≥15). (**D** and **E**) Fluorescent micrographs and densitometry quantification of the intestinal fluorescence of *hsp-16.2p::GFP* after heat shock (n≥24). (**F** and **G**) Fluorescent micrographs and quantification of fluorescent puncta in the nerve ring of control and *rab-3p::hpk-1* L4 animals expressing *rgef-1p::GFP::LGG-1/Atg8* (n≥21). (**H** and **I**) Fluorescent micrographs (H) and quantification (I) of puncta in seam cells of control and *rab-3p::hpk-1* animals expressing *lgg-1p::GFP::LGG-1/Atg8* (n≥43). (**J** and **K**) Fluorescent micrographs (J) and quantification (K) of puncta in proximal intestinal cells of control and *rab-3p::hpk-1* animals expressing the *lgg-1p::GFP::LGG-1/Atg8* autophagosome reporter (n≥17). *T*-test analysis with **P* < 0.05, ***P* < 0.01, ****P* < 0.001 and *****P* < 0.0001. See *Supplementary Files 13 and 14* for details and additional trials.

474 molecular chaperones (Das et al., 2017), neuronal HPK-1 primes inducibility of the HSR
475 within specific tissues, rather than in a systemic manner throughout the organism.

476 We next tested whether increased neuronal HPK-1 activity is sufficient to induce
477 autophagy. Using two LGG-1/Atg8 fluorescent reporter strains to visualize
478 autophagosome levels in neurons (*rgef-1p::GFP::LGG-1),* hypodermal seam cells and
479 intestine (*lgg-1p::GFP::LGG-1)* (Kumsta et al., 2017), we found that increased neuronal
480 *hpk-1* expression significantly induces autophagy in neurons and hypodermal seam cell
481 (*Figure 6F-I*), but not in the intestine (*Figure 6J, K*). Sustained autophagy and
482 transcriptional activation of autophagy genes are important components for somatic
483 maintenance and organismal longevity (Lapierre et al., 2015). Consistently *hpk-1* is
484 required for the induction of autophagy gene expression induced by TORC1 inactivation
485 (Das et al., 2017). Thus, increased HPK-1 activity within the nervous system is sufficient
486 to induce basal levels of autophagy both cell-intrinsically and non-autonomously, which
487 likely extends longevity.

488 **GABAergic and Serotonergic HPK-1 differentially regulate longevity and acute**
489 **stress signaling.**

490 *hpk-1* is broadly expressed within the *C. elegans* adult nervous system (Das et al.,
491 2017), but the neuronal cell-types responsible for extending longevity are unknown. We
492 overexpressed *hpk-1* in different subtypes of neurons and assessed changes in muscle
493 proteostasis (*unc-54p::Q35::YFP*). Increased *hpk-1* expression in glutamatergic or
494 dopaminergic neurons was not sufficient to decrease the formation of fluorescent foci or
495 reduce paralysis (*Figure supplement 7*), suggesting that HPK-1 does not act within these
496 neuronal subtypes to cell non-autonomously regulate proteostasis. In contrast, increased

497 expression of *hpk-1* in either serotonergic (*tph-1p::hpk-1*) or GABAergic (*unc-47p::hpk-1*)
498 neurons was sufficient to improve proteostasis in muscle tissue (*Figure 7A-D*).
499 Accordingly, we found that *hpk-1* is expressed in serotonergic and GABAergic neurons,
500 based on colocalization between *hpk-1* and neuronal cell-type specific reporters (*Figure*
501 *7E, F -see figure supplement 8*), consistent with the notion that HPK-1 initiates pro-
502 longevity signals from these neurons.

503 We sought to determine whether signals initiated from serotonergic and
504 GABAergic neurons induced similar or distinct components of the PN in distal tissues,
505 and assessed the overall consequence on organismal health. Since pan-neuronal

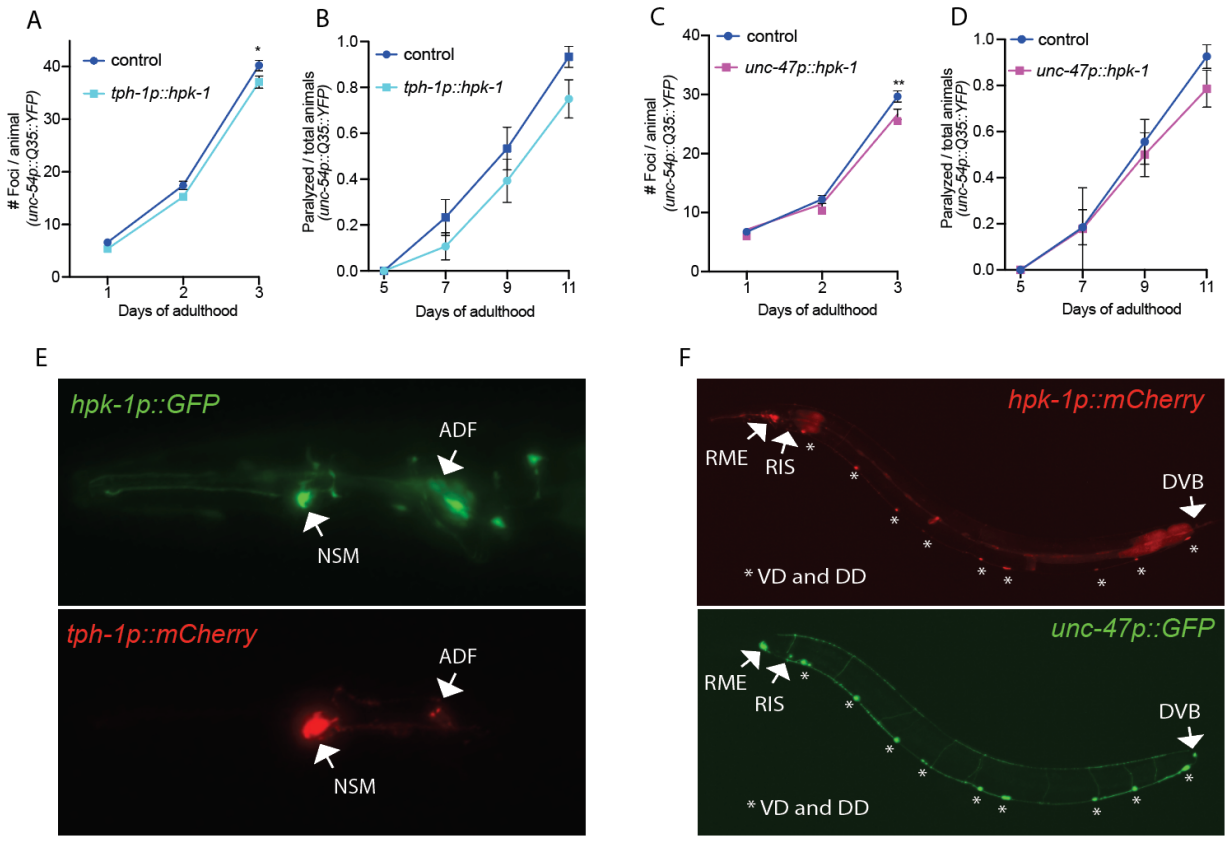

Figure 7. Expression of HPK-1 in serotonergic and GABAergic prevents the decline in proteostasis in muscle tissue.
(A and **B)** Quantification of foci (A) and paralysis rate (B) of animals expressing *hpk-1* in serotonergic neurons (n≥17 for A and n≥28 for B). **(C** and **D)** Quantification of foci (C) and paralysis rate (D) of animals expressing *hpk-1* in GABAergic neurons (n≥19 for C and n≥27 for D). **(E)** Representative fluorescent micrographs of *hpk-1* expression in serotonergic neurons. **(F)** Representative fluorescent micrographs of *hpk-1* expression in GABAergic neurons. *T* test analysis performed to each time point with $^{*}P < 0.05$ and $^{**}P < 0.01$. See *Supplemental Files 11 and 12* for details and additional trials.

506 expression of *hpk-1* was sufficient to induce autophagy, improve thermotolerance, and

507 increase lifespan, we chose to dissect whether these three phenotypes were regulated

508 within distinct neuronal cell-types. Increased HPK-1 serotonergic signaling was sufficient

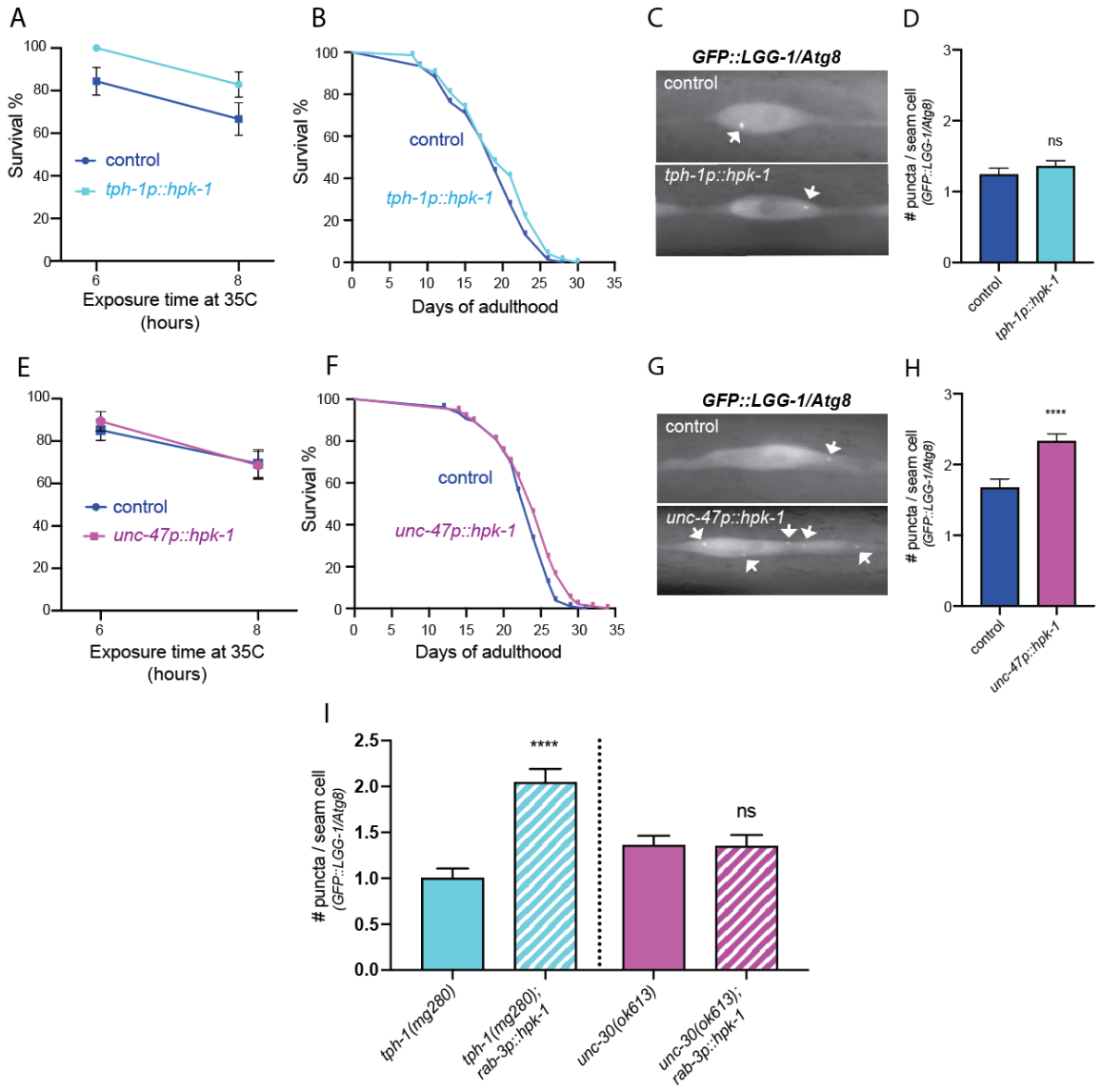

Figure 8. Serotonergic and GABAergic HPK-1 signaling activates distinct adaptive responses to regulate stress resistance and longevity.
(A) Survival of serotonergic HPK-1 expressing day 1 adult animals after heat shock (n≥32). **(B)** Lifespan of serotonergic HPK-1 expressing animals (n≥76). **(C** and **D)** Representative fluorescent micrographs (C) and quantification (D) of autophagosomes in hypodermal cells of serotonergic HPK-1 day 1 adult animals (n≥80). **(E)** Survival of GABAergic HPK-1 expressing day 1 adult animals after heat shock (n≥47). **(F)** Lifespan of GABAergic HPK-1 expressing animals (n≥119). **(G** and **H)** Representative fluorescent micrographs (G) and quantification of autophagosomes in hypodermal cells of GABAergic HPK-1 day 1 adult animals (n≥64). **(I)** Quantification of autophagosomes in hypodermal cells of mutant animals of serotonin and GABAergic signaling (*tph-1* and *unc-30*, respectively), expressing pan-neuronal *hpk-1* (day 1 adults, n≥ 67). *T* test analysis with **P* < 0.05, ***P* < 0.01 and *****P* < 0.0001. See *Supplementary Files 1, 3 and 14* for details and additional trials.

509 to improve thermotolerance, without altering lifespan or autophagy (*Figure 8A-D*). In
510 contrast, increased *hpk-1* expression in GABAergic neurons did not alter
511 thermotolerance, but induced autophagy and slightly but significantly increased lifespan
512 (*Figure 8E-H*).

513 To identify the mechanism through which increased neuronal HPK-1 activity
514 induces autophagy in distal tissues, we examined serotonergic neurons. As expected,
515 loss of *tph-1,* which encodes the *C. elegans* tryptophan hydroxylase 1 essential for
516 biosynthesis of serotonin (Sze et al., 2000), failed to block the induction of autophagy by
517 increased neuronal *hpk-1* expression (*Figure 8I*, *tph-1(mg280);rab-3p::hpk-1*). *unc-30*
518 encodes the ortholog of human paired like homeodomain 2 (PITX2) and is essential for
519 the proper differentiation of type-D inhibitory GABAergic motor neurons (Jin et al., 1994;
520 McIntire et al., 1993). Consistent with our previous result demonstrating that only
521 GABAergic expression of *hpk-1* promotes autophagy, loss of *unc-30* was sufficient to
522 completely abrogate the induction of autophagy in seam cells after increased pan-
523 neuronal expression of *hpk-1* (*Figure 8I*, *unc-30(ok613);rab-3p::hpk-1*). We conclude that
524 HPK-1 activity in serotonergic neurons promotes systemic thermotolerance, whereas
525 HPK-1 in GABAergic neurons promotes autophagy. We surmise that the two neuronal
526 subtypes are likely to contribute synergistically to the extension of longevity.

527 We sought to fortify our previous findings that: 1) TORC1 negatively regulates *hpk-*
528 *1* under basal conditions; 2) *hpk-1* is essential for decreased TORC1 signaling to increase
529 longevity and induce autophagy; and 3) HPK-1-mediated longevity requires *mxl-2*, the
530 ortholog of mammalian Mlx transcription factor (Das et al., 2017). From these data, we
531 predicted that TOR-mediated longevity might require *mxl-2* via *hpk-1.* Indeed, we find that

532 inactivation of either *daf-15* (Raptor) or *let-363* (TOR), increased lifespan and required
533 *mxl-2*, as *mxl-2(tm1516)* null mutant animals failed to increase lifespan in the absence of
534 TORC1 (*Figure Supplement 9*). MXL-2 functions as a heterodimer with MML-1 (Pickett et
535 al., 2007), which have similar roles in *C. elegans* longevity (Johnson et al., 2014).
536 Interestingly, one of the human homologs of MML-1, Carbohydrate Response Element
537 Binding Protein (ChREBP/MondoB/MLXIPL/WBSCR14), maps within a deleted region in
538 Williams-Beuren Syndrome patients, which among other symptoms causes metabolic
539 dysfunction, silent diabetes, and premature aging (Pober, 2010). This further supports
540 our model and is consistent with other studies linking the Myc-family of transcription
541 factors to longevity, autophagy, and TORC1 signaling (Johnson et al., 2014; Nakamura
542 et al., 2016; Samuelson et al., 2007). Collectively, we conclude that HPK-1 regulates
543 serotonergic signals to improve survival in acute thermal stress, likely through HSF-1, and
544 initiates GABAergic signals to extend longevity through increased autophagy, which is
545 linked to decreased TORC1 signaling and regulation of the Myc TFs.

546 **Discussion**

547 It has been known that a core group of TFs integrates various types of metabolic
548 and stress signals; moreover, this group of TFs can extend longevity when
549 overexpressed, and conversely hasten aging when lost (reviewed in (Denzel et al.,
550 2019)), but whether the activity or expression of these longevity-associated transcriptional
551 regulators are activated by signals of increasing damage or dysfunction during normal
552 aging was unknown. Recently, single-cell RNA sequencing has revealed that these
553 longevity-associated TFs increase in expression during aging in wild-type animals across
554 multiple somatic tissues (Roux et al., 2022). This comprehensive empirical dataset

555 provides foundational support for a key theme in aging research: during aging in wild-type
556 animals, increasing damage and dysfunction is mitigated by the activation of stress
557 response programs. Our findings that: 1) *hpk-1* expression is upregulated during normal
558 aging in more neurons and non-neuronal cells than any other kinase, and 2) that *hpk-1* is
559 co-expressed in cell-clusters that overlap with longevity-associated TFs, including *daf-16,*
560 *hlh-30, skn-1* and *hif-1*, implies that HPK-1 is a key regulator of an emerging
561 transcriptional anti-aging circuit. This protective transcriptional program is activated in the
562 nervous system during normal aging in wild-type animals as a cellular response to
563 increasing stress in the nervous system. Consistently, the presence of human
564 neurodegenerative disorders, a severe form of neuronal proteotoxic stress, correlates
565 with activation of human *hpk-1* expression: for example*,* human HIPK2 is activated in
566 frontal cortex samples of patients with AD, in motor neurons of ALS patients, and in
567 mouse models of ALS, (Lee et al., 2016). Thus, our results suggest that overexpression
568 of *hpk-1* in the *C. elegans* nervous system may extend longevity by preemptively delaying
569 the accumulation of age-associated damage and dysfunction to the proteome (*Figure 9A*).
570 However, *hpk-1* homologs in more complex metazoans can also promote cell death, a
571 key homeostatic component of tissue regeneration, indicating that chronic activation of
572 HIPKs is not always beneficial (Calzado et al., 2007; Lee et al., 2016; Wang et al., 2020;
573 Zhang et al., 2020). Whether activated HIPKs will fortify proteostasis and extend
574 longevity, or promote cell death is likely to be dependent on many factors, including the
575 specific homolog, levels of expression, physiological context, genetic background, and
576 cell-type.

577 We find that *hpk-1* prevents age-associated decline of axonal and synaptic
578 integrity, which together preserve neuronal function during the aging process and thus
579 also promote longer healthspan. In support of this concept, adult *hipk2 -/-* mice display
580 normal neurogenesis but manifest delayed-onset severe psychomotor and behavioral
581 deficiencies, as well as degeneration of dopaminergic neurons, reminiscent of
582 Parkinson's Disease (Zhang et al., 2007). Loss of *hpk-1* results in dysregulation of
583 neuronal gene expression by early adulthood; some changes are consistent with neuronal
584 aging but in other cases we observe an inverse correlation. For example, one third of all
585 neuropeptides are induced in the absence of *hpk-1*; yet increased neuropeptide signaling
586 has been associated with extended *C. elegans* longevity and is considered protective in
587 AD (Chen et al., 2018; Hodge et al., 2022; Petrella et al., 2019). One possibility is in the
588 absence of *hpk-1*, attenuated inducibility of the proteostatic network accelerates age-
589 associated cellular dysfunction (*Figure 9A*), and upregulation of neuropeptide signaling
590 compensates in the nervous system for the loss of proteostatic response. This concept is
591 consistent with our finding that increasing neuronal HPK-1 activity does not require
592 neuropeptides to improve proteostasis in distal tissues. An alternative possibility for the
593 connection between protective effects of HPK-1 and neuropeptides in neurons is that
594 HPK-1 may reduce insulin signaling by suppressing the processing of *ins* peptides,
595 thereby decreasing ILS to activate DAF-16 (FOXO) transcriptional quality control
596 programs. For example, loss of *egl-3*, a neuropeptide processing gene, extends longevity
597 by inactivating processing of insulins (Hamilton et al., 2005), and *egl-3* is upregulated in
598 *hpk-1* loss of function.

599 Impairment of the proteostatic network after loss of *hpk-1* results in broad
600 upregulation of gene expression, which may be provide additional levels of compensatory
601 mechanisms to mitigate neuronal dysfunction. For example, loss of *hpk-1* induces
602 expression of intraflagellar transport (IFT) components in sensory cilia. Mutations within
603 sensory neurons can alter longevity (Alcedo and Kenyon, 2004; Apfeld and Kenyon,
604 1999), and decreased IFT during *C. elegans* aging impairs sensory perception and
605 metabolism (Zhang et al., 2021). Deficiencies in primary cilia impairs neurogenesis in AD
606 transgenic mice, resulting in accumulation of $A\beta_{42}$ and tau protein and disease
607 progression (Armato et al., 2013; Chakravarthy et al., 2012; Ma et al., 2022; Morelli et al.,
608 2017). However, our bulk RNA-seq analysis cannot decipher changes in gene expression
609 at the level of individual neurons after loss of *hpk-1. hpk-1* and orthologs are known to
610 have roles in development, differentiation and cell fate-specification (Berber et al., 2013;
611 Blaquiere and Verheyen, 2017; Calzado et al., 2007; Hattangadi et al., 2010; Rinaldo et
612 al., 2007; Rinaldo et al., 2008; Steinmetz et al., 2018), therefore we cannot preclude the
613 possibility that HPK-1 may function to broadly limit neuronal gene expression during the
614 course of normal development and differentiation, thereby specifying neuronal
615 transcriptional programs. Misdifferentiation of the nervous system in the absence of *hpk-*
616 *1* could result in both intracellular transcriptional noise and cell non-autonomous noise
617 across cell-types and tissues.

618 We show that HPK-1 expression in serotonergic neurons activates a cell non-
619 autonomous signal to prime induction of molecular chaperones in muscle cells, whereas
620 HPK-1 expression in GABAergic neurons signals induces autophagy in hypodermal
621 tissue (*Figure 9B*). Our findings place HPK-1 within a selective cohort of transcriptional

622 regulators within the *C. elegans* nervous system that are activated in response to
623 metabolic, environmental, and intrinsic cues; thereby initiating distinct cell non-
624 autonomous signals to regulate components of the PN in peripheral tissues (Douglas et
625 al., 2015; Durieux et al., 2011; Frakes et al., 2020; Imanikia et al., 2019; Prahlad et al.,
626 2008; Prahlad and Morimoto, 2011; Silva et al., 2013; Tatum et al., 2015; Taylor and
627 Dillin, 2013). Loss of serotonin production in *tph-1* mutant animals has a minimal impact
628 on lifespan at basal temperature (Murakami and Murakami, 2007). However,
629 simultaneous loss of both serotonin and dopamine biosynthesis shortens lifespan
630 (Murakami and Murakami, 2007). Serotonin biosynthesis is also required for several
631 conditions that extend longevity: animals treated with an atypical antidepressant serotonin
632 antagonist (mianserin) (Petrascheck et al., 2007), changes in food perception (Entchev
633 et al., 2015), and neuronal cell non-autonomous induction of the mitochondrial unfolded
634 protein response (Berendzen et al., 2016; Zhang et al., 2018). In contrast, loss of either
635 of the serotonin receptors *ser-1* or *ser-4* have opposing effects on lifespan, suggesting
636 antagonistic activity between serotonin receptors (Murakami and Murakami, 2007).

637 Surprisingly, we find that increased HPK-1 activity in serotonergic neurons does
638 not increase lifespan, but is sufficient to improve muscle proteostasis and amplify the
639 expression of molecular chaperones that maintain proteostasis within the cytosol and
640 nucleus. Interestingly, neuronal HSF-1 regulation of the HSR through thermosensory
641 circuits is also separable from lifespan (Douglas et al., 2015). Serotonin signaling and the
642 serotonin receptor *ser-1* are essential for the induction of the HSR (Prahlad et al., 2008;
643 Tatum et al., 2015). ADF serotoninergic neurons receive upstream stress signals from
644 the thermosensory circuit, consisting of the amphid sensory neurons (AFD) and the AIY

645 interneurons, which regulate HSF-1 activity in the germline in a serotonin-dependent
646 manner (Tatum et al., 2015). However, increased serotonergic HPK-1 activity is not
647 equivalent to altered of thermosensory signals: *hpk-1* improves proteostasis within body
648 wall muscles but not intestinal cells through neurotransmitters and independent from
649 dense core vesicles. In contrast, loss of the guanylyl cyclase (*gcy-8*) in AFD
650 thermosensory neurons or the LIM-homeobox transcription factor (*ttx-3*) in AIY
651 interneurons improves intestinal proteostasis through dense core vesicle neurosecretion
652 (i.e., *unc-31*). *hpk-1* is expressed in AFD, but only at very low levels in AIY neurons (data
653 not shown and (Taylor et al., 2021)), and *hpk-1* is essential for the induction of the HSR
654 within intestinal cells (Das et al., 2017). Whether *hpk-1* activity within thermosensory
655 neurons functions within the canonical thermosensory-serotonin circuit to regulate the
656 intestinal HSR or proteostasis is not mutually exclusive from our findings and will be
657 interesting to pursue in future studies. Our results suggest serotonergic HPK-1 is an
658 important regulator of the HSR, potentially functioning in parallel to the thermosensory-
659 serotonin circuit to restore proteostasis in response to acute thermal stress.

660 We posit that increased serotonergic HPK-1 activity further activates HSF-1 in
661 response to heat (*Figure 9B*). This would be consistent with known hyperphosphorylation
662 of HSF-1 and amplification of the HSR in response to increasingly severe heat stress
663 (reviewed in (Lazaro-Pena et al., 2022)). Interestingly, HPK-1 limits SUMOylation of HSF-
664 1, SUMO limits the heat shock response in both *C. elegans* and mammals, and severe
665 heat shock results in HSF1 deSUMOylation (Das et al., 2017; Hietakangas et al., 2003;
666 Hietakangas et al., 2006). To our surprise, while increased neuronal *hsf-1* expression
667 increases longevity (Douglas et al., 2015; Morley and Morimoto, 2004), we could find no

668 study that has identified specific neuronal cell-types in which increased HSF-1 activity is
669 sufficient to extend longevity or enhance the HSR. Whether or not HPK-1 regulates HSF-
670 1 within the nervous system and/or in peripheral muscle cells through cell non-
671 autonomous signals will be interesting to determine in future studies. HPK-1 co-localizes
672 with HSF-1 in neurons, *hpk-1* is essential for induction of the HSR, and *hsf-1* and *hpk-1*
673 are mutually interdependent to extend longevity (Das et al., 2017); albeit the latter finding
674 was obtained via RNAi in animals without enhanced neuronal RNAi. Thus, while HPK-1
675 and HSF-1 may have overlapping neuronal functions, it is probable that *hsf-1* is required
676 outside of the nervous system for HPK-1 to extend longevity and the health of the
677 proteome (*Figure 9B*).

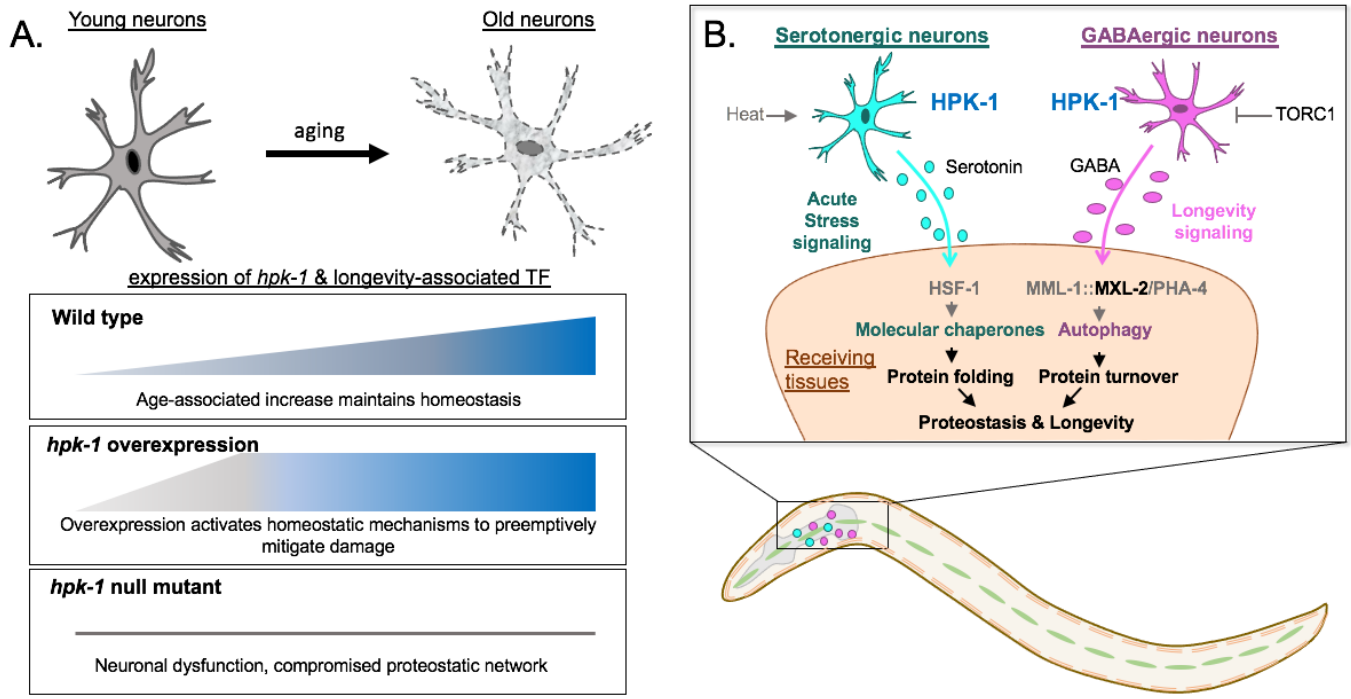

Figure 9. Differential regulation of the proteostatic network through HPK-1 activity in serotonergic and GABAergic neurons.
(A) During normal aging *hpk-1* expression increases broadly throughout the nervous system in response to accumulating damage and dysfunction. Overexpression of *hpk-1* within the nervous system fortifies proteostasis by priming and preemptively activating mechanisms that delay the progression of aging. In the absence of *hpk-1* the proteostatic network is compromised, resulting in neuronal dysfunction and increased expression compensatory mechanisms to maintain homeostasis (see text for details). **(B)** HPK-1 activity in serotonergic and GABAergic neurons initiates distinct adaptive responses, either of which improve proteostasis in a cell non-autonomous manner. Serotonergic HPK-1 protects the proteome from acute heat stress, while GABAergic HPK-1 fortifies the proteome by regulating autophagy activity in response to metabolic stress, such as changes in TORC1 activity. Gray indicates predicted interactions based on our prior genetic analysis (Das et al., 2017). MML-1 and MXL-2 heterodimerize and encode the orthologs of the Myc-family of transcription factors Mondo A/ChREBP and Mlx, respectively. *pha-4* is orthologous to the FoxA transcription factor.

678 Increased HPK-1 activity in GABAergic neurons induces autophagy in peripheral
679 cells, improves proteostasis and longevity. Whether HPK-1 functions in GABAergic
680 neurons through alteration of GABA or another neurotransmitter is unknown, but proper
681 differentiation of GABAergic neurons is essential for neuronal HPK-1 activation of
682 autophagy in distal tissue. We posit HPK-1 cell non-autonomous signaling occurs via
683 antagonism of GABA signaling. Loss of GABA increases *C. elegans* lifespan (Chun et al.,
684 2015; Yuan et al., 2019). However, not all neurotransmitters regulate lifespan, as only
685 mutants for the GABA biosynthetic enzyme, *unc-25*, increase lifespan. This GABAergic-
686 mediated control in lifespan seems to be mediated by the *gbb-1* metabotropic $GABA_B$
687 receptor (Chun et al., 2015). Interestingly, GABA signaling inhibits autophagy and causes
688 oxidative stress in mice, which is mitigated via Tor1 inhibition (Lakhani et al., 2014). In
689 fact, we previously found that neuronal expression of HPK-1 is inhibited by TORC1 and
690 *hpk-1* is required for TORC1 inactivation to extend longevity and the induction of
691 autophagy gene expression (Das et al., 2017). Both TORC1 inactivation and *hpk-1*
692 overexpression requires the Myc-family member *mxl-2* to extend longevity (Das et al.,
693 2017; Johnson et al., 2014; Nakamura et al., 2016) (*Figure 9B*). Consistently, TORC1
694 also acts within neurons to regulate aging (Zhang et al., 2019); our results suggest that
695 GABAergic neurons might be the specific neuronal cell-type through which alterations in
696 TORC1 activity regulate longevity. Collectively, our results position HPK-1 activity in
697 GABAergic neurons as the likely integration point for cell non-autonomous regulation of
698 autophagy via TORC1 (*Figure 9B*).

699 This work reveals a new level of specificity in the capacity of the nervous system
700 to initiate adaptive responses by triggering distinct components of the proteostatic

701 network across cell types. Results elucidating how neuronal cell-types generate
702 heterotypic signals to coordinate the maintenance of homeostasis are just beginning to
703 emerge. For example, a previous study discovered that activating non-autonomous
704 signaling of the endoplasmic reticulum unfolded protein response (ER-UPR) via the XBP-
705 1 transcription factor can be initiated from serotonergic neurons and dopaminergic
706 neurons; these signals are unique and converge to activate distinct branches of the ER-
707 UPR within the same distal tissues (intestinal cells) (Higuchi-Sanabria et al., 2020). In
708 contrast, our work demonstrates differential, yet specific, activation of cytosolic
709 components of the PN in separate peripheral tissues through neurotransmitters. Our work
710 suggests the nervous system partitions neuronal cell-types to coordinate the activation of
711 complementary proteostatic mechanisms across tissues, despite utilizing the same
712 transcriptional regulator within each neuronal cell-type. One possibility is that HPK-1
713 regulates specific adaptive responses based on the unique epigenetic states between
714 differentiated neuronal subtypes, which would be consistent with recent findings: during
715 development and differentiation, transcriptional rewiring of cells set chaperoning
716 capacities and alter usage of mechanisms that maintain protein quality control (Nisaa and
717 Ben-Zvi, 2021; Shemesh et al., 2021). Our work reveals HPK-1 as a novel transcriptional
718 regulator within the nervous system of metazoans, which integrates diverse stimuli to
719 coordinate specific adaptive responses that promote healthy aging.

720

721 **Materials and Methods**

722 **Key resources table**

723 *C. elegans* strains, strain background

Strain name	Genotype
N2	*Wild type*
AVS392/EK273	*hpk-1(pk1393) X*
AVS543	*artEx41 [rab-3p::hpk-1::CFP + pCFJ90 (myo-2p::mCherry)]*
AVS609	*artEx43 [myo-3p::hpk-1 + pCFJ90 (myo-2p::mCherry)] line 1*
AVS614	*artEx48 [dpy-7p::hpk-1 + pCFJ90 (myo-2p::mCherry)] line 1*
AVS627	*artEx52 [ges-1p::hpk-1 + pCFJ90 (myo-2p::mCherry)] line 1*
AVS420	*hpk-1(pk1393) X; artEx41 [rab-3p::hpk-1::CFP + pCFJ90 (myo-2p::mCherry)]*
AVS602/CZ13799	*juIs76 [unc-25p::GFP + lin-15(+)] II*
AVS608	*hpk-1(pk1393); juIs76 [unc-25p::GFP + lin-15(+)] II*
AVS752	*artEx41 [rab-3p::hpk-1::CFP + pCFJ90 (myo-2p::mCherry)]; hpk-1(pk1393); juIs76 [unc-25p::GFP + lin-15(+)] II*
AVS832	*rmIs132 [unc-54p::Q35::YFP] I; artEx58 [rab-3p::hpk-1 + pCFJ90 (myo-2p::mCherry)] line 1*
AVS833	*rmIs132 [unc-54p::Q35::YFP] I; artEx59 [rab-3p::hpk-1 + pCFJ90 (myo-2p::mCherry)] line 2*
AVS834	*rmIs132 [unc-54p::Q35::YFP] I; artEx60 [rab-3p::hpk-1 + pCFJ90 (myo-2p::mCherry)] line 3*
AVS835	*rmIs132 [unc-54p::Q35::YFP] I; artEx61 [rab-3p::hpk-1 + pCFJ90 (myo-2p::mCherry)] line 4*
AVS744	*artEx75 (rab-3p::hpk-1(K176A) + pCFJ90 (myo-2p::mCherry); rmIs132 [Punc-54::Q35::YFP] I line 1*
AVS748	*artEx79 (rab-3p::hpk-1(D272N) + pCFJ90 (myo-2p::mCherry); rmIs132 [Punc-54::Q35::YFP] I line 1*
AVS562	*rmIs132 [unc-54p::Q35::YFP] I; artEx41 [rab-3p::hpk-1::CFP + pCFJ90 (myo-2p::mCherry)] line 5*
AVS563	*rmIs110 [F25B3.3p::Q40::YFP]; artEx41 [rab-3p::hpk-1::CFP + pCFJ90 (myo-2p::mCherry)] line 1*
AVS837	*rmIs110 [F25B3.3p::Q40::YFP]; artEx92 [rab-3p::hpk-1::CFP + pCFJ90 (myo-2p::mCherry)] line 2*
AVS838	*rmIs110 [F25B3.3p::Q40::YFP]; artEx93 [rab-3p::hpk-1::CFP + pCFJ90 (myo-2p::mCherry)] line 3*
AVS839	*rmIs110 [F25B3.3p::Q40::YFP]; artEx94 [rab-3p::hpk-1::CFP + pCFJ90 (myo-2p::mCherry)] line 4*
AVS214/HC196	*sid-1(qt9) V*
AVS265/TU3401	*sid-1(pk3321)V; uIs69 [unc-119p::sid-1; myo-2p::mCherry]V*
AVS540	*rmIs132 [unc-54p::Q35::YFP] I; sid-1(pk3321)V; uIs69[unc-119p::sid-1; myo-2p::mCherry]V*
AVS541	*rmIs110 [F25B3.3p::Q40::YFP]; sid-1(pk3321)V; uIs69[unc-119p::sid-1; myo-2p::mCherry]V*
AVS713	*rmIs132 [unc-54p::Q35::YFP] I; artEx41(rab-3p::hpk-1::CFP + pCFJ90 (myo-2p::mCherry)]; unc-31(e169)V*
AVS810	*rmIs132 [unc-54p::Q35::YFP] I; artEx41 [rab-3p::hpk-1::CFP + pCFJ90 (myo-2p::mCherry)]; unc-13(e51)I*
AVS84/TJ375	*gpIs1 [hsp-16.2p::GFP] IV*
AVS397	*gpIs1 [hsp-16.2p::GFP]; artEx35 [sur-5p::hpk-1::CFP +pCFJ90 (myo-2p::mCherry)]*
AVS399	*gpIs1 [hsp-16.2p::GFP]; artEx33 [rab-3p::hpk-1::CFP +pCFJ90 (myo-2p::mCherry)]*
AVS715	*artEx41 [rab-3p::hpk-1::CFP + pCFJ90 (myo-2p::mCherry)]; sqIs24 [rgef-1p::GFP::lgg-1 + unc-122p::RFP]*
AVS716	*artEx41 [rab-3p::hpk-1::CFP + pCFJ90 (myo-2p::mCherry)]; sqIs13 [lgg-1p::GFP::lgg-1 + odr-1p::RFP]*
AVS682	*artEx62 [tph-1p::hpk-1 + pCFJ90 (myo-2p::mCherry)] line 1; rmIs132 [unc-54p::Q35::YFP] I*
AVS683	*artEx63 [tph-1p::hpk-1 + pCFJ90 (myo-2p::mCherry)] line 2; rmIs132 [unc-54p::Q35::YFP] I*
AVS685	*artEx65 [unc-47p::hpk-1 + pCFJ90 (myo-2p::mCherry)] line 1; rmIs132 [unc-54p::Q35::YFP] I*
AVS686	*artEx66 [unc-47p::hpk-1 + pCFJ90 (myo-2p::mCherry)] line 2; rmIs132 [unc-54p::Q35::YFP] I*
AVS691	*artEx71 [eat-4p::hpk-1 + pCFJ90 (myo-2p::mCherry)] line 1; rmIs132 [unc-54p::Q35::YFP] I*
AVS692	*artEx72 [eat-4p::hpk-1 + pCFJ90 (myo-2p::mCherry)] line 2; rmIs132 [unc-54p::Q35::YFP] I*
AVS693	*artEx73 [cat-2p::hpk-1 + pCFJ90 (myo-2p::mCherry)] line 1; rmIs132 [unc-54p::Q35::YFP] I*
AVS694	*artEx74 [cat-2p::hpk-1 + pCFJ90 (myo-2p::mCherry)] line 2; rmIs132 [unc-54p::Q35::YFP] I*
AVS809	*artEx62 [tph-1p::hpk-1 + pCFJ90 (myo-2p::mCherry)] line 1; sqIs13 [lgg-1p::GFP::lgg-1 + odr-1p::RFP]*
AVS794	*artEx65 [unc-47p::hpk-1 + pCFJ90 (myo-2p::mCherry)] line 1; sqIs13 [lgg-1p::GFP::lgg-1 + odr-1p::RFP]*
AVS709	*artEx62 [tph-1p::hpk-1 + pCFJ90 (myo-2p::mCherry)] line 1*
AVS710	*artEx65 [unc-47p::hpk-1 + pCFJ90 (myo-2p::mCherry)] line 1*
AVS888	*artEx99 [unc-47p::hpk-1 + pCFJ90 (myo-2p::mCherry)] line 2*
AVS816	*artEx41(rab-3p::hpk-1::CFP + pCFJ90 (myo-2p::mCherry); sqIs13 [lgg-1p::GFP::lgg-1 + unc-122p::RFP]; unc-30(ok613)*
AVS872	*artEx41(rab-3p::hpk-1::CFP + pCFJ90 (myo-2p::mCherry); sqIs13 [lgg-1p::GFP::lgg-1 + unc-122p::RFP]; tph-1(mg280)*
AVS836	*artEx91 [hpk-1p::GFP + tph-1p::mCherry] line 1*
AVS757	*artEx87 [hpk-1p::mCherry + unc-47p::GFP] line 1*
AVS001/CB1370	*daf-2(e1370)*
AVS022/GR1309	*daf-2(e1370); daf-16(mgDf47)*
AVS495/CL6264	*uIs60 [unc-119p::YFP + unc119p::sid-1]; eri-1(mg366)*

AVS817	*artIs1 [sur-5p::HPK-1::CFP + pCFJ90 (myo-2p::m-cherry)]; uIs60 [unc-119p::YFP + unc119p::sid-1]; eri-1(mg366)*
AVS488	*mxl-2(tm1516)*

Strains with both an AVS# and an external designation were generated in another laboratory. In these cases, an AVS# is assigned for internal record keeping and for purposes of increased rigor and reproducibility.

C. elegans strains and details

All strains were maintained at 20°C on standard NGM plates with OP50. For all experiments, animals were grown in 20x concentrated HT115 bacteria seeded on 6cm RNAi plates. Details on the strains, mutant alleles, and transgenic animals used in this study are listed in the Key resources table (above).

Generation of transgenic strains

To assemble tissue-specific constructs for increased *hpk-1* expression, the *hpk-1* cDNA was amplified and inserted into a pPD95.75 plasmid backbone containing the following promoters: hypodermal *dpy-7p* (Gilleard et al., 1997), body wall muscle *myo-3p* (Okkema et al., 1993), pan-neuronal *rab-3p* (Nonet et al., 1997), dopaminergic neurons *cat-2p* (Lints and Emmons, 1999), glutamatergic neurons *eat-4p* (Lee et al., 1999), serotonergic neurons *tph-1p* (Sze et al., 2000), and g-aminobutyric acid (GABA)ergic neurons *unc-47p* (Gendrel et al., 2016). All the assembled plasmids were validated by sequencing prior to microinjection. These constructs were injected at 5 ng/ml together with *myo-2p::mCherry* construct at 5 ng/ml as injection marker and *pBlueScript* at 90ng/ml as DNA carrier.

RNAi feeding

The *hpk-1* RNAi clone was originated from early copies of *E. coli* glycerol stocks of the comprehensive RNAi libraries generated in the Ahringer and Vidal laboratories. The control empty vector (L4440) and *hpk-1* RNAi colonies were grown overnight in Luria broth with 50 µg ml–1 ampicillin and then seeded onto 6cm RNAi agar plates containing 5 mM isopropylthiogalactoside (IPTG) to induce dsRNA expression overnight at room

748 temperature. RNAi clones used in this study were verified by DNA sequencing and
749 subsequent BLAST analysis to confirm their identity.

750 **Lifespan analysis**

751 Traditional lifespan assays were performed essentially as described in: (Das et al., 2017;
752 Lee et al., 2003). Briefly, animals were synchronized by egg prep bleaching followed by
753 hatching in M9 solution at 20°C overnight. The L1 animals were seeded onto 6cm plates
754 with HT115 bacteria and allowed to develop at 20°C. At L4 stage, FUdR was added to a
755 final concentration of 400 uM. Viability was scored every day or every other day as
756 indicated in each figure. Prism 7 was used to for statistical analyses and the *P* values
757 were calculated using log-rank (Mantel-Cox) method.

758 For lifespan with RNAi-mediated knockdown of TOR (*Figure Supplement 9*),
759 animals for the *let-363* (TOR RNAi) condition were first raised on empty vector RNAi
760 during development, and transferred to plates with *let-363* RNAi bacteria at L4 to avoid
761 developmental arrest at L3. In addition to having IPTG present in the media of the RNAi
762 plates, an additional 200uL of 0.2 M IPTG was added directly to the bacterial lawn of all
763 plates and allowed to dry immediately before adding animals. The assays were otherwise
764 performed as just described.

765 For lifespan assays in *Figure Supplement 3G*, assay plates and animal populations
766 were prepared as just described, and then lifespan was determined from analysis of time-
767 series image data collected for a given animal at approximately hour intervals throughout
768 adult life on modified Epson V800 flatbed scanners with our instance of the *C. elegans*
769 "lifespan machine" (Oswal et al., 2021; Stroustrup et al., 2013).

770 For replica set lifespan experiments (*Figure Supplement 3*), animals were
771 synchronized as previously described, followed by moving animals to 16°C during
772 development (L1 – L4), after which FUdR was added, and animals were moved to 20 or
773 25 °C as indicated. Replica set lifespan was trials were setup, scored, and results were
774 analyzed as described in (Cornwell et al., 2018; Cornwell and Samuelson, 2020).
775 In all cases: scoring of viability was blinded with respect to genotype and values
776 obtained at previous timepoints, and animals that died due to rupturing, desiccation on
777 the side of the plate or well, or clear body morphology defects were censored.

778 **Thermotolerance assay.**

779 Survival assays at high temperature were conducted as previously described in (Johnson
780 et al., 2014). In brief, synchronized L1 animals were allowed to develop at 20°C and FUdR
781 was added at the L4 stage. At day 1 adulthood, animals were moved to 35°C for a period
782 of 6 and 8 hours. Animals were allowed to recover for 2 hours at 20°C, and viability was
783 scored. In all cases, scoring of viability was blinded with respect to genotype and values
784 obtained at previous timepoints; animals that died due to rupturing, desiccation on the
785 side of the plate or well, or had clear body morphology defects were censored. Statistical
786 testing between pairs of conditions for differences in the number of foci was performed
787 using student's *t* test analysis.

788 **Induction of *hsp-16.2p*::*GFP* after heat shock.**

789 The *hsp-16.2p*::*GFP* animals were heat shocked on day 1 of adulthood for 1 hour at 35°C
790 and imaged after 4 hours of recovery. Images were acquired using a Zeiss Axio Imager
791 M2m microscope with AxioVision v4.8.2.0 software. The GFP a.u. values from the head
792 and intestine of the animals were acquired using the area selection feature from

793 AxioVision software. Two independent trials with a minimum of 20 animals per experiment
794 were performed.

795 **Measurement of autophagosome formation using the *GFP::LGG-1/Atg8* reporter.**

796 *GFP::LGG-1/Atg8* foci formation was visualized as described in (Kumsta et al., 2017).
797 Briefly, L4 stage and day 1 adult animals were raised on HT115 bacteria at 20°C and
798 imaged using a Zeiss Axio Imager M2m microscope with AxioVision v4.8.2.0 software at
799 63X magnification. Two independent trials where at least 20 seam cells from 15-20
800 different animals were scored for *GFP::LGG-1* puncta accumulation. In all cases scoring
801 of puncta was blinded with respect to genotype.

802 **Measurement of neurodegeneration in motor neurons.**

803 Animals carrying the *unc-25p::GFP* reporter strain to visualize VD and DD motor neurons
804 were synchronized and allowed to developed at 20°C and FUdR was added at L4 stage.
805 At L4, D2 and D9 of adulthood, animals were imaged in a Zeiss Axio Imager M2m
806 microscope and the number of animals showing axonal breaks in the VD and DD motor
807 neurons were scored. Axonal breaks were defined as an area of discontinued
808 fluorescence in either the ventral or dorsal nerve cords.

809 **Polyglutamine aggregation in neurons and locomotion analyses.**

810 The visualization and quantification of the progressive decline in proteostasis in the
811 nervous system (specifically the nerve ring) was performed as described in (Brignull et
812 al., 2006; Lazaro-Pena et al., 2021). In brief, synchronized *rgef-1p*::*polyQ40*::*YFP* L4
813 animals were treated with FUdR. Then, z-stack images from the nerve ring were acquired
814 using a Zeiss Axio Imager M2m microscope with AxioVision v4.8.2.0 software at 63X

815 magnification. The fluorescent foci form compressed *z*-stack images from 20 animals per
816 technical replicate were scored blind every other day from four to eight days of adulthood.
817 To assess locomotion capacity, at day two of adulthood, 40 animals were
818 transferred to a drop of 10ul of M9 solution and the number of body bends performed in
819 a period of 30 seconds from each animal was scored (as described in (Lazaro-Pena et
820 al., 2021)). Statistical testing between pairs of conditions for differences in the number of
821 foci was performed using student's *t* test analysis.

822 **Polyglutamine aggregation in muscle and paralysis analyses.**

823 The visualization and quantification of the progressive decline in proteostasis in muscle
824 tissue was performed as described in (Lazaro-Pena et al., 2021; Morley et al., 2002).
825 Briefly, synchronized *unc-54p*::*Q35*::*YFP* L4 animals were treated with FUdR. Then,
826 fluorescent foci from 20 animals per technical replicate were scored blind daily from days
827 one to three of adulthood. To assess paralysis, at days 5, 7, 9, and 11 of adulthood,
828 prodded animals that responded with head movement (and were therefore still alive) but
829 no backward or repulsive motion were scored as paralyzed (as described in (Lazaro-Pena
830 et al., 2021)). Statistical testing between pairs of conditions for differences in the number
831 of foci was performed using student's *t* test analysis. Two to five independent transgenics
832 lines were tested.

833 **Aldicarb assay.**

834 The aldicarb assay was performed as described in (Mahoney et al., 2006; Oh and Kim,
835 2017). Plates containing Aldicarb 1mM were prepared the day before the assay and
836 stored at 4°C. Animals were synchronized by picking at L4 stage and placing them in a
837 plate with HT115 bacteria. After 24 hours, one aldicarb plate per strain were brought out

838 of 4°C and a small drop of OP50 was placed in the center of the plate a let dry for 30
839 minutes. Approximately 25 animals were placed on each plate, and the number of
840 paralyzed animals were scored every hour up to 5 hours. The assay was performed at
841 room temperature.

842 **Exogenous 5-HT immobilization assay.**

843 Animals were synchronized by picking at L4 stage and placing them in a plate with HT115
844 bacteria. After 24 hours, serotonin (5-HT) was dissolved in M9 buffer to a 20mM
845 concentration (Hart, 2006). Twenty worms were placed on a glass plate well with 400ul
846 of 20mM serotonin for 10 minutes. The same number of control animals were placed in
847 400ul of M9 buffer. The locomotion of worms (mobilize or immobilized) was annotated at
848 the following time points: 2, 4, 6, 8, and 10 minutes. The assay was performed at room
849 temperature.

850 **Sample preparation and sequencing for RNA-Seq.**

851 10 cm RNAi plates were seeded with 1 mL of 10x concentrated HT115 EV bacteria from
852 an overnight culture, and allowed to dry for 1-2 days. N2 or *hpk-1(pk1393)* Approximately
853 1,000 synchronized L1 animals were added to each plate (~3000 animals per condition
854 across multiple plates). At the L4 stage, 600 µL of 4 mg/mL FUdR was added. Animals
855 were kept at 20 °C for the duration of the experiment.

856 Day 2 adult animals were collected in M9 buffer, washed 2x in M9, and a final wash
857 with DEPC-treated RNase-free water. Approximately two times the volume of the animal
858 pellet of TRIzol® reagent was added to each animal preparation, followed by brief mixing
859 and freezing overnight at -80 °C. Tubes were then allowed to partially thaw, and were
860 vortexed for five minutes to assist with disrupting the cuticle. Samples were transferred

861 to new tubes, and 200 µL of chloroform per 1 mL of TRIzol was added, followed by 20s
862 vortexing; the tubes settled at RT for 10 minutes. Supernatants were transferred to new
863 tubes, and an equal amount of 100% ethanol was added and mixed before proceeding to
864 column purification with the Qiagen RNAeasy Mini kit according the manufacturer's
865 instructions. Samples were eluted with 30 – 50 µL of DEPC-treated water, and checked
866 for initial concentration and quality with a Nanodrop ND-1000 spectrophotometer.
867 Biological replicate samples were prepared from independently synchronized populations
868 of animals.

869 Isolated RNA was provided to the University of Rochester Genomics Research
870 Center for library preparation and sequencing. Prior to library preparation, RNA integrity
871 of all samples was confirmed on an Agilent 2100 Bioanalyzer. Libraries for sequencing
872 were prepared with the Illumina TruSeq Stranded mRNA kit, according to the
873 manufacturer's instructions. Quality of the resulting libraries was checked again with a
874 Bioanalyzer prior to sequencing to ensure integrity. Sequencing was performed on an
875 Illumina HiSeq2500 v4, yielding an average of approximately 31 million single-ended 100
876 bp reads per sample. Quality of the output was summarized with FastQC (Andrews, 2010)
877 and reads were trimmed and filtered with Trimmomatic to remove adapter sequence and
878 any low-quality content occasionally observed toward the ends of reads (Bolger et al.,
879 2014). After filtering out low-quality reads, an average of 30 million reads per sample
880 remained, and were used for the rest of the analysis.

881 **Analysis of *hpk-1* null and wild-type control RNA-Seq dataset.**

882 RNA-Seq reads were aligned to the *C. elegans* genome (assembly WBcel235) with STAR
883 2.4.2a (Dobin et al., 2013) using gene annotation from Ensembl (version 82)

884 (Cunningham et al., 2022). An average of 90.2% of reads per sample were uniquely and
885 unambiguously mapped to the genome. These alignments were used as input to
886 featureCounts (version 1.4.6-p5) for gene-level counts (Liao et al., 2014). Ambiguous or
887 multi-mapping reads, comprising an average of approximately 9% of the reads per
888 sample, were not included in the gene-level count results. Transcript-level quantification
889 was also performed with RSEM (Li and Dewey, 2011) to obtain TPM (Transcripts Per
890 Million) expression estimates.

891 Further analysis was performed primarily in the R statistical software environment
892 (version 4.0.2) (Team, 2013), utilizing custom scripts and incorporating packages from
893 Bioconductor. Both count and TPM expression matrices were filtered to remove genes
894 with low or no expression, keeping genes with at least 10 read counts in at least one
895 sample. Genes were further filtered to keep only those annotated as protein coding,
896 pseudogene, ncRNA, lincRNA, antisense, or snRNA, which could have been included in
897 the sequenced libraries after poly-A selection; 96.3% of genes included in the final set
898 are protein-coding. Gene identifiers have been updated as necessary from newer
899 versions of WormBase (WS284) for integration with recent resources and datasets.

900 Differential expression analysis was performed with DESeq2, and the optional fold-
901 change shrinkage procedure was applied to moderate fold-changes for low-expression
902 genes (Love et al., 2014). Genes significantly differentially expressed between *hpk-*
903 *1(pk1393)* and N2 animals were taken as those with FDR-adjusted p-value less than 0.05
904 and absolute value of $\log_2$ foldchange of at least 1 (on a linear scale, down- or up-
905 regulated by at least two-fold). Functional and over-representation analysis for
906 differentially expressed genes was performed with GOSeq (Young et al., 2010)using gene

907 sets and pathways from the Gene Ontology (Harris et al., 2004), KEGG (Kanehisa and
908 Goto, 2000), and Reactome (Jassal et al., 2020).

909 **Integration with public tissue-specific and single-cell RNA-Seq datasets.**

910 *C. elegans* Aging Atlas and CenGen single-cell datasets

911 We obtained differential expression results for old (days 8, 11, 15) vs young (days 1, 3,
912 5) animals across 200 cell clusters from the Aging Atlas single-cell RNA-Seq project
913 (Roux et al., 2022). Significantly differentially expressed genes within each cluster were
914 taken as those with adjusted p-value < 0.05, and $\log_2$ fold-change magnitude of at least
915 0.5 (approximately 1.4 fold up- or down-regulated on a linear scale). Additional neuron
916 identity information was obtained by mapping Aging Atlas neuron clusters to clusters
917 identified in late-larval stage animals in the CeNGEN single-cell neuronal transcriptome
918 project (Taylor et al., 2021), assisted by correlations between clusters of the two datasets
919 already provided with the Aging Atlas. Chemical signaling subtypes of neurons were
920 determined by expression of marker genes commonly used in the field for fluorescent
921 labeling of neurons: *tph-1* for serotonergic, *unc-47* for GABAergic, *eat-4* for glutamatergic,
922 *cat-2* for dopaminergic, *cat-2* for cholinergic. Where a high correlation had been
923 established between a cluster in the Aging Atlas and CeNGEN, a signaling type was
924 assigned if the cluster expressed the associated marker gene at TPM greater than 75
925 based on the provided pre-normalized expression matrix available from the CeNGEN
926 website. Ten Aging Atlas neuron clusters did not have an obvious corresponding cluster
927 in the CeNGEN dataset; for these clusters neuron signaling class was based on marker
928 genes having average cluster counts > 0.5 across all cells in a cluster and, where
929 possible, a consensus of the six Aging Atlas timepoints.

930 Genes uniquely expressed in neurons, or significantly enriched compared to other
931 tissues were obtained from tissue-specific bulk RNA-Seq reported by (Kaletsky et al.,
932 2018) due to the additional dynamic range provided over current single-cell sequencing
933 technology.

934 *C. elegans* kinome, transcription factors, neuronal genome, and longevity-associated
935 genes

936 A collection of *C. elegans* kinases was assembled based on Zaru *et al.* 2017 (Zaru et al.,
937 2017) and cross-referenced against current gene annotation in WormBase version
938 WS284 (Harris et al., 2020) to keep only protein-coding genes and remove pseudogenes
939 or "dead" genes. This produced a list of 438 kinases in the *C. elegans* kinome (See Figure
940 Supplement 4, Supplementary File 5). *C. elegans* transcription factors were identified
941 from a previously published compendium (Nye et al., 1989). Genes with known or
942 predicted functions important to neurons, and their associated roles, were assembled
943 from tables curated in (Hobert, 2013). Genes with lifespan phenotypes primarily from
944 perturbation studies in *C. elegans* utilizing RNAi or mutant strains were assembled from
945 annotation in WormBase (WS282) as well as the GenAge database (de Magalhaes and
946 Toussaint, 2004).

947 **Statistical analysis for *in vivo* assays.**

948 Unless otherwise specified, GraphPad PRISM version 7 software was used for statistical
949 analyses. Data were considered statistically significant when P value was lower than 0.05.
950 In figures, asterisks denote statistical significance as (*, $P < 0.05$, **, $P < 0.001$, ****, $P <$
951 0.0001) as compared to appropriate controls. N number listed in figure legend indicates
952 the number of one representative experiment among all biological trials.

953 **Appendices.**

954 **Appendix 1.** In non-neuronal clusters we found a positive correlation between *hpk-1* and
955 a much smaller subset of TFs, only three of which have previously been implicated in
956 longevity: *fkh-9* (FOXG), *sea-2*, and *zfh-2* (ZFHX3) (Walter et al., 2011). Conversely, only
957 three longevity-associated TFs had inverse expression changes with age relative to *hpk-*
958 *1* outside of the nervous system: *xbp-1, mdl-1,* and *hlh-6* (achaete-scute family bHLH
959 transcription factor 3) (*Figure supplement 1*). Previously, it has been found that *xbp-1*
960 expression decreases broadly across 153 cell clusters (Roux et al., 2022); thus, whether
961 inverse co-expression with *hpk-1* has biological significance cannot be ascertained from
962 this analysis.

963 **Appendix 2.** During normal aging, only 14 kinases are downregulated in 10 or more cell-
964 clusters, four of which have been previously associated with longevity: *akt-1* (AKT1, a
965 canonical component of the insulin-signaling pathway (Paradis and Ruvkun, 1998)), *nipi-*
966 *3*, *dlk-1* (MAP3K12, a positive retrograde longevity response to mitochondrial electron
967 transport chain disruption (Munkacsy et al., 2016)), and *mkk-4* (MAP2K4) (*Figure*
968 *supplement 4*). Interestingly, *dlk-1* and *mkk-4* are both required for axon regeneration
969 after laser injury (Hammarlund et al., 2009).

970 Kinases often function in tandem in signal transduction cascades. We examined
971 whether any were co-expressed during aging in over-lapping cell-clusters with *hpk-1*,
972 which would be consistent with age-associated pathway activation via changes in gene
973 expression. Each kinase had a unique signature of cell clusters: *akt-1* and *dlk-1* are
974 broadly downregulated both within and outside the nervous system, conversely *gcy-28*
975 and *hpk-1* are broadly upregulated. Other kinases with age-associated changes in

976 expression across multiple cell-types displayed more specific patterns. For instance, *mkk-*
977 *4* was downregulated in a restricted set of clusters across cell-types, while *nipi-3*
978 expression was both strongly up and downregulated across many clusters. We failed to
979 identify any obvious correspondence, suggesting that putative HPK-1 regulatory
980 cascades either are not co-regulated via increased age-associated expression across cell
981 types or are cell-type specific.

982 **Appendix 3.** Loss of *hpk-1* upregulates expression of a number of neuronal genes
983 including those involved in: neuropeptide signaling, neurotransmission, release of
984 synaptic vesicles, calcium homeostasis, and function of sensory neurons. In addition to
985 upregulation of *ins* neuropeptides, 12 FMRFamide-related (flp) peptides, 19
986 neuropeptide-like proteins (nlp), nine neuropeptide maturation genes (e.g., *egl-3*
987 (proprotein convertase subtilisin/kexin type 2) and *egl-21*(carboxypeptidase E)), and nine
988 putative GPCR neuropeptide receptors were also significantly upregulated in *hpk-1* null
989 mutants. Neurotransmitters are signaling molecules that trigger a response by binding to
990 ionotropic or metabotropic neurotransmitter receptors in recipient neurons or tissues; we
991 find that mainly the latter are upregulated in *hpk-1* null mutant animals, including:
992 acetylcholine (*gar-1, gar-2* and *gar-3*), GABA (*gbb-2*) and glutamate (*mgl-3* and
993 uncharacterized *C30A5.10*). In total nine metabotropic and two ionotropic gluatamate
994 receptors, 14 vesicular glutamate transport family genes, nine acetylcholine receptor
995 ligand-gated ion channels, and nine GABA receptor ligand-gated ion channels were
996 upregulated. Additionally, *ace-2*, *ace-3* and *cha-1*, involved in acetylcholine degradation
997 and synthesis (respectively), were upregulated. *comt-4*, a catechol-O-methyltransferase

998 expected to be involved in the degradation of dopamine, was significantly down-
999 regulated.

1000 Synaptic transmission, the formation and release of synaptic vesicles, carry
1001 neurotransmitters and rely on proteins necessary for docking, priming and fusing to the
1002 axon terminal plasma membrane, which releases cargo into the synaptic cleft.
1003 Interestingly, loss of *hpk-1* causes the upregulation of synaptic proteins such as *unc-13*,
1004 *unc-10* and *rab-3*, which are essential for vesicle priming, recruitment and sequestration
1005 of vesicles, respectively. The process of vesicle release is highly dependent on a Ca^{2+}
1006 signal detected by synaptotagmins proteins, which promotes vesicle fusion to the plasma
1007 membrane (Deak, 2014). In *hpk-1* null mutant animals, we observed upregulation of
1008 synaptotagmin *snt-1*, *snt-3* and *snt-4* Ca^{2+} sensor proteins for vesicle release.

1009 Neuronal function is regulated by changes in calcium levels: a decrease in calcium
1010 uptake reduces neuronal function by a reducing neurotransmitter release (Scriabine and
1011 Kazda, 1989). In contrast, increasing calcium influx triggers activation of proteases and
1012 phospholipases, resulting in cell damage and cell death (Cheung et al., 1986; Siesjo,
1013 1989). Voltage-gated Ca^{2+} channels (VGCCs) are composed of 24 transmembrane
1014 alpha-1 subunits and associate with auxiliary beta-1 and alpha-2-delta subunits. *hpk-1*
1015 null mutant animals have increased expression of two of five alpha-1 subunits (*egl-19* and
1016 *unc-2*), and both alpha-2-delta subunits (*unc-36* and *tag-180*). Previous research
1017 describes the role of *egl-19* voltage-gated Ca^{2+} channel in the induction of the heat stress
1018 response (Silva et al., 2013): moderate upregulation of acetylcholine signaling improves
1019 muscle proteostasis by the activation of HSF-1, triggered by the *egl-19*-dependent Ca^{2+}
1020 influx.

1021 Neuronally expressed cilia are essential for cell motility, sensory perception and
1022 signaling. The assembly and maintenance of sensory cilia depends on IFT: bidirectional
1023 movement of cargo to and from the base and tip of the axoneme. The *C. elegans* IFT
1024 machinery is composed of: anterograde IFT motors, heterotrimeric kinesin-II and
1025 homodimeric OSM-3, retrograde dynein motors; and the IFT-A, -B and BBSome particle
1026 complexes (Hao et al., 2009; Scholey et al., 2004). Loss of *hpk-1* induces the expression
1027 of a high number of IFT machinery components including: *klp-11* (kinesin II motor), *che-*
1028 *3* (dynein motor), three and seven members of the IFT-A and -B complexes (respectively),
1029 and five members of BBSome complex. In mammals, there is a link between primary cilia
1030 signaling and age-related brain disease, including neurodegenerative disorders (Ma et
1031 al., 2022).

1032 **Data availability.**

1033 All data supporting the findings of this study are available within the article, its
1034 Supplementary Information files, the peer-review file, or are available upon request. RNA-
1035 Seq data for *hpk-1(pk1393)* and N2 is available from GEO, accession GSE220744.

1036 All scripts for data analysis are available upon reasonable request.

1037 **Acknowledgments.**
1038
1039 We would like to thank members of the Samuelson laboratory, past and present, for their
1040 thoughtful insight and assistance related to this project, especially: Zachary Ward, Rachel
1041 Kitt, and Dr. Sara Farrell. We would like to thank members of the Western New York
1042 Worm Group for their input and discussions. We would like to thank Dr. Doug Portman
1043 (URMC) and his laboratory for strains and advice. Some strains were provided by the
1044 CGC, which is funded by NIH Office of Research Infrastructure Programs (P40

1045 OD010440). We would like to personally thank Drs. Dirk Bohmann (URMC), Gary Ruvkun
1046 (Massachusetts General Hospital/Harvard Medical School), Arjumand Ghazi (University
1047 of Pittsburgh), Seung-Jae Lee (Korea Advanced Institute of Science and Technology)
1048 and Mary Wines-Samuelson for critical reading of this manuscript. We would like to thank
1049 Drs. Cynthia Kenyon and David Kelley (Calico Life Sciences) for providing us the full
1050 scRNA-seq results for the old vs young differential expression analysis results for each
1051 cell cluster in the *C. elegans* Aging Atlas. We would like to thank Dr. John Ashton for
1052 assistance and the University of Rochester Genomics Research Center for conducting
1053 RNA-sequencing. Research reported in this publication was supported by the National
1054 Institute On Aging of the National Institutes of Health under Award Number
1055 RF1AG062593. CADB was supported by F32HD105323. The content is solely the
1056 responsibility of the authors and does not necessarily represent the official views of the
1057 National Institutes of Health.
1058

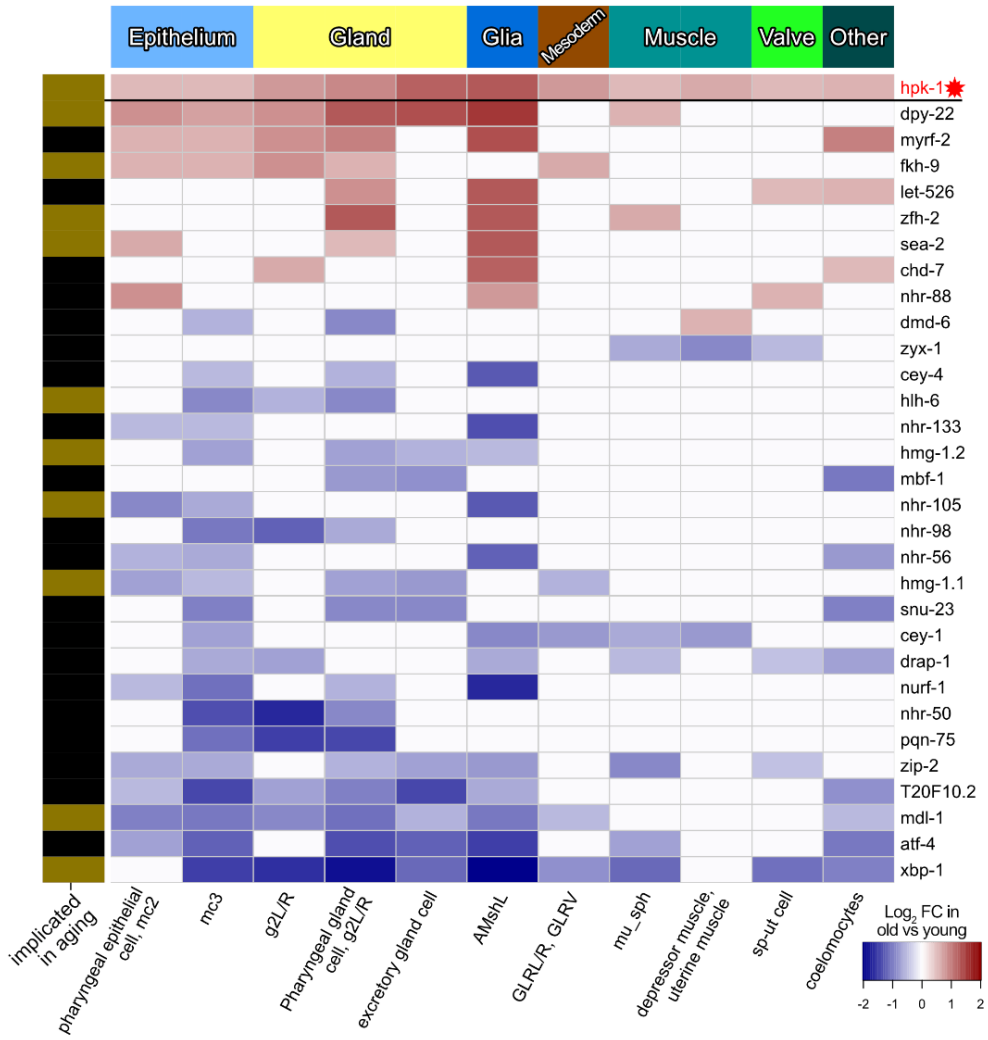

Figure Supplement 1. During normal aging *hpk-1* is co-expressed with transcription factors in cell-clusters outside of the nervous system.
Heat map of non-neuronal cell clusters in which *hpk-1* expression increases during normal aging along with TFs differentially expressed in 3 or more neuron cell-clusters. Fold-changes of a given TF from old versus young animals are shown, upregulation with aging in red and downregulation with aging in blue. Neuronal types, neurotransmitter subtypes are indicated in the top, names of the cell cluster or individual neuronal pair are given at the bottom, and whether a TF has previously been implicated in aging is indicated by the black and gold on the left side (genes with gold bars have previously published aging-associated phenotypes). Primary data for this analysis was generated in the *C. elegans* Aging Atlas (Roux et al., 2022) and differential expression with aging was based on adjusted p-values <0.05 and a $\log_2$ FC magnitude of at least 0.5 (between days 8,11,15 and days 1,3,5). Note *hpk-1* is included for reference and is a transcriptional co-factor, but is not a *bona fide* transcription factor. See *Supplementary Files 4 and 5* for dataset.

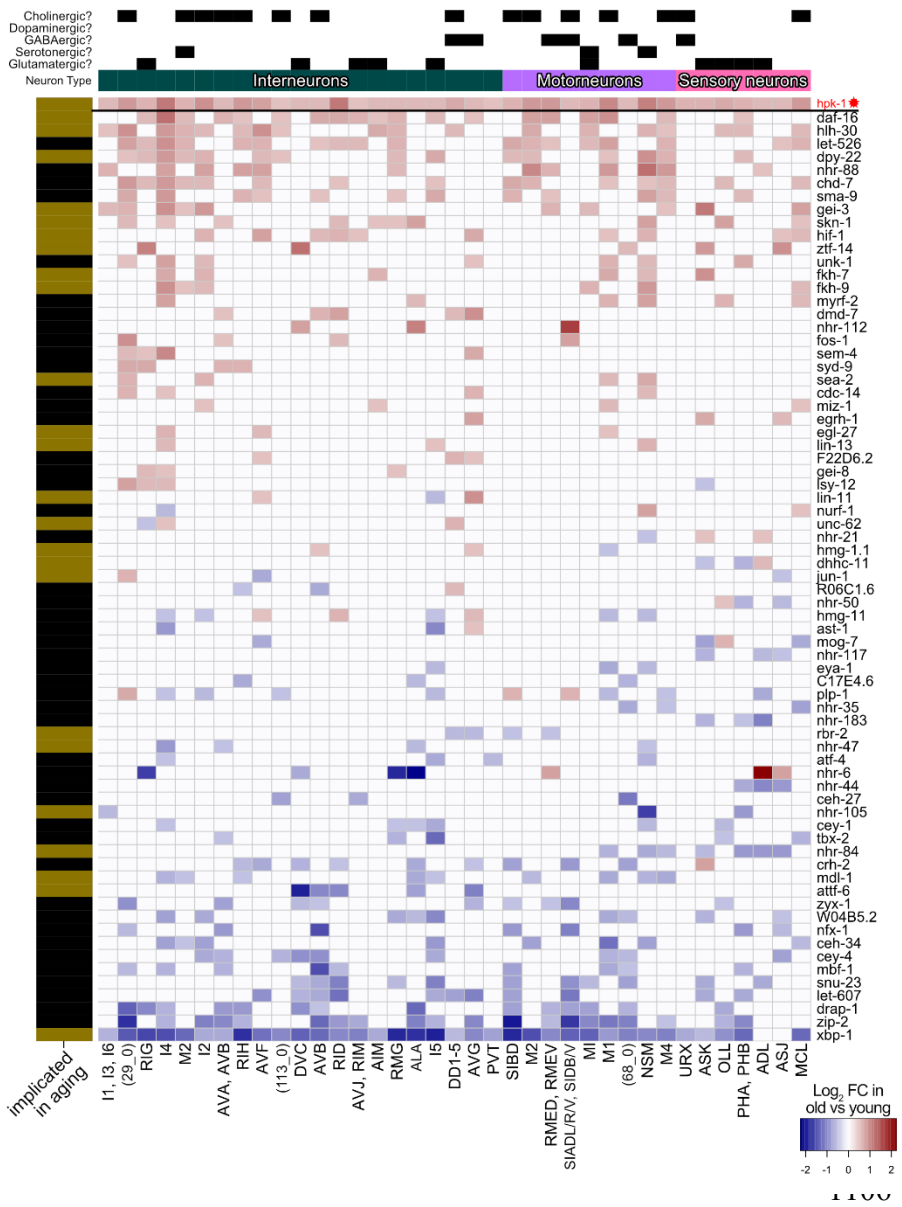

Figure Supplement 2. *hpk-1* neuronal co-expression with transcription factors during aging. Heat map of neuronal cell clusters in which *hpk-1* expression increases during normal aging along with TFs differentially expressed in 3 or more neuron cell-clusters. Fold-changes of a given TF from old versus young animals are shown, upregulation with aging in red and downregulation with aging in blue. Neuronal types, neurotransmitter subtypes are indicated in the top, names of the cell cluster or individual neuronal pair are given at the bottom, and whether a TF has previously been implicated in aging is indicated by the black and gold on the left side (genes with gold bars have previously published aging-associated phenotypes). Primary data for this analysis was generated in the *C. elegans* Aging Atlas (Roux et al., 2022) and differential expression with aging was based on adjusted p-values <0.05 and a $\log_2$ FC magnitude of at least 0.5 (between days 8,11,15 and days 1,3,5). Note *hpk-1* is included for reference and is a transcriptional co-factor, but is not a *bona fide* transcription factor. See *Supplementary Files 4 and 5* for dataset.

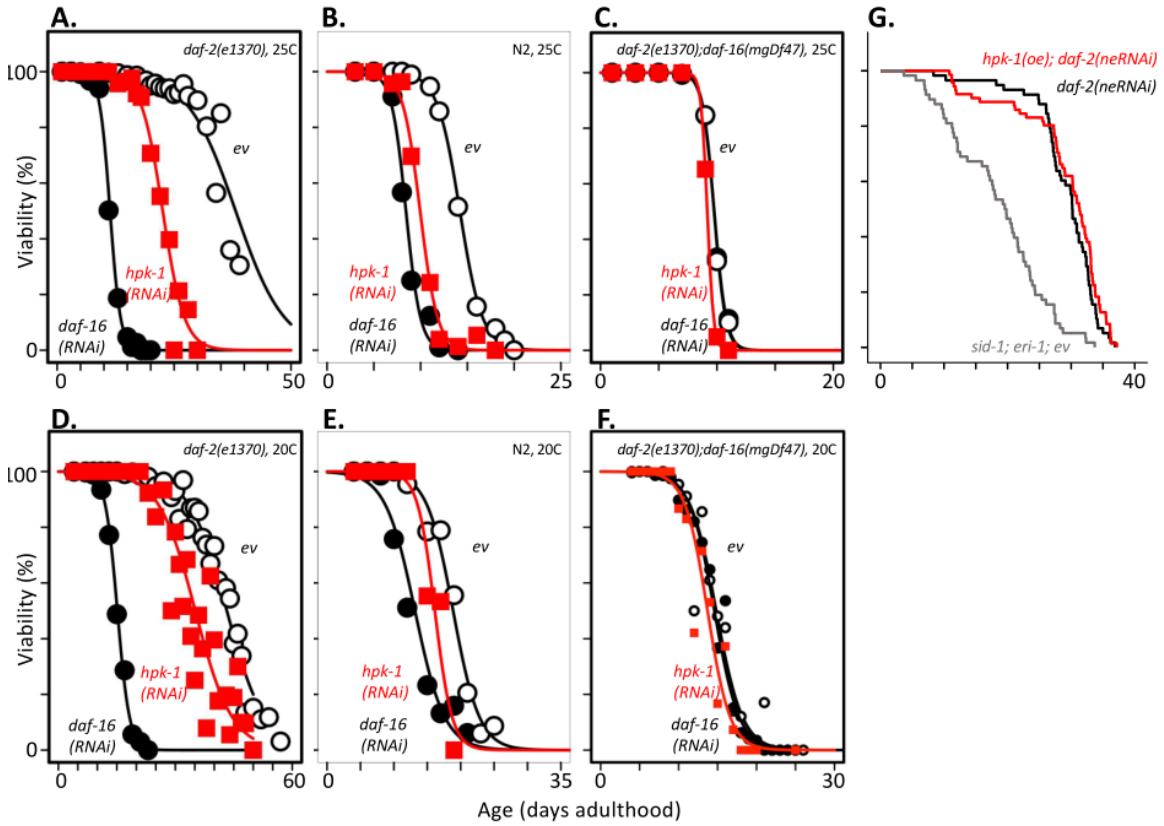

Figure Supplement 3. Genetic analysis of lifespan between *hpk-1* and alterations of ILS.

(A-C) Lifespan of *daf-2(e1370)* mutant animals treated with either empty vector (*ev)*, *hpk-1(RNAi)*, or *daf-16(RNAi)* at 25°C in either *daf-2(e1370)* (A), wild-type (B), or *daf-2(e1370);daf-16(mgDf47)* mutant animals (C). Primary lifespan data for (A-C) was generated in (Samuelson et al., 2007) and can be found in Supplemental Table 2 of that study. **(D-F)** Lifespan of *daf-2(e1370)* mutant animals treated with either empty vector (*ev)*, *hpk-1(RNAi)*, or *daf-16(RNAi)* at 20°C in either *daf-2(e1370)* (D), wild-type (E), or *daf-2(e1370);daf-16(mgDf47)* mutant animals (F). Primary data for (D-F) can be found in *Supplementary File 1* (this study). Lifespan experiments in **(A-F)** used the replicate set method (for detailed protocols see (Cornwell et al., 2018; Cornwell and Samuelson, 2020), which is as accurate and precise as traditional approaches to assess changes in *C. elegans* lifespan and have high resolution to detect differences (Cornwell et al., 2022): in *daf-2(e1370);daf-16(mgDf47)* the p-value comparisons (empty vector to *hpk-1(RNAi)*) are significant at both 25 and 20°C, but result in small absolute decreases in median lifespan (0.68 and 1.12 days, respectively). Curves were plotted using WormLife (https://github.com/samuelsonlab-urmc/wormlife) (Cornwell et al., 2018). **(G)** Lifespan of *C. elegans* with enhanced sensitivity to RNAi within the nervous system (*unc-119p::sid-1; eri-1(mg366)*) treated with either empty vector (grey line) or *daf-2(RNAi)* (red line) or *unc-119p::sid-1; eri-1(mg366); sur-5p::hpk-1* animals treated with *daf-2(RNAi)* (black line) using the Lifespan Machine method (Stroustrup et al., 2013). See *Supplementary File 1* for primary data.

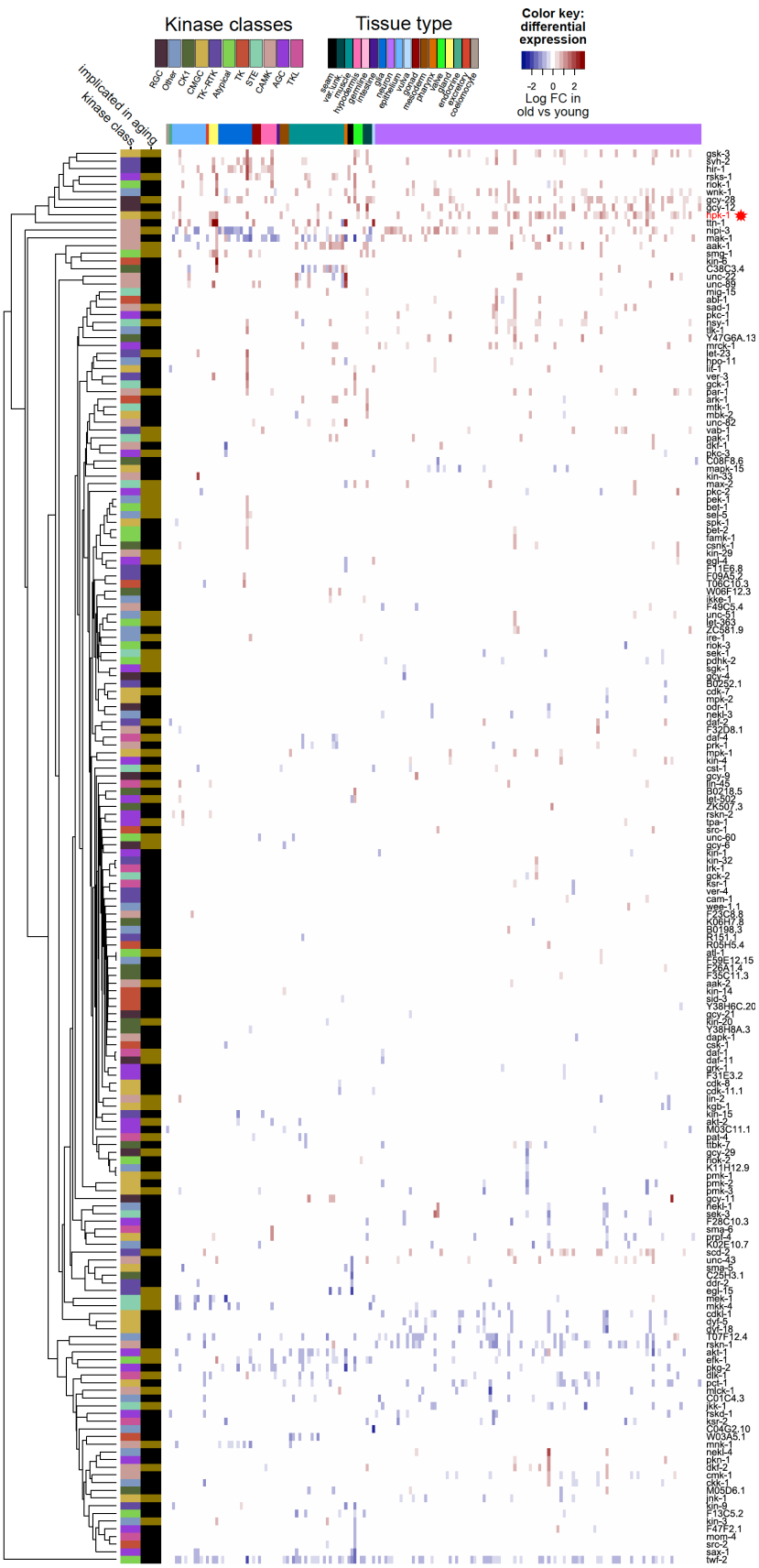

Figure Supplement 4. Only a limited subset of kinases change expression during normal aging. Heat map of 184 kinases that change expression during normal aging in any cell cluster in the aging atlas dataset, of the 438 total kinases identified in *C. elegans*. Increased (red) and decreased (blue) expression with aging of a given kinase is shown. Major tissue types, kinase classes, as well as whether a kinase has previously been implicated in aging is indicated in the top and side bars, respectively. Primary data for this analysis was generated in the *C. elegans* Aging Atlas (Roux et al., 2022) and differential expression with aging was based on adjusted p-values <0.05 and a $\log_2$ FC magnitude of at least 0.5 (between days 8,11,15 and days 1,3,5). See *Supplementary Files 4 and 5* for dataset.

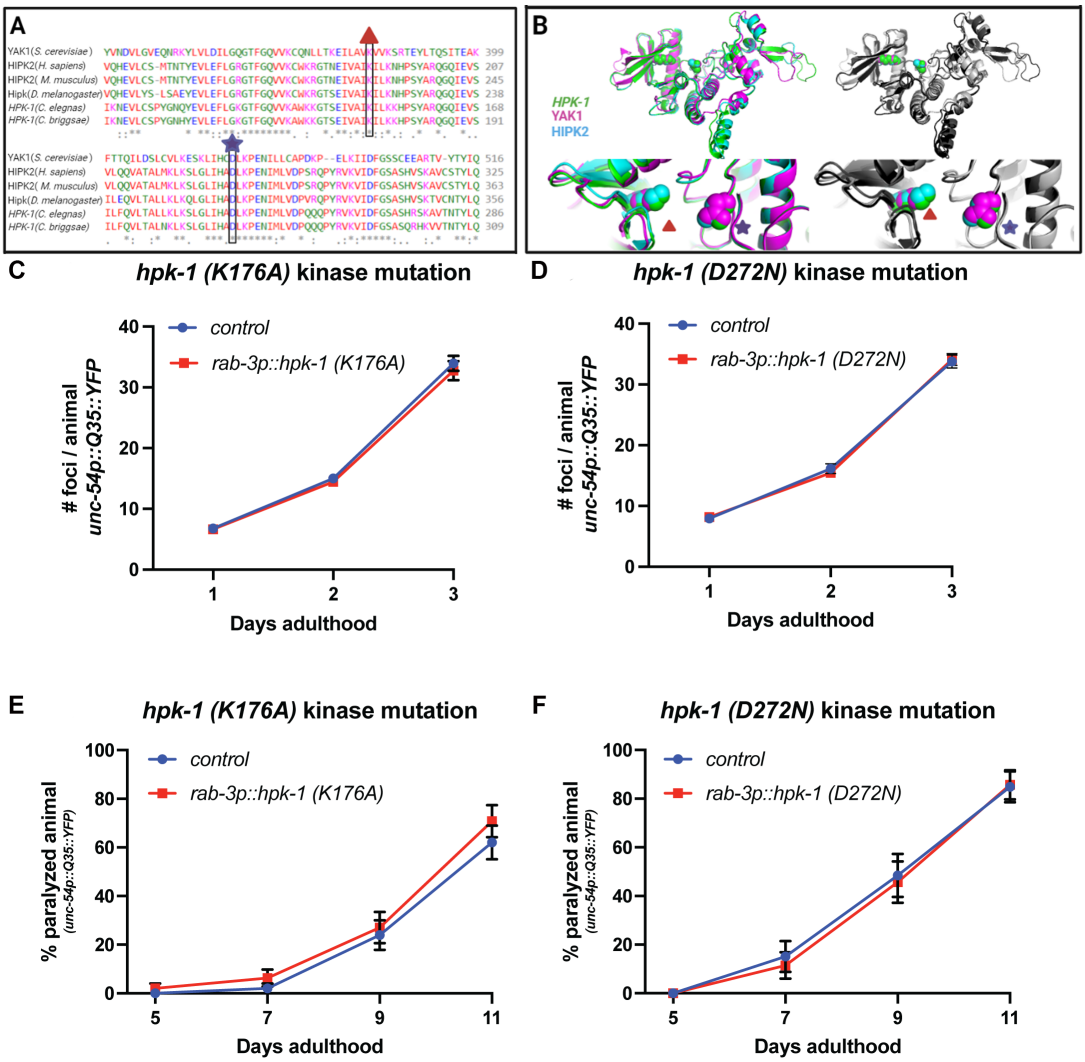

Figure Supplement 5. HPK-1 kinase activity is necessary to improve proteostasis. **(A)** Multiple sequence alignment of the HPK-1 kinase domain across evolutionarily distant species. Alignment was conducted using Clustal Omega (Sievers et al., 2011), with sequence IDs: HIPK2 (NP_073577.3), HPK-1 (F20B6.8a), HIPK2 *(M. musculus*, NP_001281073.1), HIPK (*D. melanogaster*, CG17090), HPK-1 (*C. briggsae*, CBP26904), and Yak1 (SGDID:S000003677). **(B)** Overlap between the predicted tertiary structures of the kinase domain of *C. elegans* HPK-1 (green), *S. cerevisiae* Yak1 (pink), and *H. sapiens* HIPK2 (blue). The K176A and D272N mutations are indicated by a red triangle and purple star, respectively, falling within the catalytic domain (He et al., 2010). Predicted structures for these genes were downloaded from AlphaFold (Jumper et al., 2021; Varadi et al., 2022): HPK-1(Q8MQ70 HIPK_CAEEL), Yak1 (A0A7C8V8P7_ORBOL), (H7BXX9_HUMAN). Highly conserved regions observed using multiple sequence alignment where then aligned in 3D using PyMol alignment tool (DeLano, 2002). **(C-F)** Quantification of foci in muscle (C, D) and paralysis rate (E, F) of transgenic animals with neuronal overexpression of *hpk-1(K176A)* (C, E) and *hpk-1(D272N)* (D, F), respectively. (n≥20 for C, n≥20 for D, n≥48 for E

1191 and n≥30 for F). *T* test analysis was performed between transgenic and non-transgenic
1192 animals at every time point. See *Supplementary Files 11 and 12* for details.
1193

1194

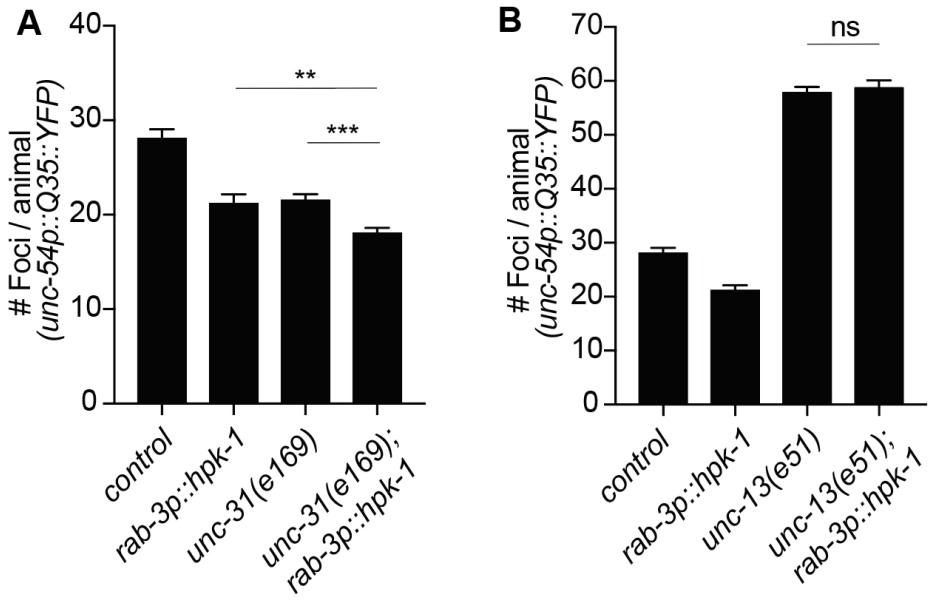

1195
1196
1197 **Figure Supplement 6. HPK-1 cell-nonautonomous regulation of proteostasis**
1198 **depends on neurotransmitter signaling.**
1199 (**A)** Quantification of *polyQ* foci in muscle of wild type and neuropeptide secretion
1200 mutants, *unc-31(e169)* (n≥21), **(B)** Quantification of foci in muscle of wild type and
1201 neurotransmitters secretion mutants, *unc-13(e51)* (n≥21). *T* test analysis with ***P* < 0.01
1202 and ****P* < 0.001. See *Supplementary File 11* for details.

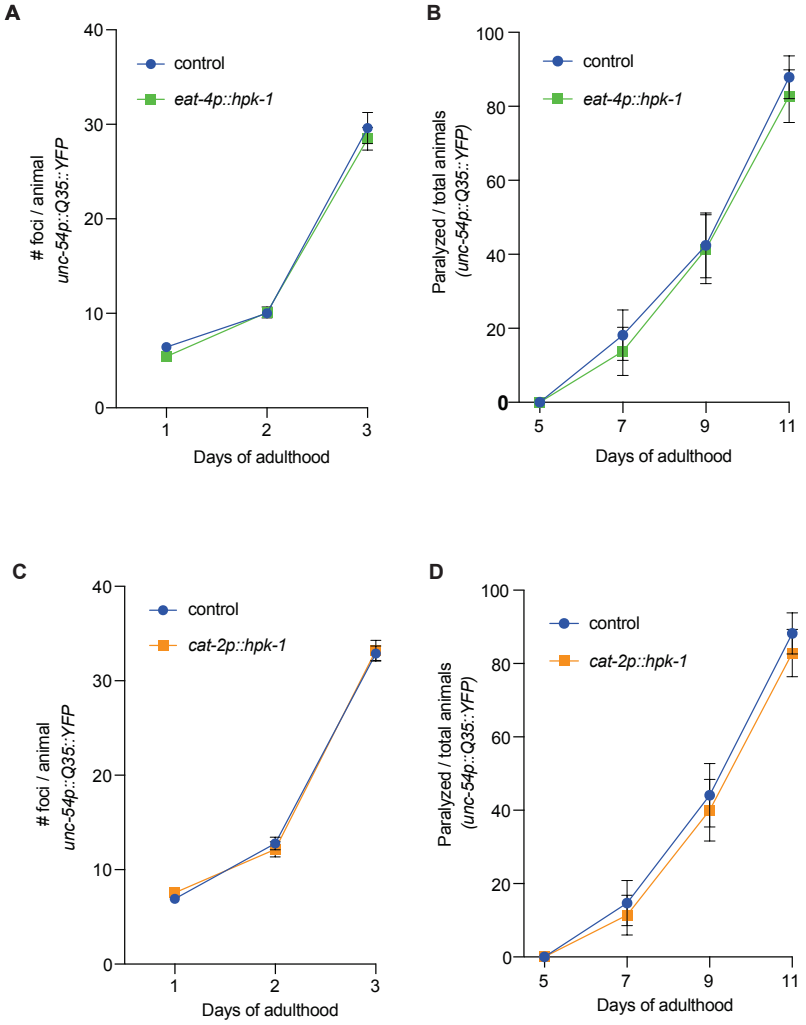

Figure Supplement 7. *hpk-1* expression in glutamatergic and dopaminergic neurons is not sufficient to prevent the decline in proteostasis.
(A and **B)** Quantification of number of foci (A) and paralysis rate (B) of animals expressing *hpk-1* in the glutamatergic neurons (*eat-4p::hpk-1*; green line) and control non-transgenic siblings (blue line) ($n \geq 18$ for A and $n \geq 29$ for B). **(C** and **D)** Quantification of number of foci (C) and paralysis rate (D) of animals expressing *hpk-1* in the dopaminergic neurons (*cat-2p::hpk-1;* orange line) and control non-transgenic siblings (blue line) ($n \geq 16$ for C and $n \geq 34$ for D). See *Supplementary Files 11 and 12* for details and additional trials.

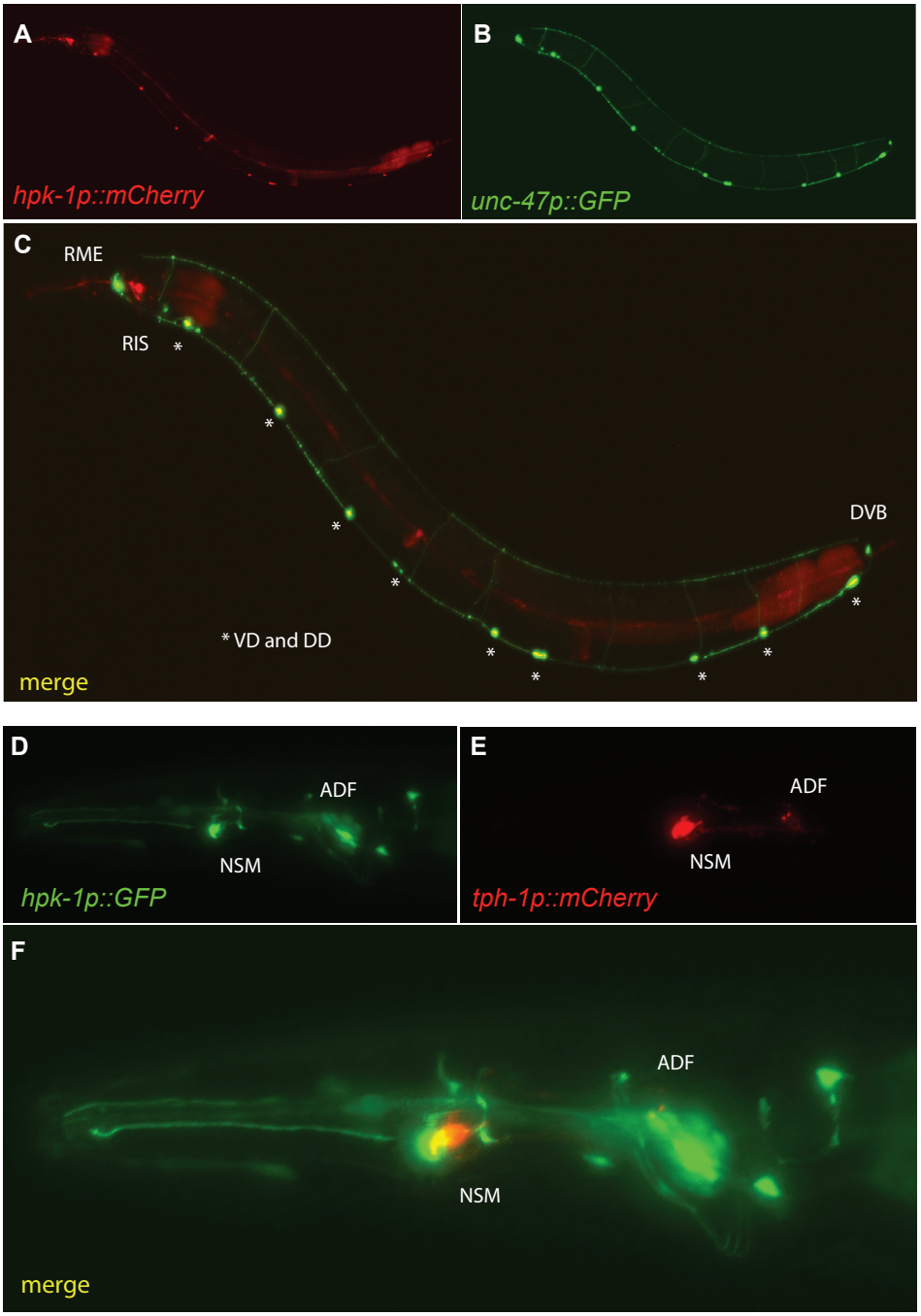

1213
1214
1215 **Figure Supplement 8. *hpk-1* is expressed in GABAergic and serotonergic neurons.**
1216 Representative fluorescent micrographs of day 1 adult animals co-expressing *hpk-*
1217 *1p::mCherry* and *unc-47p::GFP* **(A-C)**; and *hpk-1p::GFP* and *tph-1p::mCherry* **(D-F)**.
1218

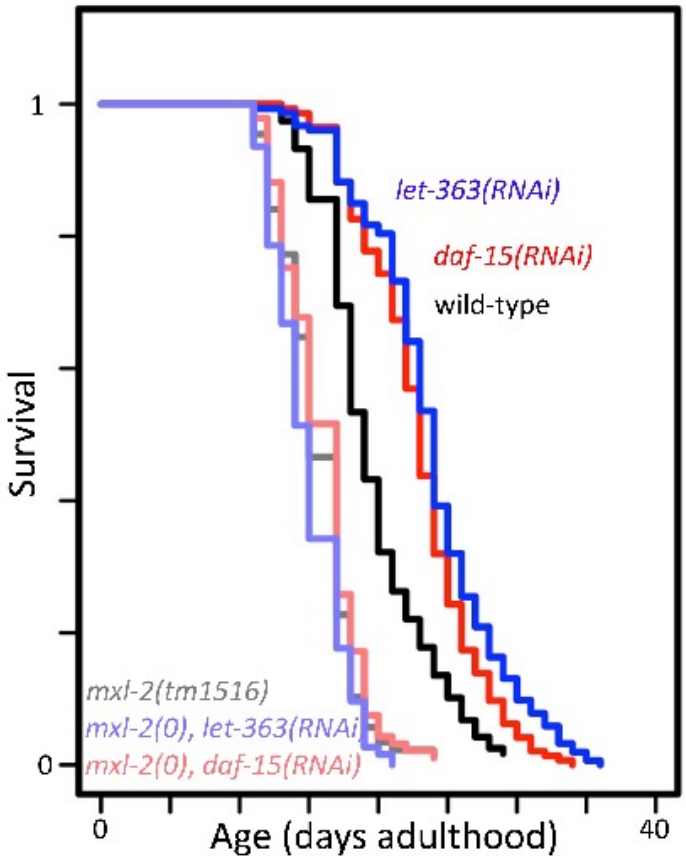

Figure Supplement 9. ***mxl-2*** **is required for decreased TORC1 signaling to increase longevity.** Lifespan of wild-type (N2, darker shades) or *mxl-2(tm1516)* null mutant animals (lighter shades) treated with either empty vector (black/gray), *let-363(RNAi)* (blues), or *daf-15(RNAi)* (reds). Lifespan graph is representative of one trial with two replicates. Curves were plotted using WormLife (https://github.com/samuelsonlab-urmc/wormlife) (Cornwell et al., 2018). See *Supplementary File 1* for details and additional trial.

Supplementary File 1. ***Lazaro-Pena SF01 Lifespan assays.xlsx.*** Trials, data, strains, genotypes, number of animals, and statistics for lifespan data presented in Figures 1a-d, 8b,f, S3a-g, and S9.

Supplementary File 2. ***Lazaro-Pena SF02 Body bends assays.xlsx.*** Experimental data, strains, genotypes, number of animals and statistical analysis for data presented in Figures 1e, and 5c,e.

Supplementary File 3. ***Lazaro-Pena SF03 Thermotolerance assays.xlsx.*** Trials, data, analysis, strains, genotypes, number of animals, and statistics for thermotolerance data presented in Figures 1f, and 8a,e.

Supplementary File 4. ***Lazaro-Pena SF04 TFs DE with aging in hpk-1 DE clusters.xlsx.*** Transcription factors differentially expressed in old vs young animals in the same cell clusters where *hpk-1* has significant expression changes with age in the Aging Atlas dataset. This includes a summary of which clusters exhibit upregulation and which exhibit downregulation for a TF, and if the gene has been previously shown to have aging or lifespan associated phenotypes in RNAi or loss-of-function mutant experiments. Primary data was from the *C. elegans* Aging Atlas, and association to aging phenotypes was determined based on curated annotations from WormBase and GenAge. File is associated with Figures 2, S1, S2, and S4.

Supplementary File 5. ***Lazaro-Pena SF05 C elegans kinome aging DE.xlsx.*** Kinases differentially expressed in old vs young animals out of any of the 200 clusters with DE analysis results from the Aging Atlas dataset. Out of 438 kinases identified in *C. elegans*, 186 have significant age-associated expression changes in at least one Aging Atlas cell cluster. For these kinases, we summarized the number of age-associated up- and down-regulated changes, if they have been previously identified as having aging or lifespan phenotypes in loss-of-function experiments, and the fold-changes in *hpk-1* null vs WT animals for significant changes in our bulk RNA-Seq experiment. Primary data was from the *C. elegans* Aging Atlas, and association to aging phenotypes was determined based on curated annotations from WormBase and GenAge. File is associated with Figures 2, S1, S2, and S4.

Supplementary File 6. ***Lazaro-Pena SF06 Neurodegeneration assay.xlsx.*** Experimental data, strains, genotypes, number of animals/cells, age and statistical analysis for data presented in Figures 3b-d.

Supplementary File 7. ***Lazaro-Pena SF07 Aldicarb assay.xlsx.*** Experimental data, strains, genotypes, number of animals, hours on aldicarb and statistical analysis for data presented in Figure 3e.

Supplementary File 8. ***Lazaro-Pena SF08 Serotonin assay.xlsx.*** Experimental data, strains, genotypes, number of animals, minutes on 5-HT and statistical analysis for data presented in Figure 3f.

Supplementary File 9. ***Lazaro-Pena SF09 hpk-1(0) and N2 D2 RNA-seq.xlsx.*** Differential expression analysis results for RNA-Seq of *hpk-1(pk1393)* null mutant animals compared to wildtype, presented in this manuscript. ***Sheet 1:*** differential expression for all 16,828 genes considered to be expressed in any sample in the experiment. ***Sheet 2:*** the subset of genes with significant expression changes between groups (adjusted p-value < 0.05, log2 fold-change magnitude ≥ 1). Additional columns in both sheets include a summary of the raw and normalized expression for each group, and the human homologs from OrthoList, where applicable. File is associated with Figure 4.

Supplementary File 10. ***Lazaro-Pena SF10 hpk-1 DE genes with neuron-associated function annotations.xlsx.*** Of the genes significantly differentially expressed in *hpk-1(pk1393)* null mutant animals vs wildtype, we found 280 overlap a set of genes with important functions in neurons (Hobert, O. (2018). *The neuronal genome of Caenorhabditis elegans*). For these genes, table includes a summary of their function, the differential expression fold-change and raw expression level in the *hpk-1(pk1393)* vs wildtype RNA-Seq comparison, and the clusters from the Aging Atlas dataset with significant age-associated expression changes (where applicable). File is associated with Figure 4.

Supplementary File 11. ***Lazaro-Pena SF11 Polyglutamine assays.xlsx.*** Trials, data, analysis, strains, genotypes, number of animals, age and statistical analysis of polyglutamine foci formation data presented in Figures 5b,d,g,i,l, 7a,c, S5c,d, S6a,b, and S7a,c.

Supplementary File 12. ***Lazaro-Pena SF12 Paralysis assays.xlsx.*** Trials, data, analysis, strains, genotypes, number of animals, age and statistical analysis of data for paralysis onset in animals expressing *polyQ::YFP* presented in Figures 5h,j, 7b,d, S5e,f, and S8b,d.

Supplementary File 13. ***Lazaro-Pena SF13 Induction of molecular chaperone.xlsx.*** Trials, fluorescent quantification, analysis, strains, genotypes, number of animals, heat shock conditions, and statistical analysis of data presented in Figure 6c,e.

Supplementary File 14. ***Lazaro-Pena SF14 Induction of autophagosomes.xlsx.*** Trials, autophagosome quantification, analysis, strains, genotypes, number of cells, age and statistical analysis of data presented in Figures 6g,i,k, and 8d,h,i.

References

Alcedo, J., and Kenyon, C. (2004). Regulation of C. elegans longevity by specific gustatory and olfactory neurons. Neuron *41*, 45-55.

An, J.H., and Blackwell, T.K. (2003). SKN-1 links C. elegans mesendodermal specification to a conserved oxidative stress response. Genes Dev *17*, 1882-1893.

Andrews, S. (2010). FastQC: a quality control tool for high throughput sequence data. [Online].

Apfeld, J., and Kenyon, C. (1998). Cell nonautonomy of C. elegans daf-2 function in the regulation of diapause and life span. Cell *95*, 199-210.

Apfeld, J., and Kenyon, C. (1999). Regulation of lifespan by sensory perception in Caenorhabditis elegans. Nature *402*, 804-809.

Armato, U., Chakravarthy, B., Pacchiana, R., and Whitfield, J.F. (2013). Alzheimer's disease: an update of the roles of receptors, astrocytes and primary cilia (review). International journal of molecular medicine *31*, 3-10.

Balch, W.E., Morimoto, R.I., Dillin, A., and Kelly, J.W. (2008). Adapting proteostasis for disease intervention. Science *319*, 916-919.

Baldari, S., Garufi, A., Granato, M., Cuomo, L., Pistritto, G., Cirone, M., and D'Orazi, G. (2017). Hyperglycemia triggers HIPK2 protein degradation. Oncotarget *8*, 1190-1203.

Berber, S., Llamosas, E., Thaivalappil, P., Boag, P.R., Crossley, M., and Nicholas, H.R. (2013). Homeodomain interacting protein kinase (HPK-1) is required in the soma for robust germline proliferation in C. elegans. Developmental dynamics : an official publication of the American Association of Anatomists *242*, 1250-1261.

Berber, S., Wood, M., Llamosas, E., Thaivalappil, P., Lee, K., Liao, B.M., Chew, Y.L., Rhodes, A., Yucel, D., Crossley, M.*, et al.* (2016). Homeodomain-Interacting Protein Kinase (HPK-1) regulates stress responses and ageing in C. elegans. Scientific reports *6*, 19582.

Berendzen, K.M., Durieux, J., Shao, L.W., Tian, Y., Kim, H.E., Wolff, S., Liu, Y., and Dillin, A. (2016). Neuroendocrine Coordination of Mitochondrial Stress Signaling and Proteostasis. Cell *166*, 1553-1563 e1510.

Blackwell, T.K., Sewell, A.K., Wu, Z., and Han, M. (2019). TOR Signaling in Caenorhabditis elegans Development, Metabolism, and Aging. Genetics *213*, 329-360.

Blaquiere, J.A., and Verheyen, E.M. (2017). Homeodomain-Interacting Protein Kinases: Diverse and Complex Roles in Development and Disease. Curr Top Dev Biol *123*, 73-103.

Bolger, A.M., Lohse, M., and Usadel, B. (2014). Trimmomatic: a flexible trimmer for Illumina sequence data. Bioinformatics *30*, 2114-2120.

Brignull, H.R., Moore, F.E., Tang, S.J., and Morimoto, R.I. (2006). Polyglutamine proteins at the pathogenic threshold display neuron-specific aggregation in a pan-neuronal Caenorhabditis elegans model. J Neurosci *26*, 7597-7606.

Calixto, A., Chelur, D., Topalidou, I., Chen, X., and Chalfie, M. (2010). Enhanced neuronal RNAi in C. elegans using SID-1. Nature methods *7*, 554-559.

Calzado, M.A., Renner, F., Roscic, A., and Schmitz, M.L. (2007). HIPK2: a versatile switchboard regulating the transcription machinery and cell death. Cell Cycle *6*, 139-143.

Chakravarthy, B., Gaudet, C., Menard, M., Brown, L., Atkinson, T., Laferla, F.M., Ito, S., Armato, U., Dal Pra, I., and Whitfield, J. (2012). Reduction of the immunostainable length of the hippocampal dentate granule cells' primary cilia in 3xAD-transgenic mice producing human Abeta(1-42) and tau. Biochem Biophys Res Commun *427*, 218-222.

Chen, D., Thomas, E.L., and Kapahi, P. (2009). HIF-1 modulates dietary restriction-mediated lifespan extension via IRE-1 in Caenorhabditis elegans. PLoS Genet *5*, e1000486.

Chen, X.Y., Du, Y.F., and Chen, L. (2018). Neuropeptides Exert Neuroprotective Effects in Alzheimer's Disease. Front Mol Neurosci *11*, 493.

Cheung, J.Y., Leaf, A., and Bonventre, J.V. (1986). Mitochondrial function and intracellular calcium in anoxic cardiac myocytes. The American journal of physiology *250*, C18-25.

Chun, L., Gong, J., Yuan, F., Zhang, B., Liu, H., Zheng, T., Yu, T., Xu, X.Z., and Liu, J. (2015). Metabotropic GABA signalling modulates longevity in C. elegans. Nature communications *6*, 8828.

Cinar, H., Keles, S., and Jin, Y. (2005). Expression profiling of GABAergic motor neurons in Caenorhabditis elegans. Curr Biol *15*, 340-346.

Cornwell, A., Llop, J.R., Salzman, P., Rasmussen, N., Thakar, J., and Samuelson, A.V. (2022). The Replica Set Method is a Robust, Accurate, and High-Throughput Approach for Assessing and Comparing Lifespan in C. elegans Experiments. Frontiers in Aging *3*.

Cornwell, A.B., Llop, J.R., Salzman, P., Thakar, J., and Samuelson, A.V. (2018). The Replica Set Method: A High-throughput Approach to Quantitatively Measure Caenorhabditis elegans Lifespan. Journal of visualized experiments : JoVE.

Cornwell, A.B., and Samuelson, A.V. (2020). Analysis of Lifespan in C. elegans: Low- and High-Throughput Approaches. In Aging: Methods and Protocols, S.P. Curran, ed. (New York, NY: Springer US), pp. 7-27.

Cunningham, F., Allen, J.E., Allen, J., Alvarez-Jarreta, J., Amode, M.R., Armean, I.M., Austine-Orimoloye, O., Azov, A.G., Barnes, I., Bennett, R.*, et al.* (2022). Ensembl 2022. Nucleic Acids Res *50*, D988-D995.

Das, R., Melo, J.A., Thondamal, M., Morton, E.A., Cornwell, A.B., Crick, B., Kim, J.H., Swartz, E.W., Lamitina, T., Douglas, P.M.*, et al.* (2017). The homeodomain-interacting protein kinase HPK-1 preserves protein homeostasis and longevity through master regulatory control of the HSF-1 chaperone network and TORC1-restricted autophagy in Caenorhabditis elegans. PLoS Genet *13*, e1007038.

de la Vega, L., Grishina, I., Moreno, R., Kruger, M., Braun, T., and Schmitz, M.L. (2012). A redox-regulated SUMO/acetylation switch of HIPK2 controls the survival threshold to oxidative stress. Mol Cell *46*, 472-483.

de Magalhaes, J.P., and Toussaint, O. (2004). GenAge: a genomic and proteomic network map of human ageing. FEBS Lett *571*, 243-247.

Deak, F. (2014). Neuronal vesicular trafficking and release in age-related cognitive impairment. J Gerontol A Biol Sci Med Sci *69*, 1325-1330.

DeLano, W.L. (2002). Pymol: An open-source molecular graphics tool. CCP4 Newsl Protein Crystallogr *40*, 82-92.

Denzel, M.S., Lapierre, L.R., and Mack, H.I.D. (2019). Emerging topics in C. elegans aging research: Transcriptional regulation, stress response and epigenetics. Mech Ageing Dev *177*, 4-21.

Dobin, A., Davis, C.A., Schlesinger, F., Drenkow, J., Zaleski, C., Jha, S., Batut, P., Chaisson, M., and Gingeras, T.R. (2013). STAR: ultrafast universal RNA-seq aligner. Bioinformatics *29*, 15-21.

Douglas, P.M., Baird, N.A., Simic, M.S., Uhlein, S., McCormick, M.A., Wolff, S.C., Kennedy, B.K., and Dillin, A. (2015). Heterotypic Signals from Neural HSF-1 Separate Thermotolerance from Longevity. Cell Rep *12*, 1196-1204.

Durieux, J., Wolff, S., and Dillin, A. (2011). The cell-non-autonomous nature of electron transport chain-mediated longevity. Cell *144*, 79-91.

Ecsedy, J.A., Michaelson, J.S., and Leder, P. (2003). Homeodomain-interacting protein kinase 1 modulates Daxx localization, phosphorylation, and transcriptional activity. Mol Cell Biol *23*, 950-960.

Entchev, E.V., Patel, D.S., Zhan, M., Steele, A.J., Lu, H., and Ch'ng, Q. (2015). A gene-expression-based neural code for food abundance that modulates lifespan. Elife *4*, e06259.

Ewald, C.Y., Landis, J.N., Porter Abate, J., Murphy, C.T., and Blackwell, T.K. (2015). Dauer-independent insulin/IGF-1-signalling implicates collagen remodelling in longevity. Nature *519*, 97-101.

Fawcett, E.M., Hoyt, J.M., Johnson, J.K., and Miller, D.L. (2015). Hypoxia disrupts proteostasis in Caenorhabditis elegans. Aging Cell *14*, 92-101.

Frakes, A.E., Metcalf, M.G., Tronnes, S.U., Bar-Ziv, R., Durieux, J., Gildea, H.K., Kandahari, N., Monshietehadi, S., and Dillin, A. (2020). Four glial cells regulate ER stress resistance and longevity via neuropeptide signaling in C. elegans. Science *367*, 436-440.

Garcia, S.M., Casanueva, M.O., Silva, M.C., Amaral, M.D., and Morimoto, R.I. (2007). Neuronal signaling modulates protein homeostasis in Caenorhabditis elegans post-synaptic muscle cells. Genes Dev *21*, 3006-3016.

Garufi, A., Ricci, A., Trisciuoglio, D., Iorio, E., Carpinelli, G., Pistritto, G., Cirone, M., and D'Orazi, G. (2013). Glucose restriction induces cell death in parental but not in homeodomain-interacting protein kinase 2-depleted RKO colon cancer cells: molecular mechanisms and implications for tumor therapy. Cell death & disease *4*, e639.

Gendrel, M., Atlas, E.G., and Hobert, O. (2016). A cellular and regulatory map of the GABAergic nervous system of C. elegans. Elife *5*.

Gidalevitz, T., Ben-Zvi, A., Ho, K.H., Brignull, H.R., and Morimoto, R.I. (2006). Progressive disruption of cellular protein folding in models of polyglutamine diseases. Science *311*, 1471-1474.

Gidalevitz, T., Kikis, E.A., and Morimoto, R.I. (2010). A cellular perspective on conformational disease: the role of genetic background and proteostasis networks. Curr Opin Struct Biol *20*, 23-32.

Gilleard, J.S., Barry, J.D., and Johnstone, I.L. (1997). cis regulatory requirements for hypodermal cell-specific expression of the Caenorhabditis elegans cuticle collagen gene dpy-7. Mol Cell Biol *17*, 2301-2311.

Hamilton, B., Dong, Y., Shindo, M., Liu, W., Odell, I., Ruvkun, G., and Lee, S.S. (2005). A systematic RNAi screen for longevity genes in C. elegans. Genes Dev *19*, 1544-1555.

Hammarlund, M., Nix, P., Hauth, L., Jorgensen, E.M., and Bastiani, M. (2009). Axon regeneration requires a conserved MAP kinase pathway. Science *323*, 802-806.

Hansen, M., Taubert, S., Crawford, D., Libina, N., Lee, S.J., and Kenyon, C. (2007). Lifespan extension by conditions that inhibit translation in Caenorhabditis elegans. Aging Cell *6*, 95-110.

Harris, M.A., Clark, J., Ireland, A., Lomax, J., Ashburner, M., Foulger, R., Eilbeck, K., Lewis, S., Marshall, B., Mungall, C*., et al.* (2004). The Gene Ontology (GO) database and informatics resource. Nucleic Acids Res *32*, D258-261.

Harris, T.W., Arnaboldi, V., Cain, S., Chan, J., Chen, W.J., Cho, J., Davis, P., Gao, S., Grove, C.A., Kishore, R*., et al.* (2020). WormBase: a modern Model Organism Information Resource. Nucleic Acids Res *48*, D762-D767.

Hart, A.C. (2006). Behavior. In The C elegans Research Community, WormBook.

Hattangadi, S.M., Burke, K.A., and Lodish, H.F. (2010). Homeodomain-interacting protein kinase 2 plays an important role in normal terminal erythroid differentiation. Blood *115*, 4853-4861.

He, Q., Shi, J., Sun, H., An, J., Huang, Y., and Sheikh, M.S. (2010). Characterization of Human Homeodomain-interacting Protein Kinase 4 (HIPK4) as a Unique Member of the HIPK Family. Molecular and cellular pharmacology *2*, 61-68.

Herndon, L.A., Schmeissner, P.J., Dudaronek, J.M., Brown, P.A., Listner, K.M., Sakano, Y., Paupard, M.C., Hall, D.H., and Driscoll, M. (2002). Stochastic and genetic factors influence tissue-specific decline in ageing C. elegans. Nature *419*, 808-814.

Hietakangas, V., Ahlskog, J.K., Jakobsson, A.M., Hellesuo, M., Sahlberg, N.M., Holmberg, C.I., Mikhailov, A., Palvimo, J.J., Pirkkala, L., and Sistonen, L. (2003). Phosphorylation of serine 303 is a prerequisite for the stress-inducible SUMO modification of heat shock factor 1. Mol Cell Biol *23*, 2953-2968.

Hietakangas, V., Anckar, J., Blomster, H.A., Fujimoto, M., Palvimo, J.J., Nakai, A., and Sistonen, L. (2006). PDSM, a motif for phosphorylation-dependent SUMO modification. Proc Natl Acad Sci U S A *103*, 45-50.

Higuchi-Sanabria, R., Durieux, J., Kelet, N., Homentcovschi, S., de Los Rios Rogers, M., Monshietehadi, S., Garcia, G., Dallarda, S., Daniele, J.R., Ramachandran, V.*, et al.* (2020). Divergent Nodes of Non-autonomous UPR(ER) Signaling through Serotonergic and Dopaminergic Neurons. Cell Rep *33*, 108489.

Hindupur, S.K., Gonzalez, A., and Hall, M.N. (2015). The opposing actions of target of rapamycin and AMP-activated protein kinase in cell growth control. Cold Spring Harbor perspectives in biology *7*, a019141.

Hobert, O. (2013). The neuronal genome of Caenorhabditis elegans. WormBook, 1-106.

Hodge, F., Bajuszova, V., and van Oosten-Hawle, P. (2022). The Intestine as a Lifespan- and Proteostasis-Promoting Signaling Tissue. Front Aging *3*, 897741.

Hofmann, T.G., Stollberg, N., Schmitz, M.L., and Will, H. (2003). HIPK2 regulates transforming growth factor-beta-induced c-Jun NH(2)-terminal kinase activation and apoptosis in human hepatoma cells. Cancer Res *63*, 8271-8277.

Huang, C., Xiong, C., and Kornfeld, K. (2004). Measurements of age-related changes of physiological processes that predict lifespan of Caenorhabditis elegans. Proc Natl Acad Sci U S A *101*, 8084-8089. Epub 2004 May 8012.

Imanikia, S., Ozbey, N.P., Krueger, C., Casanueva, M.O., and Taylor, R.C. (2019). Neuronal XBP-1 Activates Intestinal Lysosomes to Improve Proteostasis in C. elegans. Curr Biol *29*, 2322-2338 e2327.

Jaisson, S., and Gillery, P. (2014). Impaired proteostasis: role in the pathogenesis of diabetes mellitus. Diabetologia *57*, 1517-1527.

Jassal, B., Matthews, L., Viteri, G., Gong, C., Lorente, P., Fabregat, A., Sidiropoulos, K., Cook, J., Gillespie, M., Haw, R.*, et al.* (2020). The reactome pathway knowledgebase. Nucleic Acids Res *48*, D498-D503.

Jin, Y., Hoskins, R., and Horvitz, H.R. (1994). Control of type-D GABAergic neuron differentiation by C. elegans UNC-30 homeodomain protein. Nature *372*, 780-783.

Johnson, D.W., Llop, J.R., Farrell, S.F., Yuan, J., Stolzenburg, L.R., and Samuelson, A.V. (2014). The Caenorhabditis elegans Myc-Mondo/Mad complexes integrate diverse longevity signals. PLoS Genet *10*, e1004278.

Jorgensen, E.M., and Nonet, M.L. (1995). Neuromuscular junctions in the nematode C. elegans. Paper presented at: seminars in DEVELOPMENTAL BIOLOGY (Elsevier).

Jumper, J., Evans, R., Pritzel, A., Green, T., Figurnov, M., Ronneberger, O., Tunyasuvunakool, K., Bates, R., Zidek, A., Potapenko, A.*, et al.* (2021). Highly accurate protein structure prediction with AlphaFold. Nature *596*, 583-589.

Kaletsky, R., Yao, V., Williams, A., Runnels, A.M., Tadych, A., Zhou, S., Troyanskaya, O.G., and Murphy, C.T. (2018). Transcriptome analysis of adult Caenorhabditis elegans cells reveals tissue-specific gene and isoform expression. PLoS Genet *14*, e1007559.

Kamath, R.S., Fraser, A.G., Dong, Y., Poulin, G., Durbin, R., Gotta, M., Kanapin, A., Le Bot, N., Moreno, S., Sohrmann, M.*, et al.* (2003). Systematic functional analysis of the Caenorhabditis elegans genome using RNAi. Nature *421*, 231-237.

Kanehisa, M., and Goto, S. (2000). KEGG: kyoto encyclopedia of genes and genomes. Nucleic Acids Res *28*, 27-30.

Kenyon, C., Chang, J., Gensch, E., Rudner, A., and Tabtiang, R. (1993). A C. elegans mutant that lives twice as long as wild type. Nature *366*, 461-464.

Kikis, E.A., Gidalevitz, T., and Morimoto, R.I. (2010). Protein homeostasis in models of aging and age-related conformational disease. Advances in experimental medicine and biology *694*, 138-159.

Kim, E.A., Noh, Y.T., Ryu, M.J., Kim, H.T., Lee, S.E., Kim, C.H., Lee, C., Kim, Y.H., and Choi, C.Y. (2006). Phosphorylation and transactivation of Pax6 by homeodomain-interacting protein kinase 2. J Biol Chem *281*, 7489-7497.

Kraemer, B.C., Zhang, B., Leverenz, J.B., Thomas, J.H., Trojanowski, J.Q., and Schellenberg, G.D. (2003). Neurodegeneration and defective neurotransmission in a Caenorhabditis elegans model of tauopathy. Proc Natl Acad Sci U S A *100*, 9980-9985.

Kumsta, C., Chang, J.T., Schmalz, J., and Hansen, M. (2017). Hormetic heat stress and HSF-1 induce autophagy to improve survival and proteostasis in C. elegans. Nature communications *8*, 14337.

Labbadia, J., and Morimoto, R.I. (2015). The biology of proteostasis in aging and disease. Annu Rev Biochem *84*, 435-464.

Lakhani, R., Vogel, K.R., Till, A., Liu, J., Burnett, S.F., Gibson, K.M., and Subramani, S. (2014). Defects in GABA metabolism affect selective autophagy pathways and are alleviated by mTOR inhibition. EMBO Mol Med *6*, 551-566.

Lapierre, L.R., De Magalhaes Filho, C.D., McQuary, P.R., Chu, C.C., Visvikis, O., Chang, J.T., Gelino, S., Ong, B., Davis, A.E., Irazoqui, J.E.*, et al.* (2013). The TFEB orthologue HLH-30 regulates autophagy and modulates longevity in Caenorhabditis elegans. Nature communications *4*, 2267.

Lapierre, L.R., Kumsta, C., Sandri, M., Ballabio, A., and Hansen, M. (2015). Transcriptional and epigenetic regulation of autophagy in aging. Autophagy *11*, 867-880.

Lazaro-Pena, M.I., Cornwell, A.B., and Samuelson, A.V. (2021). Quantifying Tissue-Specific Proteostatic Decline in Caenorhabditis elegans. Journal of visualized experiments : JoVE.

Lazaro-Pena, M.I., Ward, Z.C., Yang, S., Strohm, A., Merrill, A.K., Soto, C.A., and Samuelson, A.V. (2022). HSF-1: Guardian of the Proteome Through Integration of Longevity Signals to the Proteostatic Network. Frontiers in Aging *3*.

Lee, P., Cho, B.R., Joo, H.S., and Hahn, J.S. (2008). Yeast Yak1 kinase, a bridge between PKA and stress-responsive transcription factors, Hsf1 and Msn2/Msn4. Mol Microbiol *70*, 882-895.

Lee, R.Y., Sawin, E.R., Chalfie, M., Horvitz, H.R., and Avery, L. (1999). EAT-4, a homolog of a mammalian sodium-dependent inorganic phosphate cotransporter, is necessary for glutamatergic neurotransmission in caenorhabditis elegans. J Neurosci *19*, 159-167.

Lee, S., Shang, Y., Redmond, S.A., Urisman, A., Tang, A.A., Li, K.H., Burlingame, A.L., Pak, R.A., Jovicic, A., Gitler, A.D.*, et al.* (2016). Activation of HIPK2 Promotes ER Stress-Mediated Neurodegeneration in Amyotrophic Lateral Sclerosis. Neuron *91*, 41-55.

Lee, S.J., Murphy, C.T., and Kenyon, C. (2009). Glucose shortens the life span of C. elegans by downregulating DAF-16/FOXO activity and aquaporin gene expression. Cell metabolism *10*, 379-391.

Lee, S.S., Kennedy, S., Tolonen, A.C., and Ruvkun, G. (2003). DAF-16 target genes that control C. elegans life-span and metabolism. Science *300*, 644-647.

Li, B., and Dewey, C.N. (2011). RSEM: accurate transcript quantification from RNA-Seq data with or without a reference genome. BMC Bioinformatics *12*, 323.

Li, N., and van der Kooy, D. (2018). Mutations in the guanylate cyclase gcy-28 neuronally dissociate naive attraction and memory retrieval. The European journal of neuroscience *48*, 3367-3378.

Liao, Y., Smyth, G.K., and Shi, W. (2014). featureCounts: an efficient general purpose program for assigning sequence reads to genomic features. Bioinformatics *30*, 923-930.

Lin, K., Dorman, J.B., Rodan, A., and Kenyon, C. (1997). daf-16: An HNF-3/forkhead family member that can function to double the life-span of Caenorhabditis elegans. Science *278*, 1319-1322.

Lints, R., and Emmons, S.W. (1999). Patterning of dopaminergic neurotransmitter identity among Caenorhabditis elegans ray sensory neurons by a TGFbeta family signaling pathway and a Hox gene. Development *126*, 5819-5831.

Lopez-Otin, C., Blasco, M.A., Partridge, L., Serrano, M., and Kroemer, G. (2013). The hallmarks of aging. Cell *153*, 1194-1217.

Love, M.I., Huber, W., and Anders, S. (2014). Moderated estimation of fold change and dispersion for RNA-seq data with DESeq2. Genome Biol *15*, 550.

Ma, R., Kutchy, N.A., Chen, L., Meigs, D.D., and Hu, G. (2022). Primary cilia and ciliary signaling pathways in aging and age-related brain disorders. Neurobiology of disease *163*, 105607.

Mahoney, T.R., Luo, S., and Nonet, M.L. (2006). Analysis of synaptic transmission in Caenorhabditis elegans using an aldicarb-sensitivity assay. Nature protocols *1*, 1772-1777.

Masse, I., Molin, L., Mouchiroud, L., Vanhems, P., Palladino, F., Billaud, M., and Solari, F. (2008). A novel role for the SMG-1 kinase in lifespan and oxidative stress resistance in Caenorhabditis elegans. PLoS One *3*, e3354.

McIntire, S.L., Jorgensen, E., and Horvitz, H.R. (1993). Genes required for GABA function in Caenorhabditis elegans. Nature *364*, 334-337.

Miller, H.A., Dean, E.S., Pletcher, S.D., and Leiser, S.F. (2020). Cell non-autonomous regulation of health and longevity. Elife *9*.

Morelli, A., Sarchielli, E., Guarnieri, G., Coppi, E., Pantano, D., Comeglio, P., Nardiello, P., Pugliese, A.M., Ballerini, L., Matucci, R., *et al.* (2017). Young Human Cholinergic Neurons Respond to Physiological Regulators and Improve Cognitive Symptoms in an Animal Model of Alzheimer's Disease. Front Cell Neurosci *11*, 339.

Morimoto, R.I. (2011). The heat shock response: systems biology of proteotoxic stress in aging and disease. Cold Spring Harb Symp Quant Biol *76*, 91-99.

Morimoto, R.I. (2019). Cell-Nonautonomous Regulation of Proteostasis in Aging and Disease. Cold Spring Harbor perspectives in biology.

Morley, J.F., Brignull, H.R., Weyers, J.J., and Morimoto, R.I. (2002). The threshold for polyglutamine-expansion protein aggregation and cellular toxicity is dynamic and influenced by aging in Caenorhabditis elegans. Proc Natl Acad Sci U S A *99*, 10417-10422.

Morley, J.F., and Morimoto, R.I. (2004). Regulation of longevity in Caenorhabditis elegans by heat shock factor and molecular chaperones. Mol Biol Cell *15*, 657-664. Epub 2003 Dec 2010.

Munkacsy, E., Khan, M.H., Lane, R.K., Borror, M.B., Park, J.H., Bokov, A.F., Fisher, A.L., Link, C.D., and Rea, S.L. (2016). DLK-1, SEK-3 and PMK-3 Are Required for the Life Extension Induced by Mitochondrial Bioenergetic Disruption in C. elegans. PLoS Genet *12*, e1006133.

Murakami, H., and Murakami, S. (2007). Serotonin receptors antagonistically modulate Caenorhabditis elegans longevity. Aging Cell *6*, 483-488.

Nakamura, S., Karalay, O., Jager, P.S., Horikawa, M., Klein, C., Nakamura, K., Latza, C., Templer, S.E., Dieterich, C., and Antebi, A. (2016). Mondo complexes regulate TFEB via TOR inhibition to promote longevity in response to gonadal signals. Nature communications *7*, 10944.

Nisaa, K., and Ben-Zvi, A. (2021). Chaperone networks are shaped by cellular differentiation and identity. Trends Cell Biol.

Nonet, M.L., Staunton, J.E., Kilgard, M.P., Fergestad, T., Hartwieg, E., Horvitz, H.R., Jorgensen, E.M., and Meyer, B.J. (1997). Caenorhabditis elegans rab-3 mutant synapses exhibit impaired function and are partially depleted of vesicles. J Neurosci *17*, 8061-8073.

Nye, K.J., Shi, Y.G., Andrews, J.M., and Wise, R. (1989). Pharmacokinetics and tissue penetration of cefepime. The Journal of antimicrobial chemotherapy *24*, 23-28.

Ogg, S., Paradis, S., Gottlieb, S., Patterson, G.I., Lee, L., Tissenbaum, H.A., and Ruvkun, G. (1997). The Fork head transcription factor DAF-16 transduces insulin-like metabolic and longevity signals in C. elegans. Nature *389*, 994-999.

Oh, K.H., and Kim, H. (2017). Aldicarb-induced Paralysis Assay to Determine Defects in Synaptic Transmission in Caenorhabditis elegans. Bio Protoc *7*.

Okkema, P.G., Harrison, S.W., Plunger, V., Aryana, A., and Fire, A. (1993). Sequence requirements for myosin gene expression and regulation in Caenorhabditis elegans. Genetics *135*, 385-404.

Oswal, N., Martin, O.M.F., Stroustrup, S., Matusiak Bruckner, M.A., and Stroustrup, N. (2021). A Hierarchical Process Model Links Behavioral Aging and Lifespan in C. elegans. bioRxiv, 2021.2003.2031.437415.

Pan, K.Z., Palter, J.E., Rogers, A.N., Olsen, A., Chen, D., Lithgow, G.J., and Kapahi, P. (2007). Inhibition of mRNA translation extends lifespan in Caenorhabditis elegans. Aging Cell *6*, 111-119.

Paradis, S., and Ruvkun, G. (1998). Caenorhabditis elegans Akt/PKB transduces insulin receptor-like signals from AGE-1 PI3 kinase to the DAF-16 transcription factor. Genes Dev *12*, 2488-2498.

Petrascheck, M., Ye, X., and Buck, L.B. (2007). An antidepressant that extends lifespan in adult Caenorhabditis elegans. Nature *450*, 553-556.

Petrella, C., Di Certo, M.G., Barbato, C., Gabanella, F., Ralli, M., Greco, A., Possenti, R., and Severini, C. (2019). Neuropeptides in Alzheimer's Disease: An Update. Current Alzheimer research *16*, 544-558.

Pickett, C.L., Breen, K.T., and Ayer, D.E. (2007). A C. elegans Myc-like network cooperates with semaphorin and Wnt signaling pathways to control cell migration. Dev Biol *310*, 226-239.

Pober, B.R. (2010). Williams-Beuren syndrome. N Engl J Med *362*, 239-252.

Prahlad, V., Cornelius, T., and Morimoto, R.I. (2008). Regulation of the cellular heat shock response in Caenorhabditis elegans by thermosensory neurons. Science *320*, 811-814.

Prahlad, V., and Morimoto, R.I. (2011). Neuronal circuitry regulates the response of Caenorhabditis elegans to misfolded proteins. Proc Natl Acad Sci U S A *108*, 14204-14209.

Rahimi, M., Sohrabi, S., and Murphy, C.T. (2022). Novel elasticity measurements reveal C. elegans cuticle stiffens with age and in a long-lived mutant. Biophys J *121*, 515-524.

Raich, W.B., Moorman, C., Lacefield, C.O., Lehrer, J., Bartsch, D., Plasterk, R.H., Kandel, E.R., and Hobert, O. (2003). Characterization of Caenorhabditis elegans homologs of the Down syndrome candidate gene DYRK1A. Genetics *163*, 571-580.

Richmond, J.E., and Jorgensen, E.M. (1999). One GABA and two acetylcholine receptors function at the C. elegans neuromuscular junction. Nature neuroscience *2*, 791-797.

Riesen, M., Feyst, I., Rattanavirotkul, N., Ezcurra, M., Tullet, J.M., Papatheodorou, I., Ziehm, M., Au, C., Gilliat, A.F., Hellberg, J.*, et al.* (2014). MDL-1, a growth- and tumor-suppressor, slows aging and prevents germline hyperplasia and hypertrophy in C. elegans. Aging (Albany NY) *6*, 98-117.

Rinaldo, C., Prodosmo, A., Siepi, F., and Soddu, S. (2007). HIPK2: a multitalented partner for transcription factors in DNA damage response and development. Biochemistry and cell biology = Biochimie et biologie cellulaire *85*, 411-418.

Rinaldo, C., Siepi, F., Prodosmo, A., and Soddu, S. (2008). HIPKs: Jack of all trades in basic nuclear activities. Biochim Biophys Acta *1783*, 2124-2129.

Roux, A.E., Yuan, H., Podshivalova, K., Hendrickson, D., Kerr, R., Kenyon, C., and Kelley, D.R. (2022). The complete cell atlas of an aging multicellular organism. bioRxiv, 2022.2006.2015.496201.

Sala, A.J., Bott, L.C., and Morimoto, R.I. (2017). Shaping proteostasis at the cellular, tissue, and organismal level. J Cell Biol *216*, 1231-1241.

Samuelson, A.V., Carr, C.E., and Ruvkun, G. (2007). Gene activities that mediate increased life span of C. elegans insulin-like signaling mutants. Genes Dev *21*, 2976-2994.

Scriabine, A., and Kazda, S. (1989). Pharmacological basis for use of calcium antagonists in hypertension. Magnesium *8*, 253-265.

Shemesh, N., Jubran, J., Dror, S., Simonovsky, E., Basha, O., Argov, C., Hekselman, I., Abu-Qarn, M., Vinogradov, E., Mauer, O.*, et al.* (2021). The landscape of molecular chaperones across human tissues reveals a layered architecture of core and variable chaperones. Nature communications *12*, 2180.

Shen, L.L., Wang, Y., and Wang, D.Y. (2007). Involvement of genes required for synaptic function in aging control in C. elegans. Neurosci Bull *23*, 21-29.

Shinkai, Y., Yamamoto, Y., Fujiwara, M., Tabata, T., Murayama, T., Hirotsu, T., Ikeda, D.D., Tsunozaki, M., Iino, Y., Bargmann, C.I.*, et al.* (2011). Behavioral choice between conflicting alternatives is regulated by a receptor guanylyl cyclase, GCY-28, and a receptor tyrosine kinase, SCD-2, in AIA interneurons of Caenorhabditis elegans. J Neurosci *31*, 3007-3015.

Shojima, N., Hara, K., Fujita, H., Horikoshi, M., Takahashi, N., Takamoto, I., Ohsugi, M., Aburatani, H., Noda, M., Kubota, N.*, et al.* (2012). Depletion of homeodomain-interacting protein kinase 3 impairs insulin secretion and glucose tolerance in mice. Diabetologia *55*, 3318-3330.

Siesjo, B.K. (1989). Calcium and cell death. Magnesium *8*, 223-237.

Sievers, F., Wilm, A., Dineen, D., Gibson, T.J., Karplus, K., Li, W., Lopez, R., McWilliam, H., Remmert, M., Soding, J.*, et al.* (2011). Fast, scalable generation of high-quality protein multiple sequence alignments using Clustal Omega. Mol Syst Biol *7*, 539.

Silva, M.C., Amaral, M.D., and Morimoto, R.I. (2013). Neuronal reprograming of protein homeostasis by calcium-dependent regulation of the heat shock response. PLoS Genet *9*, e1003711.

Song, J.J., and Lee, Y.J. (2003a). Effect of glucose concentration on activation of the ASK1-SEK1-JNK1 signal transduction pathway. J Cell Biochem *89*, 653-662.

Song, J.J., and Lee, Y.J. (2003b). Role of the ASK1-SEK1-JNK1-HIPK1 signal in Daxx trafficking and ASK1 oligomerization. J Biol Chem *278*, 47245-47252.

Steinmetz, E.L., Dewald, D.N., and Walldorf, U. (2018). Homeodomain-interacting protein kinase phosphorylates the Drosophila Paired box protein 6 (Pax6) homologues Twin of eyeless and Eyeless. Insect molecular biology *27*, 198-211.

Stroustrup, N., Ulmschneider, B.E., Nash, Z.M., Lopez-Moyado, I.F., Apfeld, J., and Fontana, W. (2013). The Caenorhabditis elegans Lifespan Machine. Nature methods *10*, 665-670.

Suriyalaksh, M., Raimondi, C., Mains, A., Segonds-Pichon, A., Mukhtar, S., Murdoch, S., Aldunate, R., Krueger, F., Guimera, R., Andrews, S.*, et al.* (2022). Gene regulatory network inference in long-lived C. elegans reveals modular properties that are predictive of novel aging genes. iScience *25*, 103663.

Sze, J.Y., Victor, M., Loer, C., Shi, Y., and Ruvkun, G. (2000). Food and metabolic signalling defects in a Caenorhabditis elegans serotonin-synthesis mutant. Nature *403*, 560-564.

Tacutu, R., Shore, D.E., Budovsky, A., de Magalhaes, J.P., Ruvkun, G., Fraifeld, V.E., and Curran, S.P. (2012). Prediction of C. elegans longevity genes by human and worm longevity networks. PLoS One *7*, e48282.

Tatum, M.C., Ooi, F.K., Chikka, M.R., Chauve, L., Martinez-Velazquez, L.A., Steinbusch, H.W., Morimoto, R.I., and Prahlad, V. (2015). Neuronal serotonin release triggers the heat shock response in C. elegans in the absence of temperature increase. Curr Biol *25*, 163-174.

Taylor, R.C., and Dillin, A. (2011). Aging as an event of proteostasis collapse. Cold Spring Harbor perspectives in biology *3*.

Taylor, R.C., and Dillin, A. (2013). XBP-1 is a cell-nonautonomous regulator of stress resistance and longevity. Cell *153*, 1435-1447.

Taylor, S.R., Santpere, G., Weinreb, A., Barrett, A., Reilly, M.B., Xu, C., Varol, E., Oikonomou, P., Glenwinkel, L., McWhirter, R.*, et al.* (2021). Molecular topography of an entire nervous system. Cell *184*, 4329-4347 e4323.

Team, R.C. (2013). R: A Language and Environment for Statistical Computing. R Foundation for Statistical Computing.

Timmons, L., Court, D.L., and Fire, A. (2001). Ingestion of bacterially expressed dsRNAs can produce specific and potent genetic interference in Caenorhabditis elegans. Gene *263*, 103-112.

Tsunozaki, M., Chalasani, S.H., and Bargmann, C.I. (2008). A behavioral switch: cGMP and PKC signaling in olfactory neurons reverses odor preference in C. elegans. Neuron *59*, 959-971.

Varadi, M., Anyango, S., Deshpande, M., Nair, S., Natassia, C., Yordanova, G., Yuan, D., Stroe, O., Wood, G., Laydon, A.*, et al.* (2022). AlphaFold Protein Structure Database: massively expanding the structural coverage of protein-sequence space with high-accuracy models. Nucleic Acids Res *50*, D439-D444.

Walter, L., Baruah, A., Chang, H.W., Pace, H.M., and Lee, S.S. (2011). The homeobox protein CEH-23 mediates prolonged longevity in response to impaired mitochondrial electron transport chain in C. elegans. PLoS Biol *9*, e1001084.

Wang, S.J.H., Sinclair, D.A.R., Kim, H.Y., Kinsey, S.D., Yoo, B., Shih, C.R.Y., Wong, K.K.L., Krieger, C., Harden, N., and Verheyen, E.M. (2020). Homeodomain-interacting protein kinase (Hipk) plays roles in nervous system and muscle structure and function. PLoS One *15*, e0221006.

Winston, W.M., Molodowitch, C., and Hunter, C.P. (2002). Systemic RNAi in C. elegans requires the putative transmembrane protein SID-1. Science *295*, 2456-2459.

Wolkow, C.A., Kimura, K.D., Lee, M.S., and Ruvkun, G. (2000). Regulation of C. elegans life-span by insulinlike signaling in the nervous system. Science *290*, 147-150.

Wu, C., Karakuzu, O., and Garsin, D.A. (2021). Tribbles pseudokinase NIPI-3 regulates intestinal immunity in Caenorhabditis elegans by controlling SKN-1/Nrf activity. Cell Rep *36*, 109529.

Young, M.D., Wakefield, M.J., Smyth, G.K., and Oshlack, A. (2010). Gene ontology analysis for RNA-seq: accounting for selection bias. Genome biology *11*, R14.

Yuan, F., Zhou, J., Xu, L., Jia, W., Chun, L., Xu, X.Z.S., and Liu, J. (2019). GABA receptors differentially regulate life span and health span in C. elegans through distinct downstream mechanisms. Am J Physiol Cell Physiol *317*, C953-C963.

Zaru, R., Magrane, M., O'Donovan, C., and UniProt, C. (2017). From the research laboratory to the database: the Caenorhabditis elegans kinome in UniProtKB. Biochem J *474*, 493-515.

Zhang, J., Pho, V., Bonasera, S.J., Holtzman, J., Tang, A.T., Hellmuth, J., Tang, S., Janak, P.H., Tecott, L.H., and Huang, E.J. (2007). Essential function of HIPK2 in TGFbeta-dependent survival of midbrain dopamine neurons. Nature neuroscience *10*, 77-86.

Zhang, J., Shang, Y., Kamiya, S., Kotowski, S.J., Nakamura, K., and Huang, E.J. (2020). Loss of HIPK2 Protects Neurons from Mitochondrial Toxins by Regulating Parkin Protein Turnover. J Neurosci *40*, 557-568.

Zhang, Q., Wu, X., Chen, P., Liu, L., Xin, N., Tian, Y., and Dillin, A. (2018). The Mitochondrial Unfolded Protein Response Is Mediated Cell-Non-autonomously by Retromer-Dependent Wnt Signaling. Cell *174*, 870-883 e817.

Zhang, Y., Lanjuin, A., Chowdhury, S.R., Mistry, M., Silva-Garcia, C.G., Weir, H.J., Lee, C.L., Escoubas, C.C., Tabakovic, E., and Mair, W.B. (2019). Neuronal TORC1 modulates longevity via AMPK and cell nonautonomous regulation of mitochondrial dynamics in C. elegans. Elife *8*.

Zhang, Y., Shao, Z., Zhai, Z., Shen, C., and Powell-Coffman, J.A. (2009). The HIF-1 hypoxia-inducible factor modulates lifespan in C. elegans. PLoS One *4*, e6348.

Zhang, Y., Zhang, X., Dai, Y., Song, M., Zhou, Y., Zhou, J., Yan, X., and Shen, Y. (2021). The decrease of intraflagellar transport impairs sensory perception and metabolism in ageing. Nature communications *12*, 1789.